AD-A146 231 COUPLING OF AIRBORNE SOUND INTO THE EARTH(U) 1/2
MISSISSIPPI UNIV UNIVERSITY PHYSICAL ACOUSTICS RESEARCH
LAB H E BASS ET AL. 01 AUG 84 PARGUM-84-01
UNCLASSIFIED ARO-17560.2-GS DAAG29-81-K-0078 F/G 17/1 NL

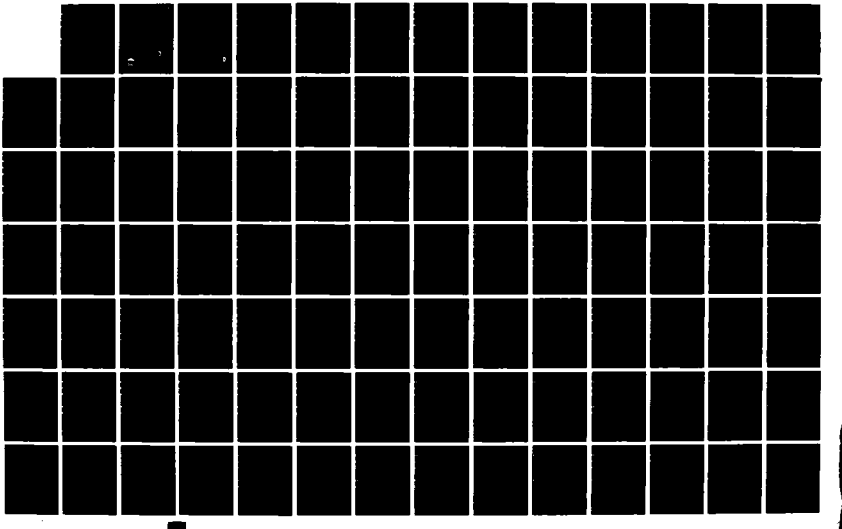

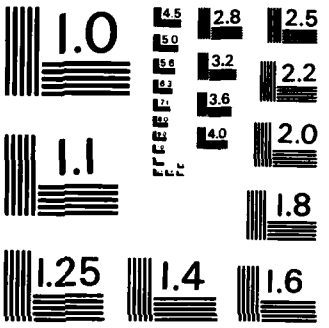

MICROCOPY RESOLUTION TEST CHART
NATIONAL BUREAU OF STANDARDS-1963-A

ARO 17560.2-GS

(2)

AD-A146 231

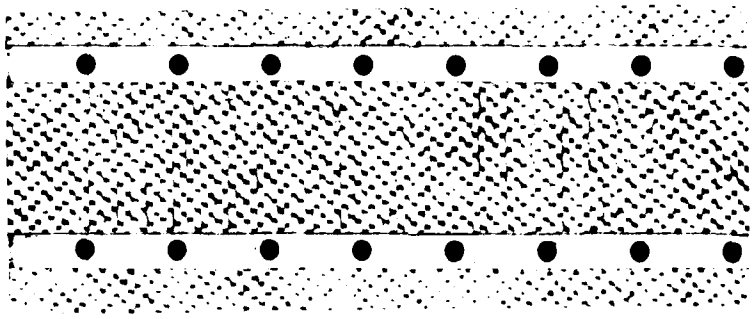

DTIC FILE COPY

DTIC
ELECTE
SEP 28 1984
S D
E

THE UNIVERSITY OF MISSISSIPPI
PHYSICAL ACOUSTICS RESEARCH GROUP
DEPARTMENT OF PHYSICS AND ASTRONOMY

84 09 25 114

2

Coupling of Airborne Sound Into the Earth

H.E. Bass and L.N. Bolen

PARGUM Report 84-01

Final Report

1 Aug. 1984

U.S. Army Research Office

DAAG-81-K-0078

Physical Acoustics Research Group

The University of Mississippi

University, MS 38677

Approved for public release;

distribution unlimited.

Foreword

The work reported here was accomplished, to a large extent, by Mr. James Sabatier, a Ph.D. candidate. This report, modified in format, will serve as his Ph.D. dissertation and will be available as such with the same title. Much of the theoretical section is based upon unpublished work by Dr. Keith Attenborough, The Open University, England. The authors gratefully acknowledge his contributions and cooperation.

UNCLASSIFIED
SECURITY CLASSIFICATION OF THIS PAGE (When Data Entered)

MASTER COPY - FOR REPRODUCTION PURPOSES

REPORT DOCUMENTATION PAGE

READ INSTRUCTIONS BEFORE COMPLETING FORM

1. REPORT NUMBER: ARO 17560.2-GS	2. GOVT ACCESSION NO.: AD-A146231 N/A
3. RECIPIENT'S CATALOG NUMBER: N/A	
4. TITLE (and Subtitle): Coupling of Airborne Sound into the Earth	5. TYPE OF REPORT & PERIOD COVERED: Final 8Jun81-7Jun84
	6. PERFORMING ORG. REPORT NUMBER: PARGUM 84-01
7. AUTHOR(s): H.E. Bass and L.N. Bolen	8. CONTRACT OR GRANT NUMBER(s): DAAG-81-K-0078
9. PERFORMING ORGANIZATION NAME AND ADDRESS: Physical Acoustics Research Laboratory, Department of Physics and Astronomy, The University of Mississippi, University, MS 38677	10. PROGRAM ELEMENT, PROJECT, TASK AREA & WORK UNIT NUMBERS: N/A
11. CONTROLLING OFFICE NAME AND ADDRESS: U. S. Army Research Office, Post Office Box 12211, Research Triangle Park, NC 27709	12. REPORT DATE 13. NUMBER OF PAGES
14. MONITORING AGENCY NAME & ADDRESS (if different from Controlling Office)	15. SECURITY CLASS. (of this report): Unclassified 15a. DECLASSIFICATION/DOWNGRADING SCHEDULE

16. DISTRIBUTION STATEMENT (of this Report)

Approved for public release; distribution unlimited.

17. DISTRIBUTION STATEMENT (of the abstract entered in Block 20, if different from Report)

NA

18. SUPPLEMENTARY NOTES

The view, opinions, and/or findings contained in this report are those of the author(s) and should not be construed as an official Department of the Army position, policy, or decision, unless so designated by other documentation.

19. KEY WORDS (Continue on reverse side if necessary and identify by block number)

Acoustic/Seismic Coupling
Outdoor Sound Propagation

20. ABSTRACT (Continue on reverse side if necessary and identify by block number)

As an acoustic wave propagates above the surface of the earth, part of the energy is transferred from motion of air to motion of the earth's surface which can be detected by a geophone. The purpose of the study described here was to establish the physical mechanisms responsible for this acoustic to seismic transfer of energy, to develop a mathematical formulation for quantitative predictions of the acoustic/seismic transfer function, and to collect data for comparison to the physical model.

DD FORM 1 JAN 73 1473 EDITION OF 1 NOV 65 IS OBSOLETE

UNCLASSIFIED
SECURITY CLASSIFICATION OF THIS PAGE (When Data Entered)

The physical model chosen to describe coupling of energy into the earth was developed by Biot and later extended by Stoll primarily for describing sound propagation in ocean sediments. The Biot-Stoll model describes sound propagation in a medium composed of fluid saturated pores and an elastic frame (matrix). The differential equations which arise from this formalism allow for a fast wave which propagates, primarily, in the frame and a slow wave which propagates, primarily, in the fluid. For our application we assume that the fluid is air and that the porous material is a layer bewteen the air (an upper semi-infinite half space) and homogenous clay (a lower semi-infinite half space). The resultant boundary value problem was solved for amplitude and phase of the acoustic wave above the surface, acoustic wave in the pores of the porous layer, seismic motion of the pore frame, and seismic motion of the lower clay half space. Shear motion was included for completeness. The incoming sound wave was assumed to be planar.

Calculations suggest that the predicted transfer functions are not strongly affected by the flow resistance of the porous layer, the elastic properties of the clay, and the thickness of the porous layer. These three quantities were independently measured. The transfer function was measured for a microphone probe buried in the porous layer, and triaxial geophones in the porous layer and underlying clay. Measurements were made for acoustic frequencies between 30 and 300 Hz, for angles of incidence for the acoustic wave between 5^{o} and 20^{o}, and various depths for buried geophones and microphone probes.

Experimental values of the various transfer functions agree with predictions within a factor of two. The experimental results show fine structure not predicted which we attribute to multiple layers. Other quantities predicted by the model (attenuation of signal with depth, little dependence on angle of incidence, acoustic surface impedance) all agree equally well with experiment.

We conclude that the Biot-Stoll model is a good physical description of acoustic to seismic energy transfer. Additional avenues for future research are also discussed. Computer programs are included along with a representative sample of the experimental data.

TABLE OF CONTENTS

LIST OF FIGURES

LIST OF TABLES

1. INTRODUCTION

The objective of this study was to establish the physical principles involved in coupling airborne sound into earth motion. The study was motivated by measurements made at the U.S. Army Corps Engineers Waterways Experiment Station (WES) in 1977. In these measurements, a speaker was suspended from a crane, the sound level in the far field was measured with a microphone above the surface, and geophone response was measured below the surface. The major findings[1,2] were:

1. The geophone response had a magnitude 1000 times larger than one would expect from calculations based upon simple acoust transmission through a boundary between two perfect fluids.

2. The magnitude of the geophone response is, within the accuracy of the measurements, independent of angle of incidence.

3. The transit time from speaker to microphone was approximately the same as from speaker to geophone and the speed of propagation was, within the accuracy of the measurements, the same as the speed of sound in air (343 m/sec).

4. The geophone signal varied in phase as one would expect of a Rayleigh Wave.

5. The geophone signal had well defined maxima and minima which could be accurately explained assuming interference in the upper boundary layer of the earth. The depth of this layer was defined by independent seismic refraction studies.

During the course of the study reported on here, a physical model consistent with these observations has been developed from which quantitative predictions can be made.

The first inquiry this laboratory received concerning this problem was from WES and was prompted by a field test during which airborne sound

sources had detonated smart mines. The first goal, then, was to develop an algorithm which would allow the sensor to discriminate against airborne sound. This was done by discriminating against geophone signals which correlate with above ground microphone signals. More recently, this correlation has been used to identify airborne sound source in a security system developed by Sandia Laboratories. The coupling between airborne and seismic signals, then, is not necessarily detrimental to military applications.

In the following sections several experiments and theoretical results will be presented which represent the progression of events leading to a physical model for the coupling process.

Initially, the theoretical approach was to treat the boundary as a separation between homogeneous half spaces and treat the shallow porous upper layer of the earth as an impedance matching layer.[3,4,5] It was thought that this approach plus consideration of Rayleigh Waves in the earth instead of compressional waves would give the measured seismic amplitudes. Even with the relatively slow Rayleigh Wave velocity, however, the acoustic resistance (ρc) ratio between air and the earth is so small that most all the impinging energy would be reflected. This approach was abandoned after one year.

The initial experimental concerns were the extent to which the speaker was decoupled from the earth and the potential contributions of the geophone signal by direct airborne waves. Several experiments were conducted to insure direct coupling though speaker supports would not account for the geophone signal. Speakers were isolated from the ground using flexible cables and inner tubes with no effect on the measured seismic signal. Perhaps the most conclusive experiment was the firing of a freely falling blank pistol - the seismic/acoustic coupling remained unchanged.

At this stage in the research (about one year after beginning), it was concluded that airborne sound is, indeed, coupled into motion of the earth

frame with an amplitude larger than can be predicted from homogeneous layer theory.

A major breakthrough in the understanding of this problem came as a result of progress on another research project in this laboratory. To explain measurements of sound propagation through ocean sediments, it is common to use what is known as the Biot-Stoll Model.[6] This model basically allows for two waves in the porous medium, one associated with the matrix, another associated with motion of the pore fluid relative to the matrix. At a meeting organized by this laboratory on the status of long range acoustic propagation research,[7] the possibility of using the Biot-Stoll Model to explain coupling of airborne sound into the earth was explored. The physical principles were consistent with this problem, but the approximations used in underwater propagation codes were of concern. Following this meeting, Dr. Attenborough of the Open University of England agreed that this model offered most promise of explaining the seismic/acoustic coupling results. It was agreed that a joint effort would be fruitful, and cooperative measurements in this laboratory the following summer (1982) were arranged.

During the time Dr. Attenborough was visiting this laboratory it was agreed to address two major questions:

1. Is there an acoustic wave in the earth which can be attributed to motion of the pore fluid relative to the matrix?

2. If such an acoustic wave exists, is the velocity sufficiently low so that the acoustic resistance for this wave will allow for sufficient energy transfer? It was felt that if the wavelength of sound in the pores was much greater than a typical pore length (a few centimeters), transfer of energy to the pore walls by viscous drag would be quite small.

Both these questions were answered, to some degree, during the summer of 1982. Using a specially designed probe microphone (see Chapter 3) the

acoustic wave attributable to motion of air in the pores was detected, the attenuation of this wave with depth was measured and favorable comparisons with calculations made assuming a rigid porous medium were shown. These results were published in Reference 8. The same model used to compute attenuation was also used to predict the velocity of the acoustic wave in the earth. It was gratifying to find that the predicted speed decreases rapidly with decreasing frequency such that for a typical soil, the wavelength becomes independent of frequency below about 500 Hz with a wavelength of a few tens of centimeters. Measurements with the probe microphone illustrated that in the same medium, an acoustic signal could be observed down to depths of a few tens of centimeters. The pore depth is, in fact, comparable to the acoustic wavelength even at very low frequencies.

These results reinforced confidence in the Biot-Stoll Model and showed that pervious knowledge in acoustic wave propagation in ocean sediments and above the surface of the earth could be applied directly to the seismic/acoustic coupling problem. The next step was to apply the Biot-Stoll Model quantitatively dropping the earlier assumption (commonly made in acoustics) that the frame is rigid. The result of that effort will be presented in Chapter 2.

2. THEORY

In this section application of the Biot-Stoll Model of sound propagation in a porous media to the air/earth boundary will be described. In the first section, the procedure for computing propagation coefficients in the media as developed by Attenborough[9,10] will be presented. In the next section the boundary value problem for this case will set up and solved. This treatment is similar to that presented by Sides[11] except a shear wave term is also included. Finally measurable quantities will be defined and calculated.

Absent from this chapter are treatments of a spherically spreading source (plane waves are assumed), impulsive sources, and a soil with porosity varying with depth. The effect of spherical waves could be to introduce a sub-surface wave similar to the surface wave known in above ground propagation and which, above the ground, is dominant for certain source receiver geometries. By transforming from frequency to time domain, the current theory should be applicable to impulsive sounds but that process has not yet been developed. Varying porosity could improve coupling into the earth frame by providing a gradual change in the acoustic resistance with depth. These two extensions to the theory will probably be necessary before all experimental results can be explained.

The Biot-Stoll Model for wave propagation in a porous elastic medium was used to describe the coupling of an airborne acoustic wave into the porous elastic earth. The first layer or few tens of centimeters of the earth's surface is porous and will allow for the propagation of an acoustic wave, whether the surface is sand or grass covered soil. The porosity of a sand results from the packing of the sand particles. A grass covered soil's porosity might result from decaying organic matter and grass roots as well as the particle packing. This first layer was modeled as a two

dimensional homogeneous porous elastic medium characterized by a frame or matrix filled with air overlying a semi-infinite nonporous elastic clay.

From a plane wave analysis of the Biot-Stoll differential equations which govern the propagation of compressional waves, the attenuation coefficients and phase velocities of the allowed wave motions can be determined. After applying the boundary conditions at the boundaries of the air-sand-clay or air-soil-clay layer to solve for the amplitudes of the matrix and fluid motions, the specific normal acoustic surface impedance, the attenuation coefficients, and the surface transfer functions for the porous medium will be found.

Determination of Propagation Constants

The Biot-Stoll[6] differential equations for compressional wave propagation are

$$\nabla^2(He-C\xi) = \frac{\partial^2}{\partial t^2}(\rho e-\rho_f \xi) \tag{1a}$$

and

$$\nabla^2(Ce-M\xi) = \frac{\partial^2}{\partial t^2}(\rho_f e-m\xi) - \frac{\eta}{\kappa}\frac{\partial \xi}{\partial t}. \tag{1b}$$

The terms H, C and M are frequency dependent constants that characterize the porous elastic matrix and will be discussed later in this section. The quantity e represents the matrix dilitation, $e = \nabla\cdot\vec{u}$ where $\vec{u}$ is the matrix displacement. The dilitation of the fluid relative to the matrix is ξ and

$$\xi = \nabla\cdot\vec{w}$$

where

$$\vec{w} = \Omega(\vec{u}-\vec{U})$$

is the relative fluid velocity; $\vec{U}$ is the fluid displacement and Ω is the porosity. The density of the matrix and the fluid are identified with the

terms ρ and ρ_f while η and κ are the dynamic fluid viscosity and the permeability of the matrix. The term $\frac{\eta}{\kappa}\frac{\partial \xi}{\partial t}$ allows for damping through viscous drag as the fluid and matrix move relative to each other. The term m is a dimensionless parameter that accounts for the fact that not all the fluid moves in the direction of the macroscopic pressure gradient because the pores do not all run normal to the surface. This term is related to the Biot added mass term and allows for damping due to inertial drag between the fluid and matrix as they move relative to each other. This quantity is expressed as $q^2\rho_f/\Omega$ where q^2, the tortuosity, is a constant greater than or equal to one and has the particular value $1/\cos\theta$ when the pores are cylindrical and are inclined at θ to the surface normal.

The terms H, C, and M are complex constants that characterize the elastic response of the matrix. These constants are determined from the bulk and shear moduli of the solid material, the bulk modulus of the fluid and the bulk modulus of the matrix. The relationships are as follows

$$H = \frac{[K_r-K_b]^2}{[D-K_b]^2} + K_b + \frac{4}{3}\mu \tag{2a}$$

$$C = K_r\frac{K_r-K_b}{D-K_b} \tag{2b}$$

$$M = \frac{K_r^2}{D-K_b} \tag{2c}$$

with

$$D = K_r[1+\Omega(\frac{K_r}{K_f}-1)]. \tag{2d}$$

In the above expressions, K_r is the bulk modulus of the solid material, K_f is the bulk modulus of the fluid and μ and K_b are the shear and bulk moduli of the matrix. The elastic constants can be made complex through a complex compressibility of the pore fluid. However, at this stage they were assumed to be real. The bulk and shear moduli were determined from the expressions for compressional and shear wave speeds in an elastic solid, which are

$$v_s = [G/\rho]^{1/2} \tag{3}$$

and

$$v_p = [(B + \frac{4}{3} G)/\rho]^{1/2} \tag{4}$$

In these expressions, B and G are the bulk and shear moduli and ρ is the density of the medium. For the porous soil, it was assumed B was the frame bulk modulus, G was the frame shear modulus and ρ was the frame density. In the non-porous clay, it was assumed the bulk modulus B was the bulk modulus of the solid material, and G was the shear modulus of the same. These assumptions imply that the porous medium is composed of the same material as the clay but that it has been made porous by some means, say weathering or cultivation.

In equation (1b), Stoll[6] replaces the viscosity by a viscosity correction factor, $\eta F(\lambda)$, where λ is a dimensionless quantity that is related to the thickness of the viscous boundary layer at the pore wall. Biot[11] developed expressions for $F(\lambda)$ for cylindrical and parallel sided pores in terms of the fluid viscosity and pore diameter. Attenborough[12] suggested that the dimensionless parameter λ for an arbitrary pore shape is

$$\lambda = \frac{\sqrt{s}}{n} \frac{[8\rho_f q^2 \omega]^{1/2}}{\Omega\phi} \tag{5}$$

where $\frac{\sqrt{s}}{n}$ is a shape factor ratio, ϕ is the flow resistivity and ω is the angular frequency. The static shape factor, n, relates λ for an arbitrary pore cross section to that of a cylindrical pore cross section while the pore shape factor, s, accounts for the fact that the pores may have varying cross sections along their lengths. The ranges of n and s as suggested by Attenborough are $1.5 > s > 1 > n > 0.5$. The viscosity correction factor $F(\lambda)$ is a complex function and is written as

$$F(\lambda) = -\frac{1}{4} \cdot \frac{\sqrt{i}\,\lambda T[\sqrt{i}\,\lambda]}{1-\frac{2}{\sqrt{i}\lambda}T[\sqrt{i}\lambda]} \tag{6}$$

with $T[\sqrt{i}\,\lambda] = J_1[\sqrt{i}\,\lambda]/J_0[\sqrt{i}\,\lambda]$, where J_0 and J_1 are the zero and first order Bessel functions of the first kind.

The Biot-Stoll equations of motion admit two plane wave solutions and thus two propagation constants or wave speeds. The waves are referred to as the type one and type two waves or simply as fast and slow waves. For each wave there is both fluid and solid displacement and each wave is distinguished by its propagation coefficients. In sands and soils the fast wave primarily moves in the matrix or solid component while the slow wave moves primarily in the fluid. The exact relationship between the fluid and solid displacement will be determined in a later paragraph. The slow wave is a diffusion wave and it is highly attenuated and very dispersive as it propagates. The fast wave is analogous to the compressional wave that propagates in a solid and it is relatively unattenuated and not dispersive.

From a plane wave analysis of equations (1a) and (1b) the frequency equation determining the propagation constants can be found. If the plane waves $e = A\exp[i(\ell x-\omega t)]$ and $\xi = B\exp[i(\ell x-\omega t)]$ are chosen as solutions to equations 1a and 1b, the following expressions

$$(H\ell^2-\rho\omega^2)A + (\rho_f\omega^2-C\ell^2)B = 0 \tag{7a}$$

and

$$(C\ell^2-\rho_f\omega^2)A + (m\omega^2-M\ell^2-i\omega F(\lambda)\tfrac{\eta}{\kappa})B = 0 \tag{7b}$$

are found after substitution. The determinant of the coefficients must be zero so one can write

$$\begin{vmatrix} H\ell^2-\rho\omega^2 & \rho_f\omega^2-C\ell^2 \\ C\ell^2-\rho_f\omega^2 & m\omega^2-M\ell^2-i\omega F(\lambda)\frac{\eta}{\kappa} \end{vmatrix} = 0. \tag{8}$$

There are two complex roots of this equation from which both the attenuation and phase velocities for the fast and slow waves can be found. The

solution to this expression must be done numerically because of the Bessel functions involved, and a routine is included in Appendix A.1.

From equation (7a) we can write down the relation between the fluid and matrix wave amplitudes for each wave type as

$$m_i = \frac{B}{A} = -\frac{(H\ell^2-\rho\omega^2)}{(\rho_f\omega^2-C\ell^2)}. \tag{9}$$

The Biot-Stoll differential equations which govern the propagation of shear waves are not included here but are found in Reference 6 along with the characteristic frequency equation for the propagation constants. In this work it was assumed that a shear wave is non-dispersive, and the wave number was determined from the measured shear wave velocity.

Now that the propagation coefficients are known the boundary value problem can be considered.

Boundary Value Problem

The first few tens of centimeters of the earth's surface was modeled as a two-dimensional porous elastic medium of depth $\underline{d}$ overlying a semi-infinite non-porous elastic medium. The intermediate medium was either a sand or soil and the lower medium was a non-porous clay. The air-soil or air-sand interface was assumed to be a free surface and the lower surface was assumed to be in welded contact with an impermeable membrane between the two media. The air is allowed to flow across the upper boundary, while it is not allowed to penetrate the elastic clay below the porous soil.

For this physical system, the boundary conditions have been developed by Deresiewiez and Sfalak.[13] The boundary conditions at the upper interface are (1) continuity of normal particle velocity, (2) continuity of fluid pressure, (3) continuity of total normal stress, and (4) continuity of tangential stress. At the lower interface the boundary conditions are (5) continuity of normal frame velocity, (6) continuity of tangential frame

velocity, (7) continuity of fluid velocity, (8) continuity of total normal stress, and (9) continuity of tangential stress.

The pressure and stress-strain relations for a porous medium in the Biot-Stoll[6] notation are:

$$\tau_{xx} = He-2\mu(e_y+e_z)-C\xi \tag{10}$$

$$\tau_{yy} = He-2\mu(e_z+e_x)-C\xi \tag{11}$$

$$\tau_{zz} = He-2\mu(e_x+e_y)-C\xi \tag{12}$$

$$\tau_{xy} = \mu\gamma_z \tag{13}$$

$$\tau_{yz} = \mu\gamma_x \tag{14}$$

$$\tau_{zx} = \mu\gamma_y \tag{15}$$

$$P_f = M\xi-Ce \tag{16}$$

where τ_{ij} are the total stresses, and P_f is the pore fluid pressure. The terms e_x, e_y, e_z, γ_x, γ_y, and γ_z are defined as

$$e_x = \frac{\partial u_x}{\partial x} \tag{17}$$

$$e_y = \frac{\partial u_y}{\partial y} \tag{18}$$

$$e_z = \frac{\partial u_z}{\partial z} \tag{19}$$

$$\gamma_x = 1/2\left(\frac{\partial u_y}{\partial z} + \frac{\partial u_z}{\partial y}\right) \tag{20}$$

$$\gamma_y = 1/2\left(\frac{\partial u_z}{\partial x} + \frac{\partial u_x}{\partial z}\right) \tag{21}$$

$$\gamma_z = 1/2\left(\frac{\partial u_x}{\partial y} + \frac{\partial u_y}{\partial x}\right) \tag{22}$$

It is informative to evaluate these relations in a medium which the porosity is either one or zero. If the porosity of the medium goes to one, $\Omega = 1$, then the medium is a fluid and the relation for the pressure reduces to

$$P_f = M\xi \tag{23}$$

because $e = \nabla \cdot \vec{u} = 0$ since there is no solid component present. In this last expression for P_f, the elastic constant, M, reduces to the bulk

modulus of the fluid. In the lowest medium, where the porosity is zero, the stress-strain relations reduce to that of an elastic solid. Specifically, the expression for τ_{zz} reduces to

$$\tau_{zz} = He - 2\mu(e_x+e_z) \tag{24}$$

since there is no fluid component present. In this last expression, the elastic frame constant, H, reduces to

$$H = K_r + \frac{4}{3}\mu. \tag{25}$$

In the following M will be set equal to the bulk modulus when $\Omega = 1$ and, for a non-porous elastic material, $\Omega = 0$, H will be evaluated using equation (25).

Next the types of allowed wave motion are chosen and then the boundary conditions are applied at the appropriate interfaces. In the air, incident and reflected waves are allowed having wave vectors $\vec{\ell}_i$ and $\vec{\ell}_r$, with $|\ell_i| = |\ell_r|$. Type one and type two dilitational waves and a shear wave are transmitted into the porous medium with respective wave vectors, $\vec{\ell}_1$, $\vec{\ell}_2$, and $\vec{\ell}_3$. At the lower interface the three waves are reflected and have wave vectors $\vec{\ell}_1'$, $\vec{\ell}_2'$ and $\vec{\ell}_3'$ with $|\ell_1| = |\ell_1'|$, $|\ell_2| = |\ell_2'|$ and $|\ell_3| = |\ell_3'|$. In the clay only a shear wave and compressional wave are transmitted with wave vectors $\vec{\ell}_4$ and $\vec{\ell}_5$, respectively. Each allowed wave is associated with an angle of incidence, reflection, etc. as indicated in Figure 2.1. In the air the incident and reflected waves are

$$\vec{U}_i = \vec{\ell}_i B_i \exp[i(\ell_i \cos\theta_i x + \ell_i \sin\theta_i z - \omega t)] \tag{26}$$

and

$$\vec{U}_r = \vec{\ell}_r B_r \exp[i(\ell_r \cos\theta_r x - \ell_r \sin\theta_r z - \omega t)] \tag{27}$$

where B_i and B_r are the fluid displacement amplitudes. In the porous medium, the matrix compressional waves are

$$\vec{u}_1 = \hat{\ell}_1 A_1 \exp[i(\ell_1 \sin\theta_1 x + \ell_1 \cos\theta_1 z - \omega t)] \tag{28}$$

$$\vec{u}_2 = \hat{\ell}_2 A_2 \exp[i(\ell_2 \sin\theta_2 x + \ell_2 \cos\theta_2 z - \omega t)] \tag{29}$$

$$\vec{u}_1' = \hat{\ell}_1' A_1' \exp[i(\ell_1' \sin\theta_2 x - \ell_1' \cos\theta_1' z - \omega t)] \tag{30}$$

$$\vec{u}_2' = \hat{\ell}_2' A_2' \exp[i(\ell_2' \sin\theta_2' x - \ell_2' \cos\theta_2' z - \omega t)] \tag{31}$$

where $\vec{u}_1$ and $\vec{u}_2$ are the type one and two waves transmitted into the porous medium and $\vec{u}_1'$ and $\vec{u}_2'$ are the type one and two waves reflected at the lower boundary. The A_i are the matrix wave displacement amplitudes. Associated with each matrix wave in the porous medium is a relative fluid wave which is expressed as

$$\vec{w}_1 = \hat{\ell}_1 B_1 \exp[i(\ell_1 \sin\theta_1 x + \ell_1 \cos\theta_1 z - \omega t)] \tag{32}$$

$$\vec{w}_2 = \hat{\ell}_2 B_2 \exp[i(\ell_2 \sin\theta_2 x + \ell_2 \cos\theta_2 z - \omega t)] \tag{33}$$

$$\vec{w}_1' = \hat{\ell}_1' B_1' \exp[i(\ell_1' \sin\theta_1' x - \ell_1' \cos\theta_1' z - \omega t)] \tag{34}$$

$$\vec{w}_2' = \hat{\ell}_2' B_2' \exp[i(\ell_2' \sin\theta_2' x - \ell_2' \cos\theta_2' z - \omega t)] \tag{35}$$

where the B_i are the relative fluid wave amplitudes. In the porous medium there are also shear waves transmitted and reflected which are expressed as

$$\vec{u}_3 = \hat{e} E \exp[i(\ell_3 \sin\theta_3 x + \ell_3 \cos\theta_3 z - \omega t)] \tag{36}$$

$$\vec{u}_3' = \hat{e}' E' \exp[i(\ell_3' \sin\theta_3' x - \ell_3' \cos\theta_3' z - \omega t)] \tag{37}$$

where E and E' are matrix displacement amplitudes. The transmitted compressional and shear waves in the clay are

$$\vec{u}_t^c = \hat{\ell}_5 A_t \exp[i(\ell_5 \sin\theta_5 x + \ell_5 \cos\theta_5 z - \omega t)] \tag{38}$$

$$\vec{u}_t^s = \hat{e}'' E_t \exp[i(\ell_4 \sin\theta_4 x + \ell_4 \cos\theta_4 z - \omega t)] \tag{39}$$

and A_t and E_t are again the displacement amplitudes. Using these plane waves, the boundary conditions at the two interfaces can be evaluated.

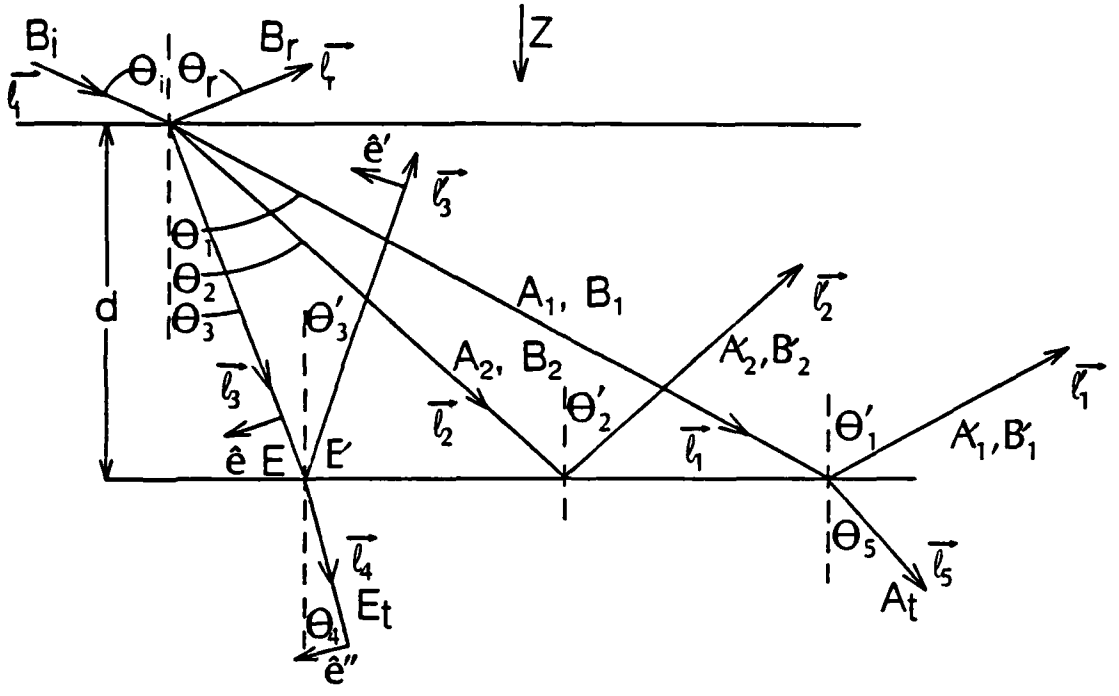

Figure 2.1. The layer model used indicating notation for angles of incidence, reflection and refraction, wave amplitudes, propagation vectors and polarizations.

At the upper boundary, the first boundary condition is continuity of normal particle velocity and is expressed as

$$\bar{\dot{U}}_\perp = (1-\Omega)\dot{u}_\perp + \dot{U}_\perp \tag{40}$$

where a bar is used to indicate wave motion in the upper medium. Using $\vec{w} = \Omega(\vec{u}-\vec{U})$, $\dot{U}_\perp$ can be eliminated from the boundary condition to yield

$$\bar{\dot{U}}_\perp = \dot{u}_\perp - \dot{w}_\perp. \tag{41}$$

Substituting in the appropriate waves yields the following equation

$$\begin{aligned} U_i\cos\theta_i - U_r\cos\theta_r = {} & u_1\cos\theta_1 + u_2\cos\theta_2 - u_i'\cos\theta_i' \\ & - u_2'\cos\theta_2' - w_1\cos\theta_1 - w_2\cos\theta_2 \\ & + w_1'\cos\theta_1' + w_2'\cos\theta_2' + u_3\sin\theta_3 - u_3'\sin\theta_3'. \end{aligned} \tag{42}$$

After substituting for z = 0, Snell's law is verified yielding:

$$\theta_i = \theta_r \tag{43}$$

$$\theta_1 = \theta_1' \tag{44}$$

$$\theta_2 = \theta_2' \tag{45}$$

$$\theta_3 = \theta_3'. \tag{46}$$

This boundary condition equation can be rewritten as

$$\begin{aligned}(B_i-B_r)\cos\theta_i = {} & A_1(1-m_1)\cos\theta_1 + A_2(1-m_2)\cos\theta_2 \\ & - A_1'(1-m_1)\cos\theta_1 - A_2'(1-m_2)\cos\theta_2 \\ & + E\sin\theta_3 - E'\sin\theta_3\end{aligned} \tag{47}$$

where the relative wave amplitudes have been replaced by the matrix wave amplitudes, using $m_i = A_i/B_i$. The second boundary condition is continuity of fluid pressure. The expression for the pressure is

$$P_f = M\xi - Ce \tag{48}$$

which when evaluated at the boundary yields

$$\begin{aligned}K_f\ell_i[B_i+B_r] = {} & A_1\ell_1(C-m_1M) + A_2\ell_2(C-m_2M) + A_1'\ell_1(C-m_1M) \\ & + A_2'\ell_2(C-m_2M).\end{aligned} \tag{49}$$

The continuity of total normal stress, τ_{zz}, is the third boundary condition and upon substitution yields the following at z = 0,

$$\begin{aligned}K_f\ell_i(B_i+B_r) = {} & A_1\ell_1[H-m_1C-2\mu\sin^2\theta_1] + A_2\ell_2[H-m_2C-2\mu\sin^2\theta_2] \\ & + A_1'\ell_1[H-m_1C-2\mu\sin^2\theta_1] + A_2'\ell_2[H-m_2C-2\mu\sin^2\theta_2] \\ & + 2E\mu\ell_3\sin\theta_3\cos\theta_3 + 2E'\mu\ell_3\sin\theta_3\cos\theta_3.\end{aligned} \tag{50}$$

In the fluid, τ_{zz} was set equal to the negative of the pressure. The last boundary condition to be evaluated at the upper interface is continuity of tangential stress,

$$\tau_{zx} = \frac{1}{2}\mu\left(\frac{\partial u_x}{\partial z} + \frac{\partial u_z}{\partial x}\right) \tag{51}$$

The fluid is assumed not to support any shears and thus τ_{zx} in the fluid was set equal to zero. This boundary condition results in

$$\begin{aligned} 0 = {} & 2A_1\ell_1\sin\theta_1\cos\theta_1 + 2A_2\ell_2\sin\theta_2\cos\theta_2 \\ & - 2A_1'\ell_1\sin\theta_1\cos\theta_1 - 2A_1'\ell_2\sin\theta_2\cos\theta_2 \\ & - E\ell_3(\cos^2\theta_3 - \sin^2\theta_3) + E'\ell_3(\cos^2\theta_3 - \sin^2\theta_3). \end{aligned} \tag{52}$$

Next, the five boundary conditions at the lower interface are evaluated. The fifth boundary condition is continuity of normal frame velocity,

$$\bar{\dot{u}}_\perp = \dot{u}_\perp. \tag{53}$$

Substitution of the plane waves at the lower interface yields

$$\begin{aligned} & u_1\cos\theta_1 + u_2\cos\theta_2 - u_1'\cos\theta_1 - u_2'\cos\theta_2 + u_3\sin\theta_3 \\ & \qquad - u_3'\sin\theta_3 = u_t^c\cos\theta_5 + u_t^s\sin\theta_4 \end{aligned} \tag{54}$$

After setting z = d in this expression, Snell's law is again verified and equation (54) may be written as

$$\begin{aligned} & A_1\cos\theta_1\exp[i\ell_1\cos\theta_2 d] + A_2\cos\theta_2\exp[i\ell_2\cos\theta_2 d] \\ & \quad - A_1'\cos\theta_1\exp[-i\ell_1\cos\theta_1 d] - A_2'\cos\theta_2\exp[i\ell_2\cos\theta_1 d] \\ & \quad + E\sin\theta_3\exp[i\ell_3\cos\theta_3 d] - E'\sin\theta_3\exp[-i\ell_3\cos\theta_3 d] \\ & \quad = A_5\cos\theta_5\exp[i\ell_5\cos\theta_5 d] + E_t\sin\theta_4\exp[i\ell_4\sin\theta_4 d]. \end{aligned} \tag{55}$$

The sixth boundary condition is continuity of tangential frame velocity,

$$\bar{\dot{u}}_t = \dot{u}_t. \tag{56}$$

This boundary condition yields

$$\begin{aligned} & u_1\sin\theta_1 + u_2\sin\theta_2 + u_1'\sin\theta_2 + u_2'\sin\theta_2 - u_3\cos\theta_3 - u_3'\cos\theta_3 \\ & \qquad = u_t^c\sin\theta_5 - u_t^s\cos\theta_4 \end{aligned} \tag{57}$$

and at z = d reduces to

$$A_1\sin\theta_1\exp[i\ell_1\cos\theta_1 d] + A_2\sin\theta_2\exp[i\ell_2\cos\theta_2 d]$$
$$+ A_1'\sin\theta_1\exp[-i\ell_1\cos\theta_1 d] + A_2'\sin\theta_2\exp[-i\ell_2\cos\theta_2 d]$$
$$- E\cos\theta_3\exp[i\ell_3\cos\theta_3 d] - E'\cos\theta_3\exp[-i\ell_3\cos\theta_3 d]$$
$$= A_t\sin\theta_5\exp[i\ell_5\cos\theta_5 d] - E_t\cos\theta_4\exp[i\ell_4\cos\theta_4 d]. \quad (58)$$

The seventh boundary condition is continuity of normal fluid velocity, however, since the fluid cannot penetrate the lower medium, the normal fluid velocity must go to zero at the boundary, $\dot{w}_\perp = 0$. Substitution in this expression yields

$$w_1\cos\theta_1 + w_2\cos\theta_2 - w_1'\cos\theta_1 - w_2'\cos\theta_2 = 0. \quad (59)$$

Using the relation between the relative wave amplitude and the matrix wave amplitude, equation (59) can be written as, at z = d,

$$A_1 m_1\cos\theta_1\exp[i\ell_1\cos\theta_1 d] + A_2 m_2\cos\theta_2\exp[i\ell_2\cos\theta_2 d]$$
$$- A_1' m_1\cos\theta_1\exp[-i\ell_1\cos\theta_1 d] - A_2' m_2\cos\theta_2\exp[-i\ell_2\cos\theta_2 d] = 0. \quad (60)$$

Continuity of normal stress, τ_{zz}, is the eighth boundary condition and it yields, at z = d,

$$A_1\ell_1[H - m_1 C - 2\mu\sin^2\theta_1]\exp(i\ell_1\cos\theta_1 d)$$
$$+ A_2\ell_2[H - m_2 C - 2\mu\sin^2\theta_2]\exp(i\ell_2\cos\theta_2 d)$$
$$+ A_1'\ell_1[H - m_1 C - 2\mu\sin^2\theta_1]\exp(-i\ell_1\cos\theta_1 d)$$
$$+ A_2'\ell_2[H - m_1 C - 2\mu\sin^2\theta_1]\exp(-i\ell_2\cos\theta_2 d)$$
$$+ 2\mu\ell_3 E\sin\theta_3\cos\theta_3\exp(i\ell_3\cos\theta_3 d)$$
$$+ 2\mu\ell_3 E'\sin\theta_3\cos\theta_3\exp(-i\ell_3\cos\theta_3 d)$$
$$= H' A_t\ell_5\exp[i\ell_5\cos\theta_5 d] - 2\mu' A_t\ell_5\cos^2\theta_5\exp[i\ell_5\cos\theta_5 d]$$
$$- 2\mu' E_t\ell_4\sin\theta_4\cos\theta_4\exp[i\ell_4\cos\theta_4 d], \quad (61)$$

where H' and μ' are elastic constants in the clay. The last boundary condition is continuity of tangential stress, $\tau_{zx} = \tau_{zx}$. Substitution in this expression yields, at z=d,

$$
\begin{aligned}
&2\mu A_1 \ell_1 \sin\theta_1 \cos\theta_1 \exp(i\ell_1 \cos\theta_1 d) \\
&\quad + 2\mu A_2 \ell_2 \sin\theta_2 \cos\theta_2 \exp(i\ell_2 \cos\theta_2 d) \\
&\quad - 2\mu A_1' \ell_1 \sin\theta_2 \cos\theta_1 \exp(-i\ell_1 \cos\theta_1 d) \\
&\quad - 2\mu A_2' \ell_2 \sin\theta_2 \cos\theta_2 \exp(-i\ell_2 \cos\theta_2 d) \\
&\quad - E\mu\ell_3(\cos^2\theta_3 - \sin^2\theta_3)\exp(i\ell_3 \cos\theta_3 d) \\
&\quad + E'\mu\ell_3(\cos^2\theta_3 - \sin^2\theta_3)\exp(-i\ell_3 \cos\theta_3 d) \\
&\quad = 2A_t \mu' \ell_5 \sin\theta_5 \cos\theta_5 \exp(i\ell_5 \cos\theta_5 d) \\
&\quad - E_t \mu' \ell_4(\cos^2\theta_4 - \sin^2\theta_4)\exp(i\ell_4 \cos\theta_4 d). \qquad (62)
\end{aligned}
$$

These nine boundary condition equations can be solved simultaneously to determine the amplitudes of the allowed types of wave motion relative to the incident wave amplitude. From these amplitudes, the acoustic propagation coefficients of the porous medium as well as the surface impedance and transfer functions for the upper boundary can be found. The routine, Ampl.Fortran, used to determine those amplitudes calls an IMSL subroutine. The main routine is included in Appendix A.2.

Measurable Quantities

Predictions of seismic/acoustic coupling in the field should, when possible, rely only upon quantities measurable in the field. Measurements of jacketed and unjacketed bulk moduli[14] are interesting in the laboratory but not practical in the field. One goal of this study was to determine which quantities must be measured in order to predict seimic/acoustic coupling.

Acoustic measurements outdoors usually require that the acoustic impedance of the surface be known. Several techniques have been developed for

this purpose. It has been found, that for many surfaces, the acoustic impedance can be computed from the flow resistance. The flow resistance can be readily measured in the field or estimated by an on-site evaluation of the surface. During the course of these measurements, the ability to measure the attenuation of the acoustic wave with depth in the soil using a buried microphone was developed. The acoustic attenuation in the soil is, typically, easier to measure than the acoustic impedance yet, as will be shown later, carries the same information about the surface. The response of a buried geophone to an airborne acoustic wave and to seismic disturbances can be measured in the field. By comparing the geophone or probe microphone signal to the signal from a microphone above the surface, one can determine the transfer function for the boundary. Finally, by mechanically disturbing the surface, the seismic velocities can be measured as well as layer depths.

Of those quantities underlined above, flow resistance, seismic velocities, and layer depths must be experimentally measured. Experimental measurements of these quantities will be described in the next chapter. The other quantities can, in principle, be computed from flow resistance, seismic velocities, layer depths, and tabulated physical properties of the soil. In the following, a description of the calculations of the other underlined quantities will be given using the Biot-Stoll Model.

Acoustic Impedance of the Surface

The normal specific acoustic impedance of a surface is the ratio of the acoustic pressure to the particle velocity at the surface divided by the acoustic resistance of air, $\rho_0 c_0$. This is a complex quantity and is expressed as

$$z = z_{real} + z_{imag}. \tag{63}$$

The surface pressure in terms of the incident and reflected wave amplitudes is

$$P_{surface}(\omega) = -iK_f\ell_i[B_i+B_r] \tag{64}$$

and the velocity at the surface is

$$V_{(surface)}(\omega) = -i\omega\cos\theta_i[B_i-B_r]. \tag{65}$$

The normal surface impedance is then

$$z = \frac{P}{V} = \frac{K_f\ell_i}{\omega_0\cos\theta_i}\frac{[B_r+B_i]}{[B_r-B_i]} \tag{66}$$

and

$$\frac{z}{z_{air}} = \frac{K_f}{\rho_0 c_0^2\cos\theta_i}\frac{[B_i+B_r]}{[B_i-B_r]}\ . \tag{67}$$

In Appendix A.3 is a subroutine, Sufimp.Fortran, used to calculate the surface impedance.

Acoustic Attenuation in the Soil

The acoustic attenuation coefficients of the porous medium are found by determining the magnitude of the acoustic pressure at two different depths below the surface. The acoustic pressure below the surface is the sum of the fluid pressure due to the fast and slow waves. Using the fast wave amplitude and equation (9), for example, the amplitude of the fast relative fluid displacement at a depth z is

$$P_{fast} = iA_1\ell_1(C-m_1M)\exp(i\ell_1\cos\theta_1 z). \tag{68}$$

Expression for the fluid pressure due to the other waves in the porous medium are

$$P_{slow} = iA_2\ell_2(C-m_2M)\exp(i\ell_2\cos\theta_2 z) \tag{69}$$

$$P'_{fast} = iA'_1\ell_1(C-m_1M)\exp(-i\ell_1\cos\theta_1 z) \tag{70}$$

$$P'_{slow} = iA'_1\ell_2(C-m_2M)\exp(-i\ell_2\cos\theta_2 z) \tag{71}$$

where again the prime indicates a wave reflected from the lower boundary. The total fluid pressure at a depth z below the surface is the sum of the pressure due to the relative fluid waves and is expressed as

$$P_{below}(\omega,z) = P_{fast} + P_{slow} + P'_{fast} + P'_{slow}. \tag{72}$$

The attenuation coefficient in dB per unit depth is then

$$\alpha = [\ell n|P_{below}(\omega,z)| - \ell n|P_{below}(\omega,z_2)|]\cdot \frac{20.0\log(e)}{(z_2-z_1)}. \tag{73}$$

This calculation is done in the routine Ampl.Fortran.

Transfer Function of the Boundary

In this section the acoustic and seismic transfer function for the air-soil interface will be determined. The acoustic transfer function is the ratio of the acoustic pressures below and above the surface. This is a complex quantity and expressions for both the magnitude and phase will be included. The acoustic pressure at a height z above the surface is due to the incident and reflected wave amplitudes and is expressed as

$$P_{above}(\omega,z) = P_{incident}(\omega,z) + P_{reflected}(\omega,z) \tag{74}$$

where

$$P_{incident}(\omega,z) = -iK_f\ell_i B_i\exp(i\ell_i\cos\theta_i z) \tag{75}$$

and

$$P_{reflected}(\omega,z) = -iK_f\ell_r B_r\exp(-i\ell_r\cos\theta_r z). \tag{76}$$

Using the expression for the acoustic pressure below the surface, equation (72), the acoustic transfer function is expressed as

$$T(\omega,z,z') = \frac{P_{below}(\omega,z)}{P_{above}(\omega,z')} \tag{77}$$

The seismic transfer function is the ratio of the seismic velocity response of the matrix below the boundary to the acoustic pressure above the boundary. The total velocity response of the matrix will be the vector sum of the frame velocity of each of the allowed matrix waves. However, the total normal velocity response of the matrix will be determined so that it can be later compared to experimental results. The total normal velocity, V_n, at a depth z below the surface is

$$\begin{aligned} V_n &= \dot{u}_{1\perp} + \dot{u}_{2\perp} + \dot{u}'_{1\perp} + \dot{u}'_{2\perp} + \dot{u}_{3\perp} + \dot{u}'_{3\perp} \\ V_n &= -i\omega A_1 \cos\theta_1 \exp(i\ell_1 \cos\theta_1 z) + i\omega A'_1 \cos\theta_1 \exp(-i\ell_1 \cos\theta_1 z) \\ &\quad - i\omega A_2 \cos\theta_2 \exp(i\ell_2 \cos\theta_2 z) + i\omega A'_2 \cos\theta_2 \exp(-i\ell_2 \cos\theta_2 z) \\ &\quad + i\omega E \sin\theta_3 \exp(i\ell_3 \cos\theta_3 z) + i\omega E' \sin\theta_3 \exp(-i\ell_3 \cos\theta_3 z). \end{aligned} \tag{78}$$

An expression for the seismic transfer function is

$$T(\omega,z,z') = \frac{V_n(\omega,z)}{P_{above}(\omega,z')}. \tag{79}$$

The radial transfer function as well as an air-clay transfer function is a simple extension of this work. Routines for calculating these transfer functions are included in Appendix A.4, A.5, and A.6.

3. EXPERIMENTAL MEASUREMENTS

During the course of this study, a variety of experimental measurements were performed to define the mechanism responsible for seismic/acoustic coupling and insure that this quantity is measured. The individual experiments along with data analysis procedures will be described in the following. In many cases, the experiments were designed to answer specific experimental questions. In those cases the results and conclusions will be presented with the experimental procedure. The major measurements were of the transfer function. Interpretation of those results will be described Chapter 5.

Preliminary Measurements

Considerable effort was expended to make certain the sound system was mechanically decoupled from the surface of the earth to eliminate direct mechanical transfer of energy. The speaker systems were either suspended from a large A frame using various elastic straps, or supported on the bed of a 3/4-ton truck which was placed on inflated rubber bags.

In order to measure the degree of isolation, two types of tests were conducted. Impulses on the side of the speaker cabinet were generated and the resulting acoustic and seismic waves measured using a collocated geophone and microphone. As isolation systems were applied the magnitude of the seismic signal was observed on the geophone. The microphone provided a time scale to permit separation of a seismic wave generated mechanically at the source and an acoustically coupled wave. In all cases it was possible to reduce the mechanical coupling below the ambient background seismic noise level. Geophone response to sweep tones generated by the speaker were also measured as the decoupling was applied. The effectiveness of the decoupling as a function of frequency was observed in this way. It was possible to ascertain that no specific resonances existed in the isolation

system which would selectively pass low frequency energy to the earth and geophone.

A geophone isolated from the ground and suspended in air would respond to airborne acoustic energy. Measurements were made to determine if acoustic waves could generate a geophone response when the geophone was placed in a variety of porous materials, but still isolated from the earth and seismic energy sources. The airborne sound produced a geophone response when the geophone was covered in isolated containers of plastic beads, of sands and gravels with a variety of porosities. The overall response of the geophone varied with the surrounding materials, but in each case the results could be explained in terms of a vibrating mass loaded system driven by the airborne acoustic energy. The data indicated no measureable contribution to geophone response due to motion of the geophone relative to the matrix material when driven in this isolated system.

Measurements of the Acoustic Wave in the Earth

The measurements of the sound pressure below the surface of the earth were made with a specially designed probe as shown in Figure 3.1. It consists of an AKG microphone and preamplifier housed in a cylindrical brass tube. The inner cylinders shown were used to increase the mass of the probe and to seal any possible air leaks. The nose cone contains small holes to allow the active element of the microphone to sense the acoustic field. A rubber membrane was stretched over the microphone elements to protect it from any particles that penetrate the nose cone when the probe was inserted in a predrilled hole. A comparison of the probe microphone response to a standard AKG microphone is shown in Figure 3.2. The frequency response for the probe is essentially flat to 3kHz where it begins to roll off to a new, less sensitive, plateau near 7kHz. The frequency response of the probe is essentially unchanged when the probe is

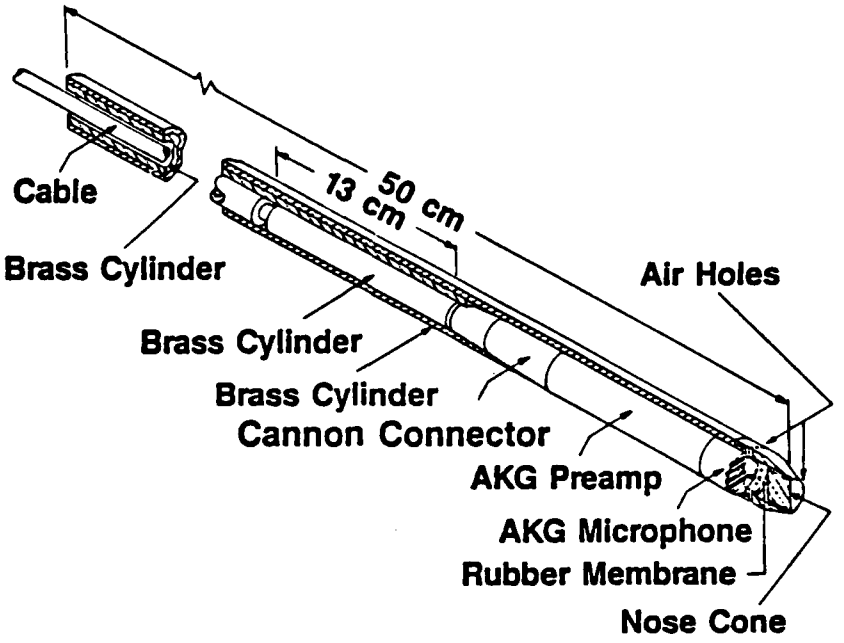

Figure 3.1. Specially designed probe microphone used to measure the acoustic sound field in the porous soil.

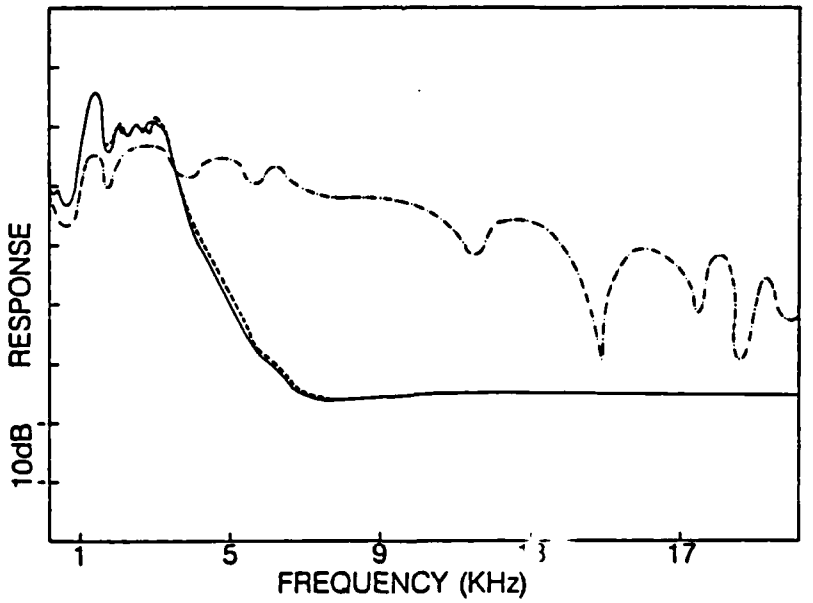

Figure 3.2. A comparison of probe microphone response (——) to a standard AKG microphone (– – –). Also shown is the response of the probe when pointed away from the sound source.

pointed away from the sound source, the normal geometry for measurements below the earth's surface.

Before the probe was inserted into the ground, a drill was used to bore a hole 1 inch in diameter to the desired depth. The probe was then forced into the hole and STP Oil Treatment was poured around the probe near ground level to further seal the probe entry. This procedure worked well giving reproducible results for sandy soil and loam. For clays, the soil in the vicinity of the probe would quite often crack providing air paths not previously available. This cracking gave results which differed from one attempt to the next. It was generally assumed that the measurement giving the smallest sound pressure at the probe was best.

Occasionally, the holes in the tip of the probe became filled with dirt when the probe was inserted. This occurance could only be detected when the probe was removed and examined, so several data runs had to be rejected after the fact.

The results of an extensive series of probe microphone measurements are published in Reference 8. In subsequent measurements, the probe microphone output was recorded along with geophone response, but the microphone depth was not varied. Referring again to Figure 3.1, when the probe is inserted in the ground where the speed of sound is less than the speed in the air, the probe microphone response with frequency could be expected to differ. There is no clear theoretical relation to predict the microphone response when it is inserted into the earth since the surrounding medium is changed dramatically. One would expect, as a minimum, that the frequency at which the response begins to roll off should be related to the wavelength of sound in the pores which scales with wavelength. If the speed of sound in the pores is 10 m/sec, one would expect the microphone response to begin to roll off at about 100 Hz. This feature of the data will be demonstrated below.

The speed of sound in the pores was measured in a hemispherical dish formed in the ground with a radius of 0.5 m and filled with sand with a measured flow resistivity of 85 rayls/cm. Figure 3.3 shows the relative

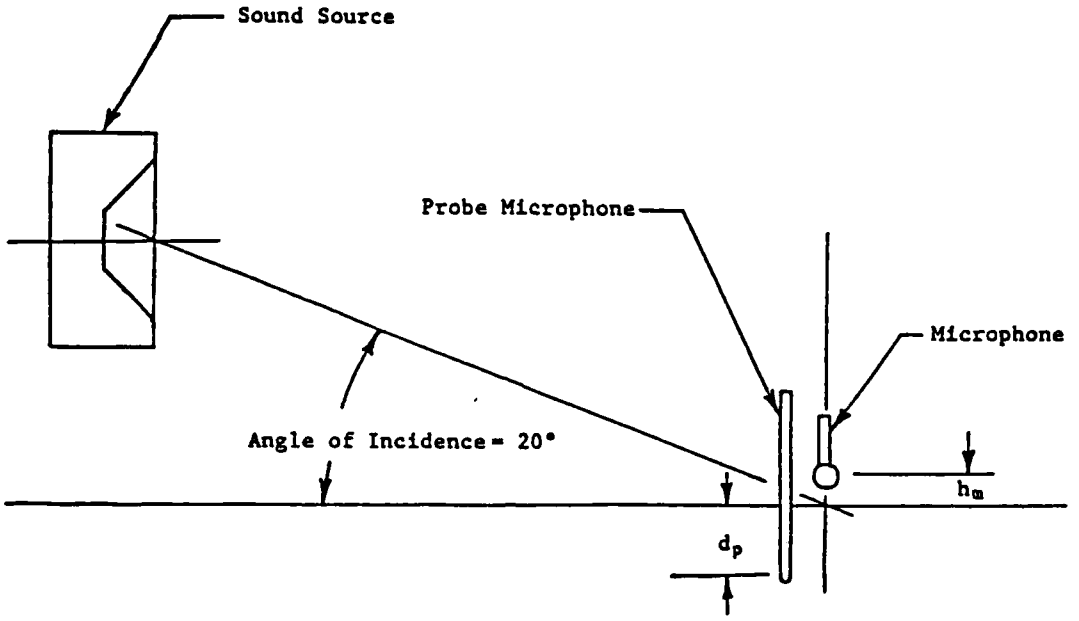

Figure 3.3. Relative positions of the sound source and sensors used to measure acoustic phase velocity and attenuation.

positions of the source and sensors used in the experiment. A reference AKG microphone was positioned approximately 5 cm above the sand and the probe microphone inserted to an approximate depth of five cm. A 50 Hz acoustic tone was broadcast at an angle of incidence of approximately 20^{o} from the horizontal. The relative delay between the probe and reference microphone was recorded using a Nicolet 3091 digital oscilloscope. Next, the probe was pushed 2.0 cm further down in the sand and the relative delay again recorded. The sound speed in the pores is the ratio of the change in the probe depth to the change in the phase. The probe was pushed down in 2.0 cm increments to a depth of 11 cm and the phase difference recorded at each probe position. This experiment was repeated at several frequencies between 50 Hz and 500 Hz. Results of the average phase speed in the pores

are plotted in Fig. 3.4. The attenuation of the acoustic wave was measured in the same sand using sweep tones, results are shown in Figure 3.5. The solid line was calculated using equation (73).

Measurements of the Transfer Function

Experimental Configuration

The experimental data were collected at two different locations, the UM test field and Sardis beach. The UM test field is two miles south of Oxford, MS and a map showing the field size, relative elevations and tree lines is included in appendix C.1. Sardis beach is located at John W. Kyle state park which is located approximately ten miles west of Oxford and a map of the park is included in appendix C.2. Several experiments were performed at each site in order to characterize the physical properties necessary for theoretical calculations.

The flow resistivity was measured using an apparatus described by Leonard[15]. A cylindrical sample of earth was taken from the ground and the rate of air flow through the sample was measured as a function of differential pressure across the sample. Measurements of flow resistance were made of each soil sample using at least three differential pressures across the sample . Consistency of these results were always within 5%. However, it was found that there were inconsistencies in the measured flow resistances from multiple samples from the same site. Values of flow resistance varied as much as a factor of two at the UM test field, however, in sand these measurements were always within 10%. It was assumed that these discrepencies occured because of variations in soil structure in the 10cm diameter plugs extracted for measurements and the effects of disturbing the soil. Results of these measurements are shown in Table 1. The density of the

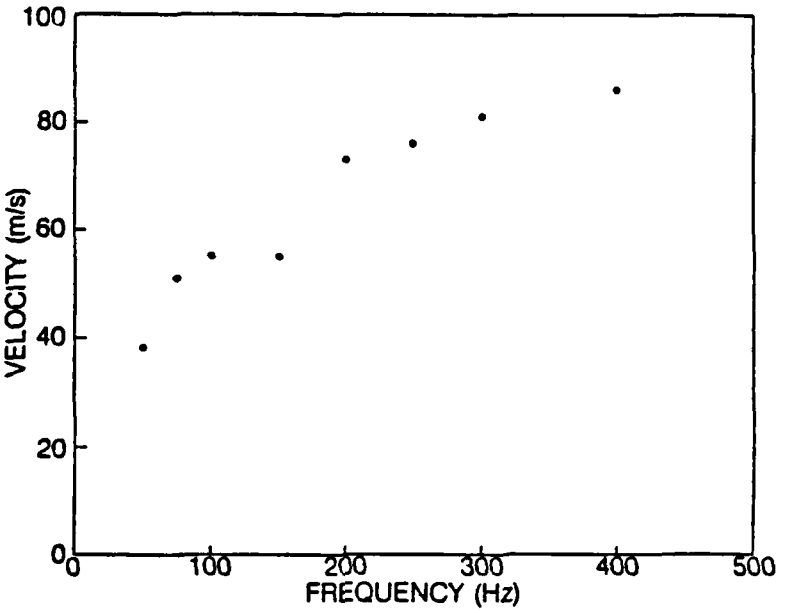

Figure 3.4. Acoustic phase velocity measured with the probe microphone in a sand with a flow resistivity of 85 rays/cm.

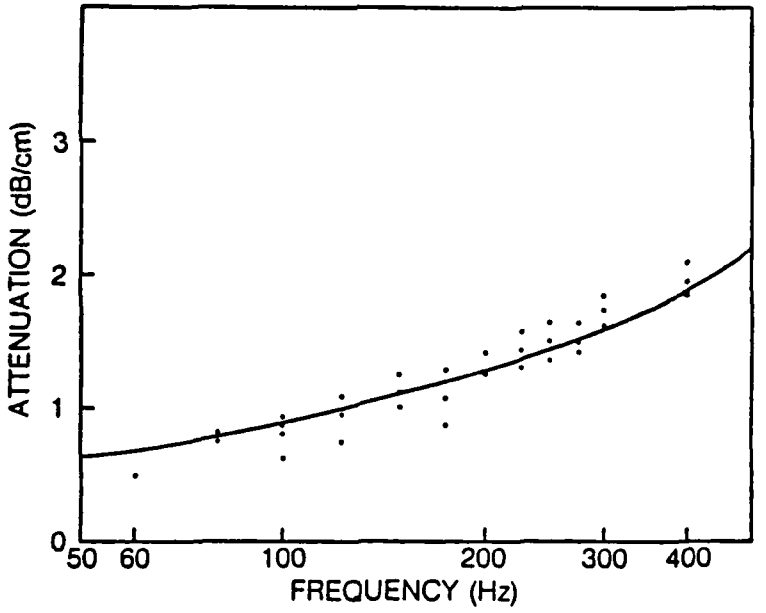

Figure 3.5. The acoustic attenuation measured with the probe microphone. The solid line was calculated using equation 73.

TABLE 1

Measured Values of Flow Resistance

Site	Average (rayls/cm)
Sardis	350
UM Test Field	550 to 1050

nonporous lower layer material at the UM test field was determined from a sample of clay extracted from approximately 0.5 meters below the surface. At Sardis beach, the density of the clay underlying the sand was assumed to be the same as at the UM test field, which was found to be $2.65 g/cm^3$.

The shear and compressional wave speeds and the depth of the porous material were determined from a ray propagation model[16] for a two layer system, see Figure 3.6. An impulse is created at x_0 by striking a metal block with a hammer. A seismic sensor is located at, say x_1 and is sensitive to both shear and compressional waves, and it is assumed that there are three possible paths to the sensor. Path one is along the surface at a wave speed of v_1 and is referred to as the direct path. The second path or reflected path is down towards the lower boundary and reflected in accordance with Snell's law. The third, the refracted path, is down towards the lower boundary, along the surface of the lower medium at a speed v_2 then back towards the upper boundary. When the seismic sensor is close to the source compared to the layer depth, the first arrival will be the direct pulse. As the seismic sensor is moved away from the source and the separation distance becomes greater than twice the layer depth, the first arrival will be the refracted pulse. A plot of arrival times versus source detector separation distance for the UM test field is plotted in Figure 3.7 and the wave velocities are the slopes of the lines drawn. From the geometry of the model, the layer depth can be expressed as

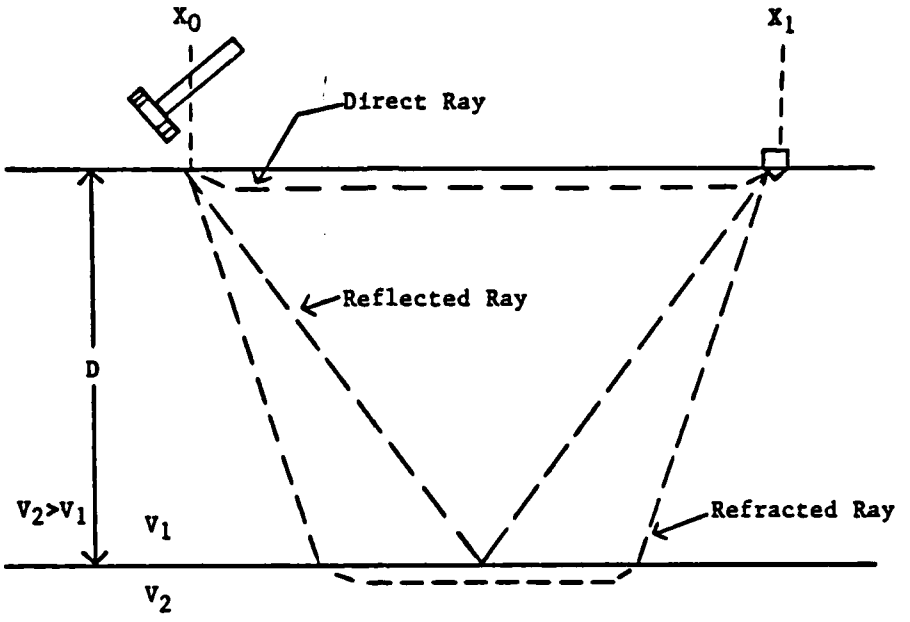

Figure 3.6. Ray propagation model used to calculate the layer depths at experimental sites.

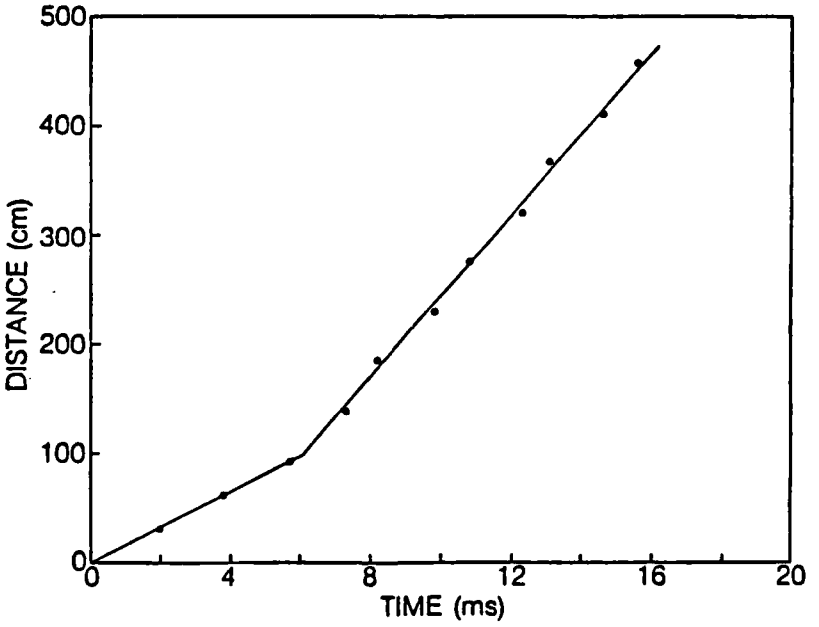

Figure 3.7. A plot of arrival times versus geophone position at the UM test field. The layer velocities are the slopes of the straight lines drawn.

$$d = \frac{x_c}{2} \frac{(V_1-V_2)}{(V_1+V_2)} \tag{80}$$

where x_c is the location of the intersection of the lines on the time-position graph. Physically, x_c is the distance from the source to the point at which the refracted pulse arrives at the same time as the direct pulse. The results of the wave speeds and the layer depths for both sites are recorded in Table 2.

TABLE 2

Seismic Wave Velocities (cm/s)

Layer depth (cm)

Sardis Beach

First Layer			Second Layer	
Compressional	Shear	Layer Depth	Compressional	Shear
1.6×10^4	1.5×10^4	26	4.6×10^4	2.6×10^4

UM Test Field

First Layer			Second Layer	
Compressional	Shear	Layer Depth	Compressional	Shear
1.6×10^4	$.95 \times 10^4$	30	3.7×10^4	2.2×10^4

Sources and Sensors

The sound source used to broadcast acoustic signals was constructed at the University of Mississippi Physics Department and a diagram of the speaker system is shown in Figure 3.8. The outer most material is 1/2 inch particle board which was nailed and glued to an internal framework constructed from two inch by two inch lumber. The speaker system consists of four independent vented boxes of which each has an internal volume of 725 liters and are each tuned to 20 hertz with a four inch diameter by six

inch depth cylindrical port. On the front face of each box is a modified Peavy 18 inch Black Widow driver. The speaker system was driven by two ADS Power Plate 100 watt amplifiers and was mounted on a truck so that it would be made mobile for field use.

A Hall Engineering acoustic signal generator was used to record two minute segments of pink noise at each one of the third octave bands from 25 Hz to 500 HZ. In the field experiments, this tape was broadcast using a Nakamichi 550 tape player. A block diagram of the acoustic broadcasting network is shown in Figure 3.9.

The seismic sensor used was a commercially available Mark Products L-4-3-D triaxial geophone. This geophone contains three coils which are sensitive to motion in the transverse, radial and vertical directions. A calibration factor supplied by the manufacturer enables the determination of the seismic velocity from the signal voltage. The calibration factor was 1.0 mV = 3.57×10^{-4} cm/sec. Using an auger, a cylindrical hole was dug slightly larger than the diameter of the geophone. The geophone was then placed in the hole, leveled, and then covered with the soil or sand that had been removed. In the transfer function experiment the geophones were buried to depths such that the top surface of the geophone was either 5 or 25 cm below the ground.

The probe microphone was of our own design and a cut-away view of the instrument is shown in Figure 3.1. At the UM test site the probe depth was 8cm and at Sardis beach the depth was 12cm. A reference AkG microphone, identical to the one in the probe, was positioned approximately 5 cm above the surface of the ground.

Figure 3.10 shows the relative positions of the sensors and sound source. Four different angles of incidence, in increments of 5°, were used during the experiment. At the largest angle, 20°, the separation distance between the source and sensors was 5.5 m while at the smallest incident

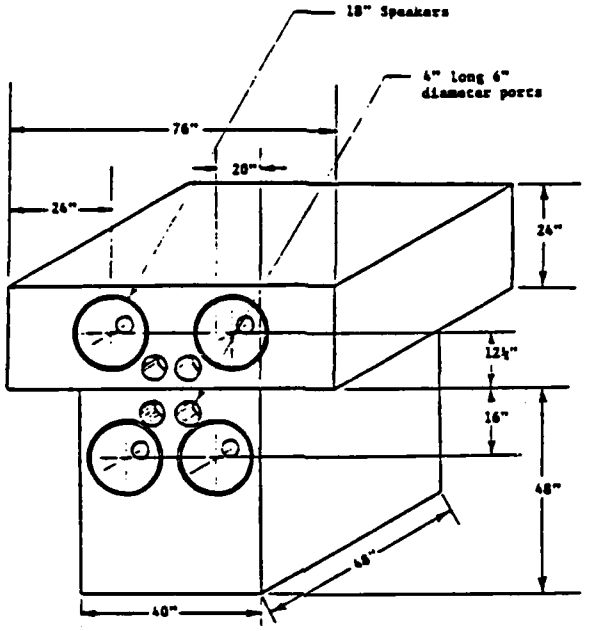

Figure 3.8. Speaker system built at the University of Mississippi Physics Department and used as a sound source in outdoor sound propagation measurements.

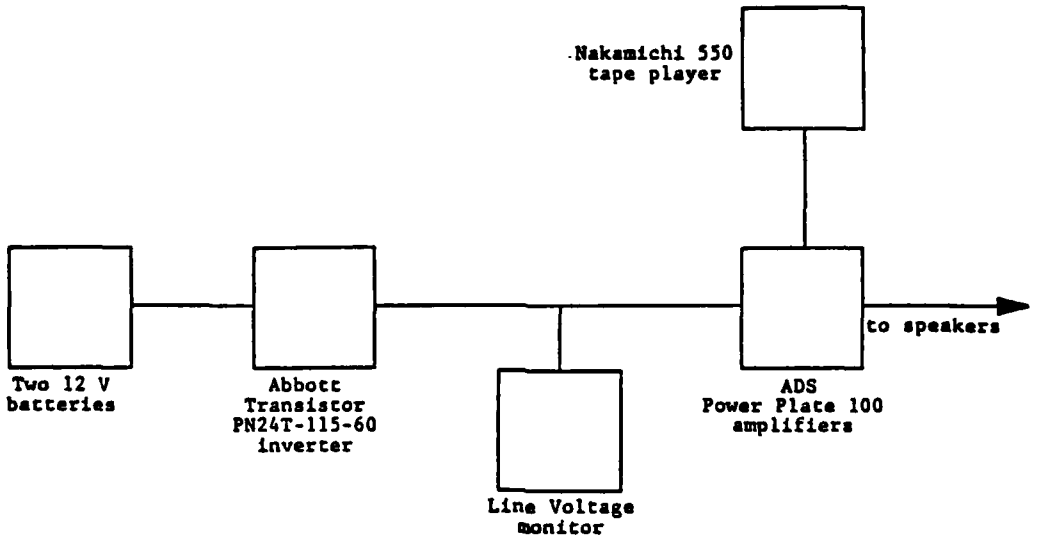

Figure 3.9. Block diagram of the acoustic broadcasting network used at experimental sites.

angle it was 23 m. The angle of incidence was changed by repositioning the truck upon which the speakers were mounted.

Each of the electronic signals from the sensors were amplfied with a Tektronix AM 502 differential amplifier and then recorded on a Teac R-81 seven channel FM cassette recorder. A block diagram of the data recording system is shown in Figure 3.11. The amplifier gains were adjusted such that the most intense sound level broadcast did not overload the amplifiers. The gains of each of the coils of the geophone and the microphones along with the recorder channel assignments are in Table 3. The output voltage of

TABLE 3

UM Test Field

CH	SENSOR	GAIN
1	Vertical Triax	500
2	Longitudinal Triax	500
3	Transverse Triax	500
5	Above Ground Microphone	100
6	Probe Microphone	5000
7	Voice Memo & DC Trigger	

Sardis

CH	SENSOR	GAIN
1	Vertical Traix	500
2	Transverse Triax	500
3	Longitudinal Triax	500
5	Above Ground Microphone	100
6	Probe Microphone	500
7	Voice Memo & DC Trigger	

each amplifier was five volts and that was the maximum input voltage of the tape recorder, thus allowing the maximum dynamic range of the recorder, 40 dB, to be used. After the gains were set, a General Radio model 1986 sound level calibrator was used to record a 94 dB calibration tone on the reference microphone. The output voltage of this reference microphone was measured and then temporarily connected to each input of the geophone

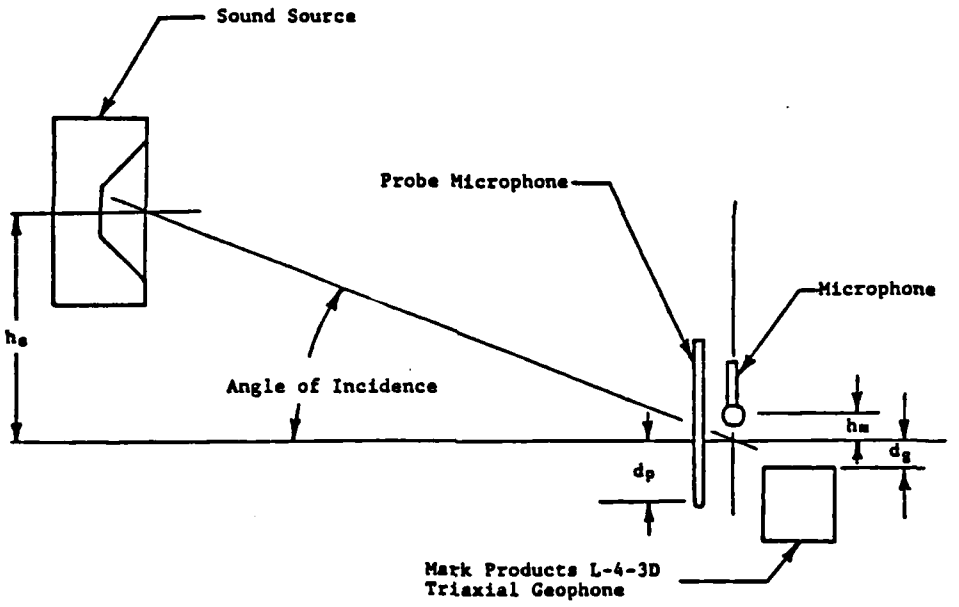

Figure 3.10. Diagram of source and sensor geometry indicating source height h_s, reference microphone position h_m, probe depth d_p and geophone depth d_g.

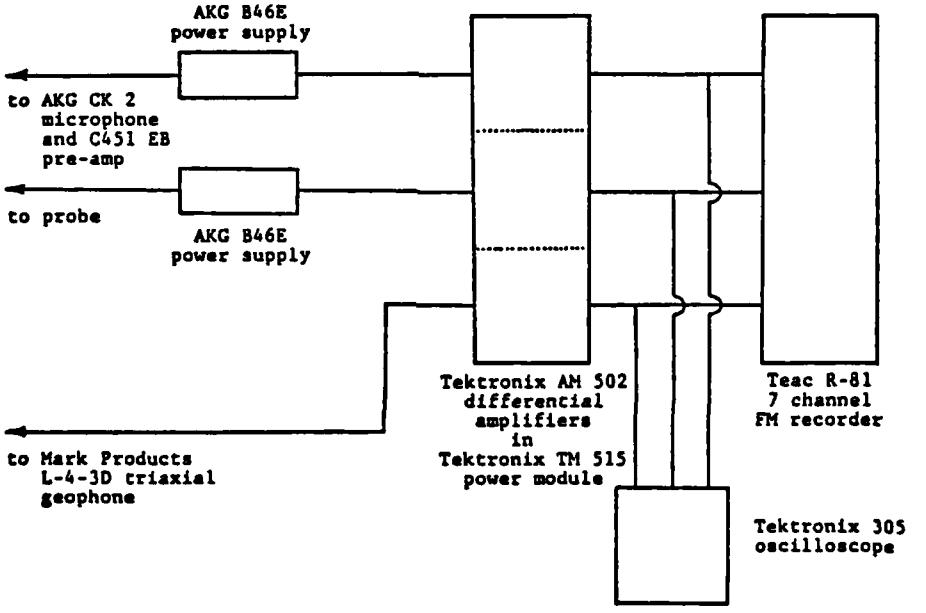

Figure 3.11. Data recording system used in the measurements of the transfer functions.

signal amplifiers, thus recording a calibration voltage for the seismic sensors. This procedure for calibration tones was repeated after the experiment was complete. Once the initial calibration tones were recorded, the test tape containing one-third octave bands of pink noise was broadcast. The geophone, probe and reference microphone responses were recorded on the assigned tape recorder channels. A five second 1.5 volt d.c. pulse was also recorded on its assigned channel (see Table 3) at the beginning of the broadcast of each one 1/3 octave band. This pulse was used as a trigger when the data were digitized. After the last 1/3 octave band was broadcast, the source tape was rewound, the truck repositioned and the broadcast repeated. This proceedure was repeated at each of the remaining incident angles.

4. DATA ANALYSIS

The primary quantity of interest in this study was the transfer function defined by

$$T(f) = \frac{\text{Signal Below the Surface (Complex)}}{\text{Sound Pressure Above the Surface (Complex)}}.$$

The transfer function, T(f), is a complex quantity which can be expressed in terms of a magnitude and phase. The data analysis procedure was designed to extract, from the FM tape records made in the field, this magnitude and phase.

Since we are concerned with the absolute magnitude of the transfer function, the first step in the analysis was to determine calibration levels of the two channels to be compared. Calibration tones were generated for each data channel used (except the probe microphone see experimental procedures). With the geophone and calibration levels used, a 1 bar acoustic sound pressure level and a geophone velocity of 1.754×10^{-4} cm/sec produced equal voltage levels at the input to the FM recorder.

The field records were digitized using a PDP 11/23 contolled A/D converter digitizing at 1000 Hz. No anti-aliasing filter was used. We assumed that the electronic and geophone frequency roll was sufficient to prevent aliasing.

The program used to analyze the data, called Tranff.Bas, is attached as Appendix A.7.

Representative results of the data analysis are given in Figures 4.1, 4.2, 4.3, and 4.4. The total amount of data precluded a complete presentation here but all data will be provided on request. A larger sample is included in Appendix B. Referring to Figure 4.2 note that the direction of phase change with frequency depends upon the sign convention chosen on

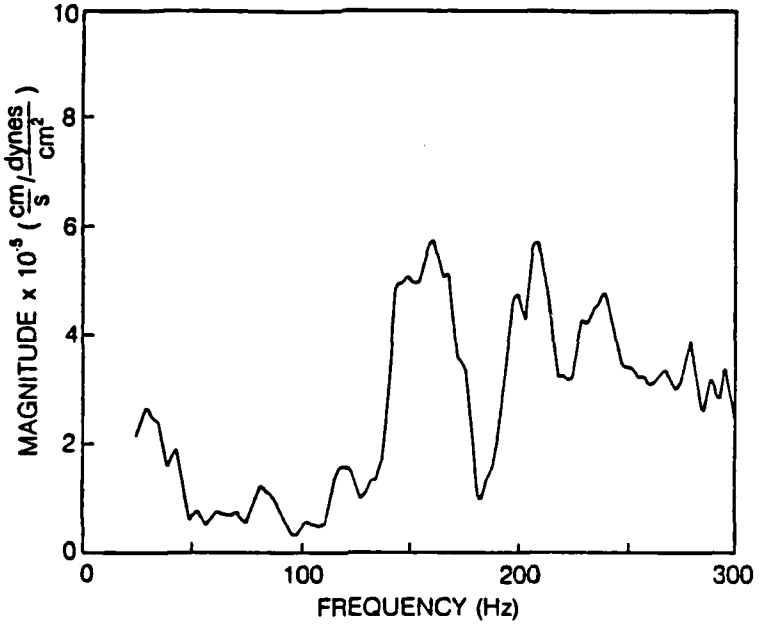

Figure 4.1. The experimental magnitude of the vertical seismic transfer function at a depth of 5cm and 20° angle of incidence at Sardis.

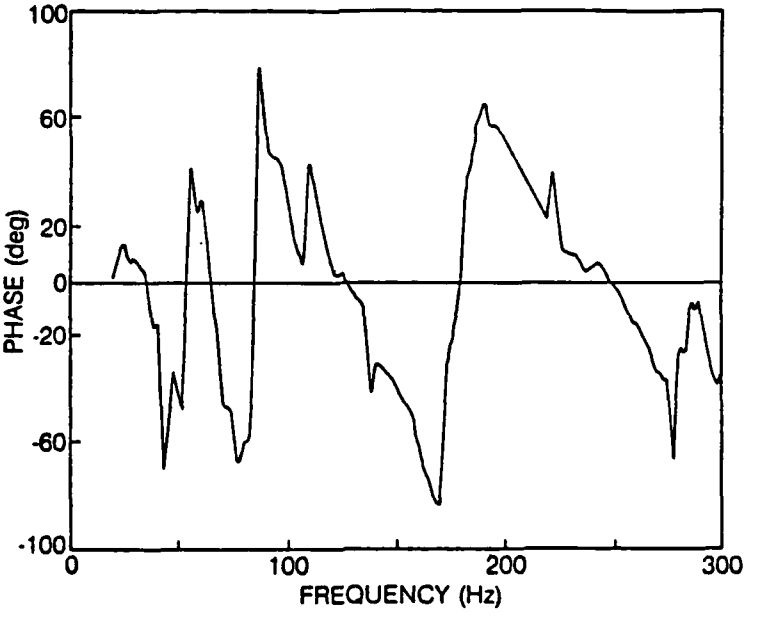

Figure 4.2. The experimental phase of the vertical seismic transfer function at a depth of 5cm and 10° angle of incidence for the UM test field.

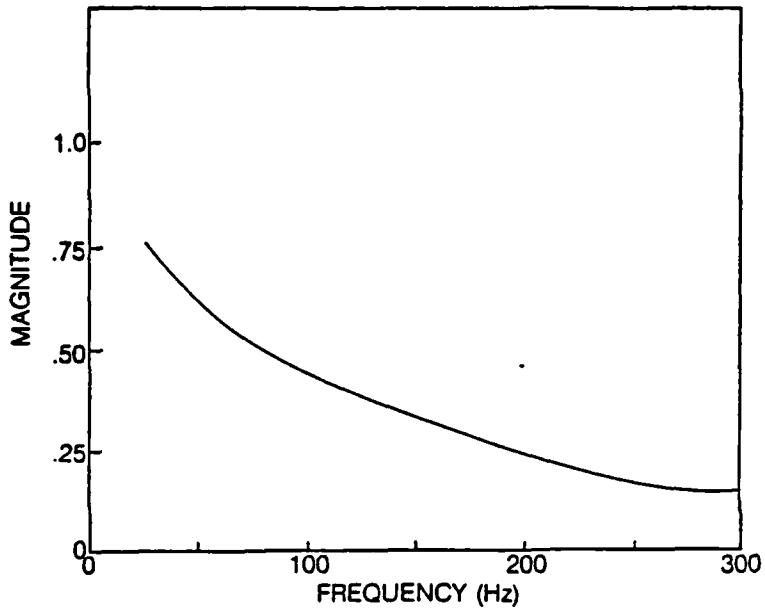

Figure 4.3. The experimental magnitude of the probe transfer function at a depth of 8cm and 20° angle of incidence for Sardis beach.

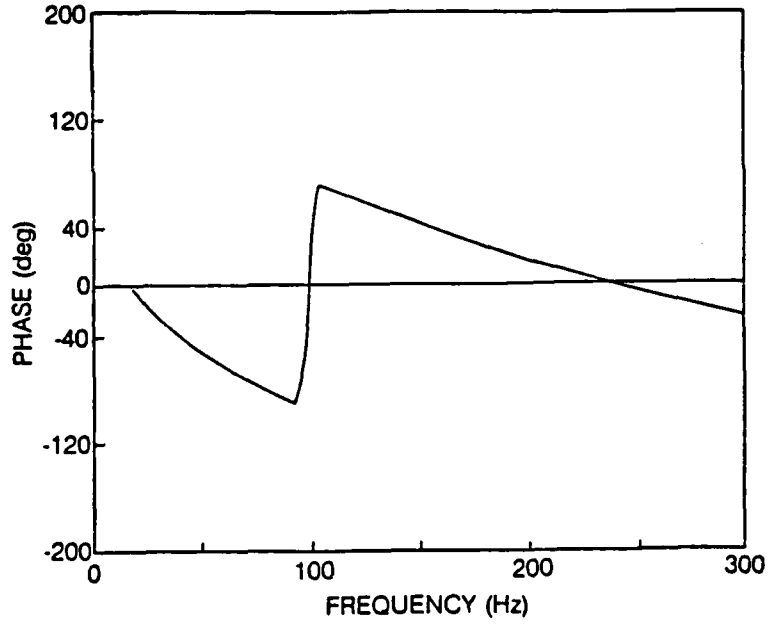

Figure 4.4. The experimental phase of the probe transfer function at a depth of 5cm and 15° angle of incidence for Sardis beach.

$\exp(i\omega t)$. Unfortunately, all data analysis was done independently of the theory development so the signs are reversed. In the data analysis program, the phase becomes more negative as the frequency increases (fixed path length difference, decreasing wavelength); in the theory program, this would result in a more positive phase. Also note, in figure 4.3 that the probe had no absolute calibration so we only measured the change in probe response as a function of frequency. For convenience in presentation, it was assumed that the probe microphone and the AKG microphone in the probe had the same sensitivity but this could be off by as much as a factor of two. Finally, note that all phases are limited between $\mp 90^{o}$ due to the ambiguity in the arctan routine. This accounts for occasional discontinuous jumps from -90^{o} to $+90^{o}$. In fact, the phase is smoothly varying at this point through an angle greater than -90^{o}.

Probe microphone data collected in the UM test field suffered from poor S/N due to the rapid attenuation of the sound field with depth at that site. The poor S/N ratio makes the phase measurements especially ragged through the trend is clear.

5. COMPARISON OF EXPERIMENTAL DATA TO THEORETICAL CALCULATION

This section provides a physical interpretation of selected experimental data and a comparison to theoretical predictions. The effects of the parameters which characterize the porous layer, viscosity, shape factor ratio, tortuosity, flow resistivity, porosity, angle of incidence, and layer depth, on the acoustic and seismic transfer functions are considered. Also, using measured values of flow resistivity, an acoustic surface impedance is calculated using a standared empirical form and compared to that which the Biot-Stoll Model (developed here) predicts and experiment.

Experimental Observations

At either depth at the UM test field, the phase of the seismic transfer function shows only a slight change when the incident angle is changed from 10^{o} to 20^{o} for frequencies above 100 Hz (See Figure 5.1 and 5.2). Similar observations can be made for the phase measurements at Sardis beach, but with less assurance due to the more rapid oscillation of the phase frequency (Figure 5.3 and 5.4). The phase of the seismic transfer function at the UM test field shows a $\frac{5}{2}\pi$ phase change over 300 Hz frequency range (Figure 5.1); at Sardis, for the same depth, there is a 3π to 4π phase change for the same frequency span (Figure 5.3). At a frequency of 100 Hz, there is approximately a 30^{o} phase difference between the 5 cm and 25 cm depths for the seismic transfer functions at the UM test field, (Figure 5.1 and 5.4) (angle of incidence 20^{o}) which would correspond to a seismic phase velocity of 2.4×10^{4} cm/s. Table 2 shows values of measured wave speeds near this value.

The magnitude of the seismic transfer function is insensitive to angle of incidence at both depths at each experimental site. However, the magnitude of the acoustic transfer function at Sardis at the 12 cm depth shows an increase with decreasing angle of incidence. At 100 Hz, there is a 40%

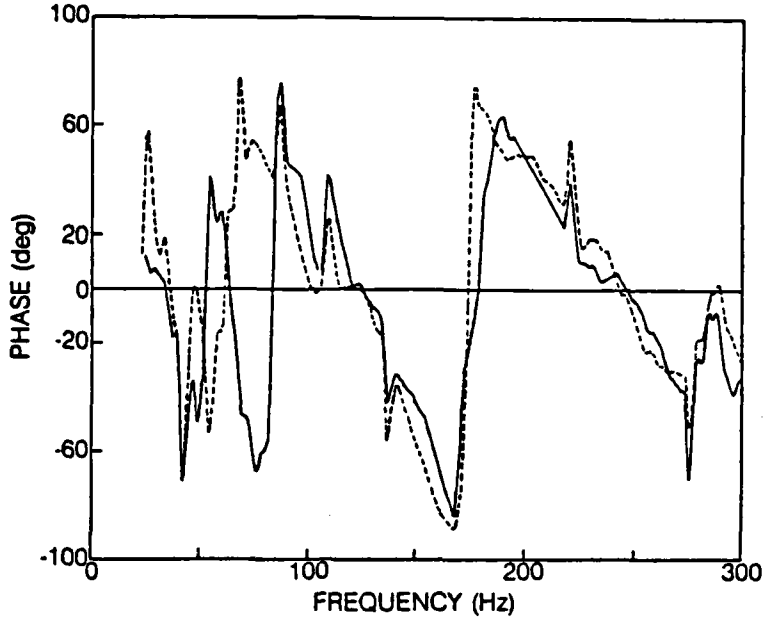

Figure 5.1. The phase of the experimental seismic transfer function at a 5cm depth at the UM test field for 10^{o} (——) and 20^{o} (---).

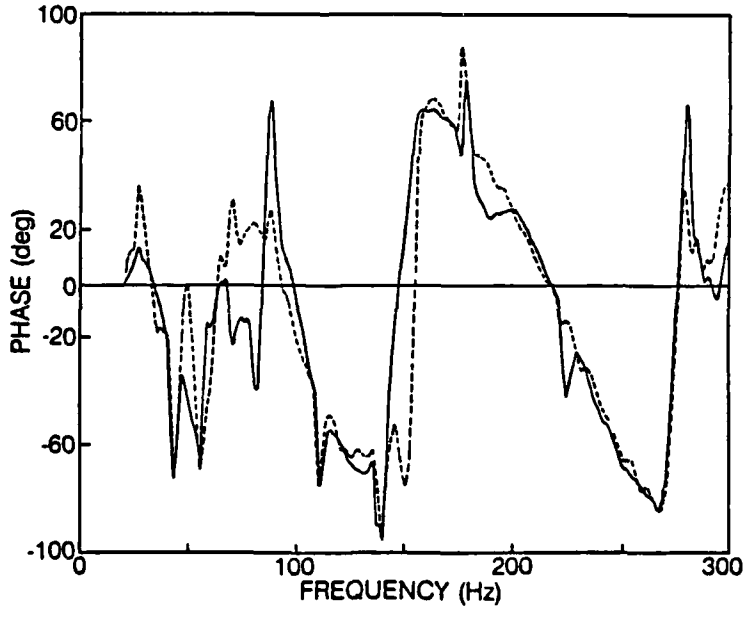

Figure 5.2. The phase of the experimental seismic transfer function at a 25cm depth at the UM test field for 10^{o} (——) and 20^{o} (---).

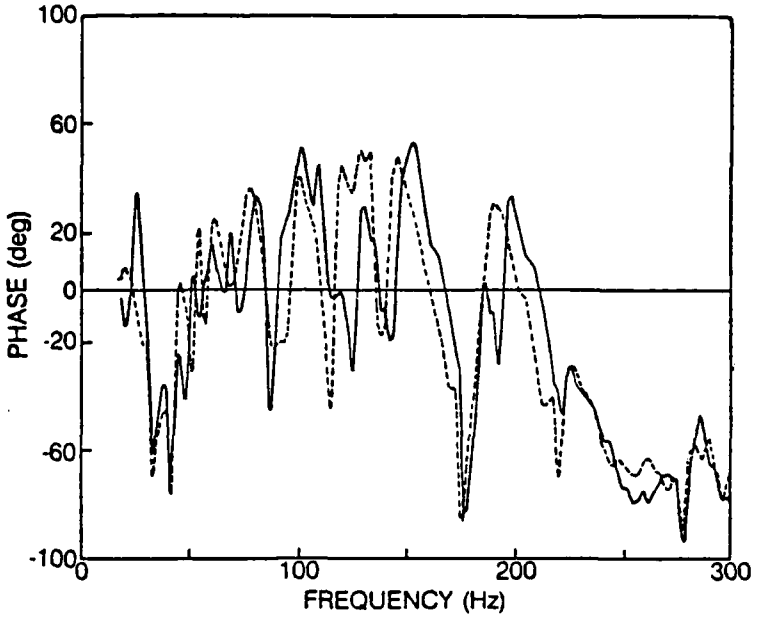

Figure 5.3. The phase of experimental seismic transfer function at a 5cm depth at Sardis beach for 10^{o} (——) and 20^{o} (— —).

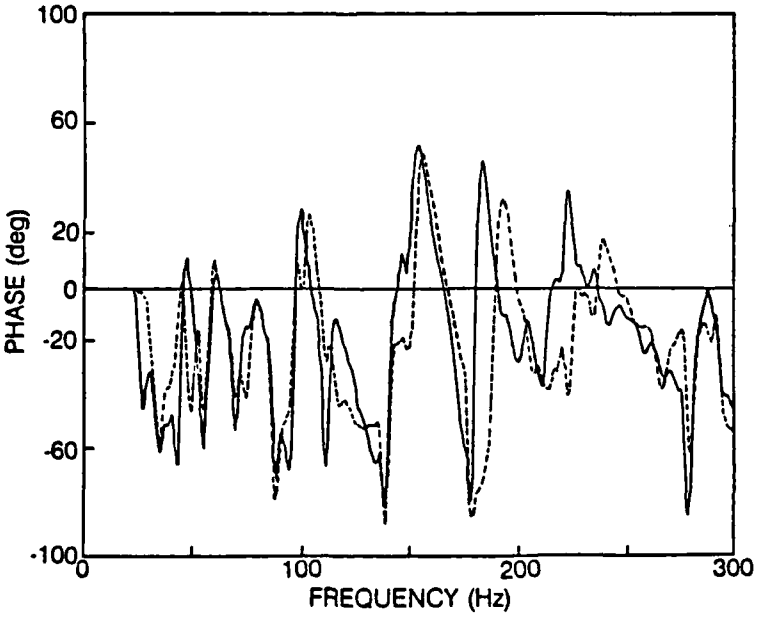

Figure 5.4. The phase of experimental transfer function at a 25cm depth at Sardis beach for 10^{o} (---) and 20^{o} (——).

increase in the magnitude when the angle of incidence is changed for 20° to 5°, (See Figure 5.5). This change is not observed at the UM test field.

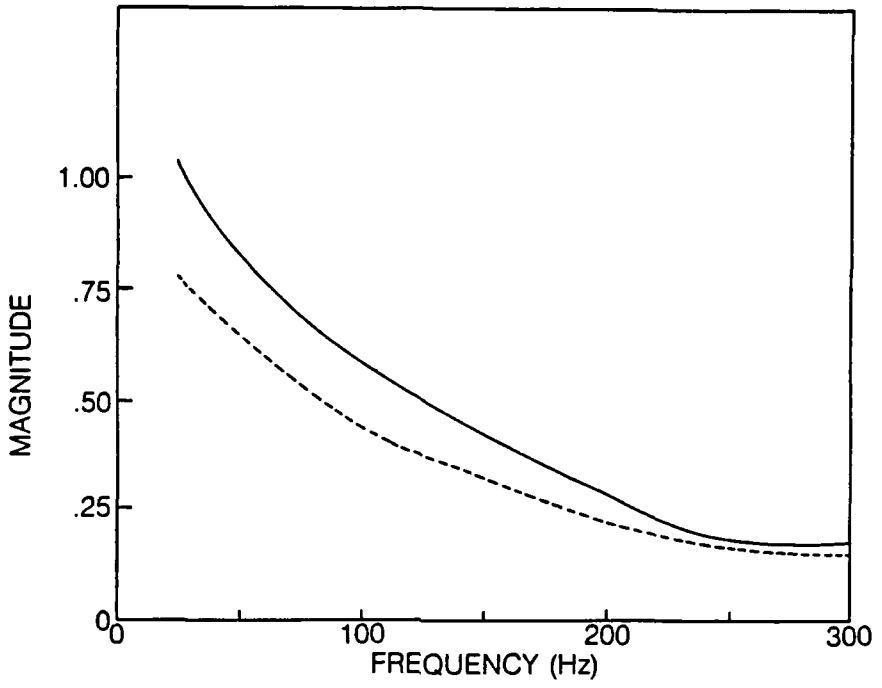

Figure 5.5. The magnitude of the experimental probe transfer function at 12cm at Sardis for 20° (——) and 5° (——).

The phase of the acoustic transfer function at Sardis is independent of angle of incidence. At the UM test field, the phase below 125 Hz is not affected by changes in the incident angle of incidence; above this frequency the S/N is so poor that a trend is not clear.

Sensitivity Analysis

In the field, only a finite number of surfaces can be studied. The theory developed in Chapter 2 can be used to determine the effects of the various physical properties required in the theory on the transfer functions.

Tortuosity and shape factor ratio have been shown by Attenborough[8] to effect attenuation of an acoustic wave in some soils and sands, however these effects were not observed in this study. For ranges of the shape

factor ratio, $0.4 \leq \frac{n}{\sqrt{s}} \leq 1.0$, or tortuosity, $1.0 \leq q \leq 4.0$, the acoustic or seismic transfer functions are changed by less than 2%. The magnitude of the transfer functions are also insensitive to changes in both dynamic and kinematic viscosities of air when changed by factors up to five. The flow resistance and porosity do have a significant effect on the transfer functions.

The effect of increasing the porosity from .3 to .5 on the magnitude of the seismic transfer function is shown in Figure 5.6. Increasing porosity results in an increase in the seismic transfer function; the magnitude of the acoustic transfer function decreases for the same increases in porosity as indicated in Figure 5.7. The increase in the seismic transfer function results from a decrease in the mass density of the frame. For the same amount of incident acoustic energy when more is coupled into the frame, less must be available as transmitted acoustic energy, consequently the acoustic transfer function decreases with the increase in porosity. In the real world, the porosity cannot change without changing the flow resistivity. The argument here is offered only to aid physical interpretation.

The effect of changing the flow resistivity from 60 rayls/cm to 420 rayls/cm to 3000 rayls/cm on the magnitude of the seismic transfer functions is shown in Figure 5.8. Figure 5.9 shows the magnitude of the acoustic transfer function for flow resistivities of 60 rayls/cm, 150 rayls/cm and 420 rayls/cm. The magnitude of the acoustic transfer function decreases as the flow resistivity is increased. The magnitude of the seismic transfer function decreases with increasing flow resistivity for frequencies above 130 Hz and increases at the lower frequencies. If the flow resistivity were to go to infinity, the magnitude of the acoustic transfer function would tend to zero because acoustic energy could not be transmitted across the boundary as the pore fluid could not move. The

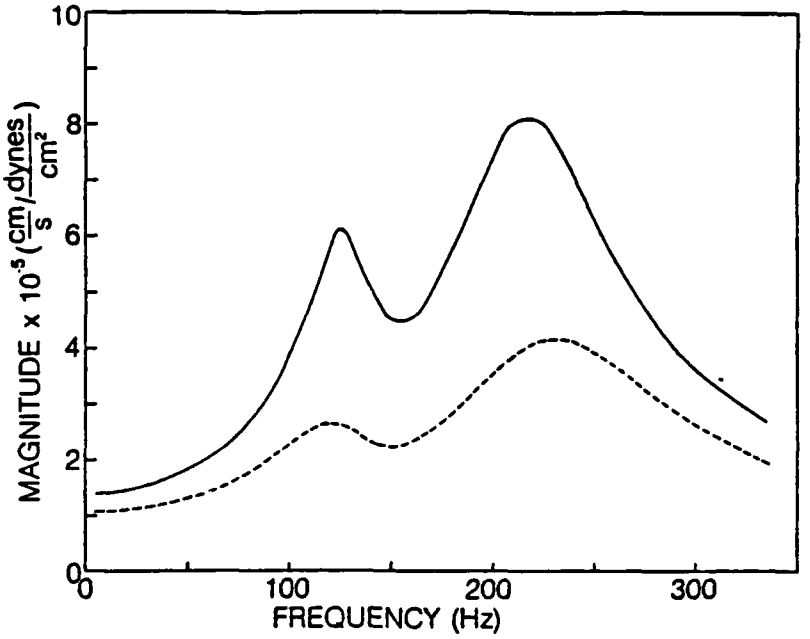

Figure 5.6. Magnitude of the calculated seismic transfer function for porosities of .3 (---) and .5 (——), 5 cm below the surface and 5° angle of incidence. All other parameters are set to values measured at Sardis.

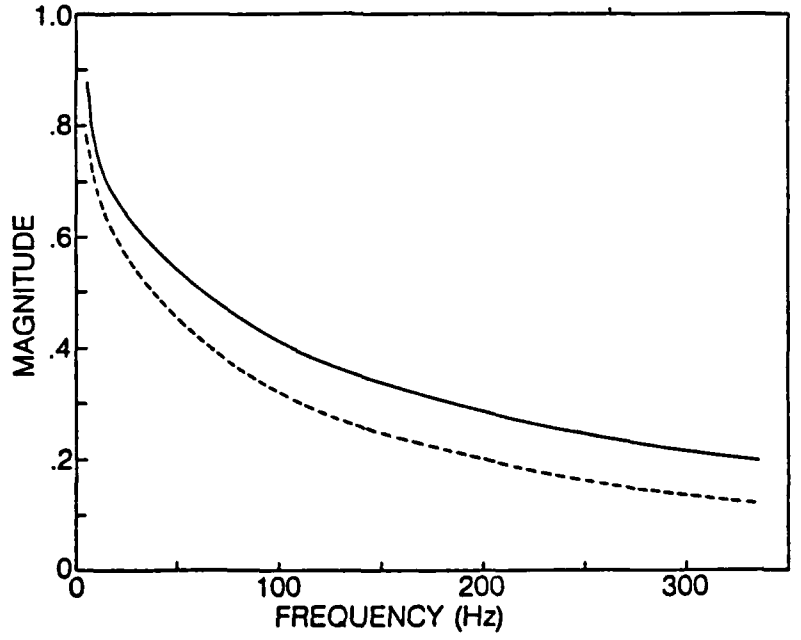

Figure 5.7. Magnitude of the calculated acoustic transfer function for porosities of .3 (——) and .5 (---), 5 cm below the surface and 5° angle of incidence. All other parameters are set to the values measured at Sardis.

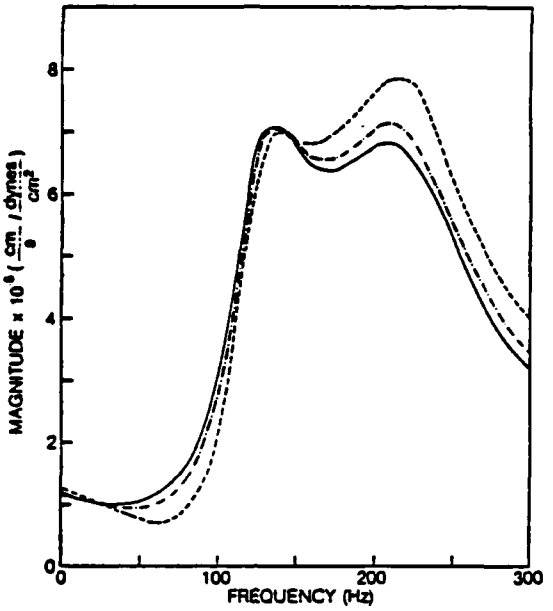

Figure 5.8. Magnitude of the calculated seismic transfer function for flow resistivities of 60 rayls/cm (——), 420 rayles/cm (-•-) and 3000 rayls/cm (——) at 23cm and 20°. The porosity is .4 and other parameters are set to the values measured at Sardis.

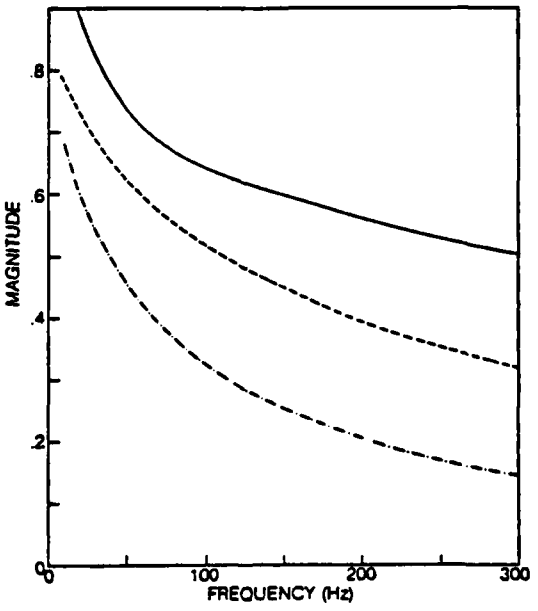

Figure 5.9. Magnitude of the calculated acoustic transfer function at 5cm for flow resistivities of 60 rayls/cm (——), 150 rayls/cm (——) and 420 rayls/cm (-•-), a porosity of .4 and angle of incidence of 5°. Other parameters are set to the values measured at Sardis.

seismic transfer function would approach zero since no acoustic energy could be coupled to motion of the frame through drag forces at the pore walls. If the flow resistivity went to zero, all the incident acoustic energy would pass through the upper boundary without attenuation but there would again be no seismic motion since there would be no frame.

By changing the layer depth, the effect of the measured wave speeds and consequently the elastic moduli on the transfer functions can be observed. Figure 5.10 shows the seismic transfer function for layer depths

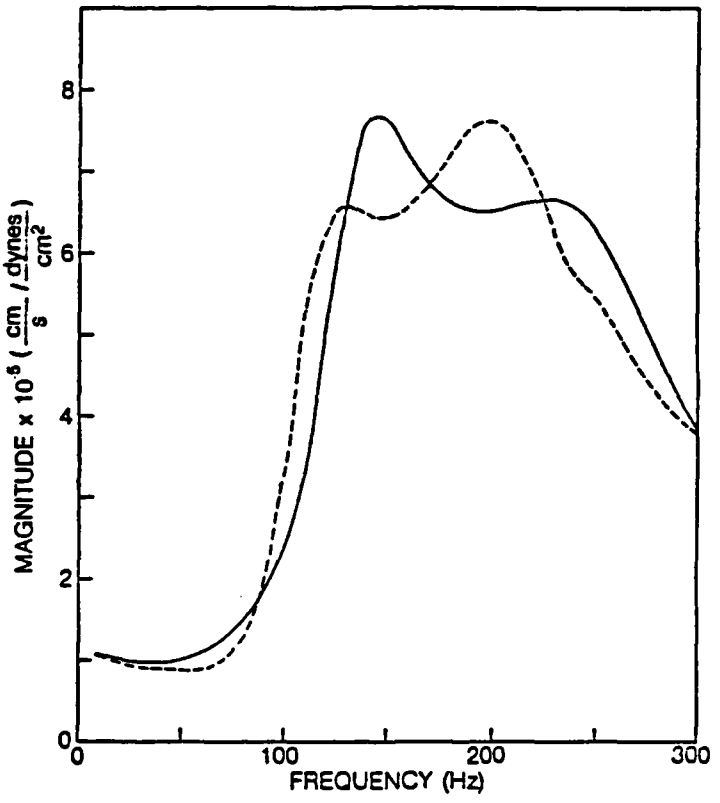

Figure 5.10. Magnitude of the calculated seismic transfer function at 23cm for layer depths of 28 cm (---) and 24 cm (——). Angle of incidence, porosity and flow resistance are 5^{o}, .4, 350 rayls/cm. Other parameters are set to those measured at Sardis.

of 28 and 24 cm. The acoustic transfer function for the same layer depths, not shown, is changed by less than 1%. The acoustic transfer function is insensitive to these changes but the seismic transfer function shows frequency shifts in the minimum and maximum indicating that some of the seismic energy is reflected from the lower boundary.

During the transfer function experiments, the angle of grazing incidence was varied from 5^{o} to 20^{o}. Figures 5.11 and 5.12 indicate the calculated effect of angle of incidence on the magnitude and phase of the seismic transfer function. The magnitude and phase of the acoustic transfer function is insensitive to the angle of incidence to less than 1 percent while the magnitude of the seismic transfer function decreases by as much as 25% at the maximum and the phase curve is shifted vertically by 4^{o} to 5^{o}.

Acoustic Transfer Function

Next, the experimental acoustic transfer function will be compared to the predicted transfer function using the measured values of flow resistivity (See Table 1) with the porosity set to 0.4 for both experimental sites. Figures 5.13 and 5.14 show the magnitude and phase of both the experimental and predicted acoustic transfer functions for the Sardis beach area at an incident angle of 20^{o} and 12 cm below the surface. The theoretical phase plotted here is the negative of what was predicted for reasons previously explained. Comparisons of transfer functions for the UM test field are not shown. The agreement is no better or worse than at Sardis.

Even when the layer depth is theoretically changed from 26 cm to 6 cm the magnitude of the transfer function 5 cm below the surface does not show interference with waves reflected from the lower boundary because the acoustic wave in the pores is rapidly attenuated; it is not reflected from the lower boundary. By the time that the acoustic wave has propagated 4 cm through the pores almost all the acoustic energy has been transferred to motion of the frame at the pore walls. The effect of the porous layer acting as an impedance matching device coupling acoustic energy into the non-porous clay will be demonstrated in the next section of this report.

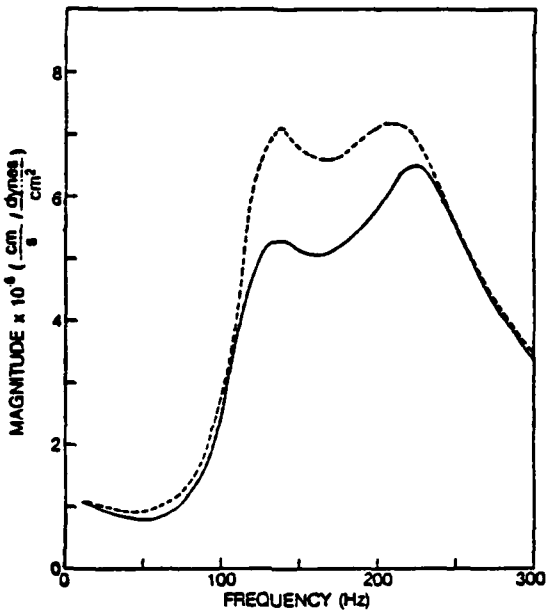

Figure 5.11. The calculated effect of angle of incidence on the magnitude of the seismic transfer function at 5^{o} (---) and 20^{o} (——) at a depth of 23cm. The porosity is 0.4 and other parameters are the values measured at Sardis.

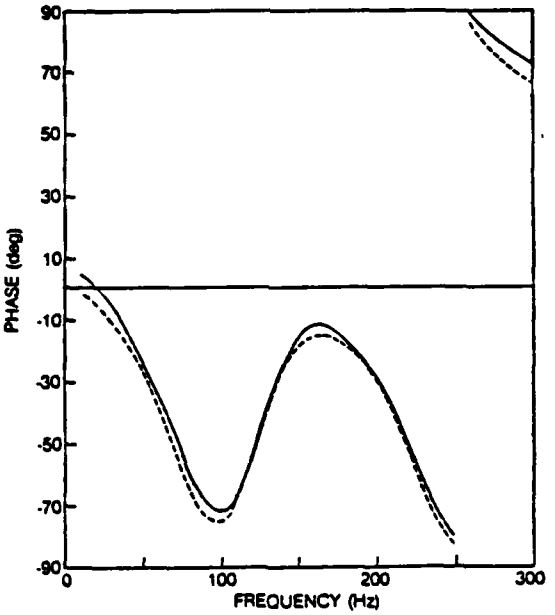

Figure 5.12. The calculated effect of angle of incidence on the phase of the seismic transfer function at 5^{o} (---) and 20^{o} (——) at a depth of 23cm. The porosity is 0.4 and other parameters are the values measured at Sardis.

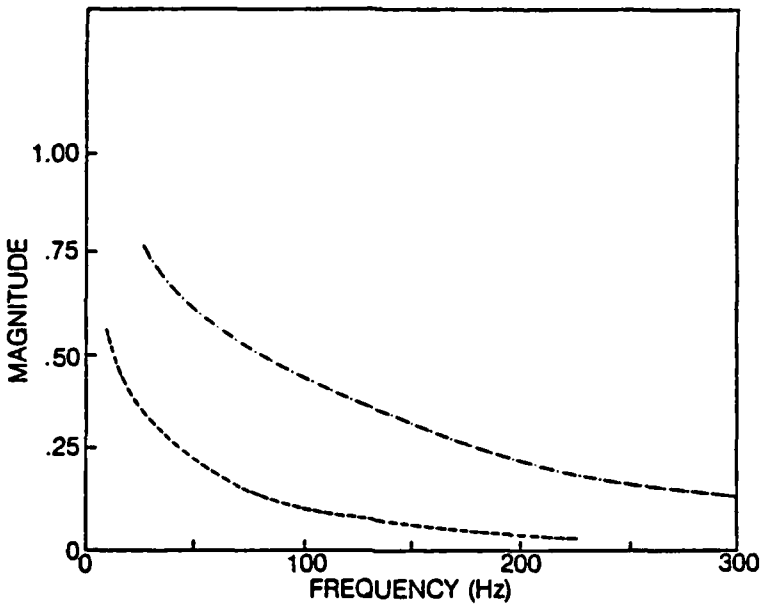

Figure 5.13. The calculated (——) and experimental (-·-) magnitudes of the acoustic transfer function at Sardis at 20° and 12 cm below the ground surface. Porosity is 0.4 and other parameters are the value measured at Sardis.

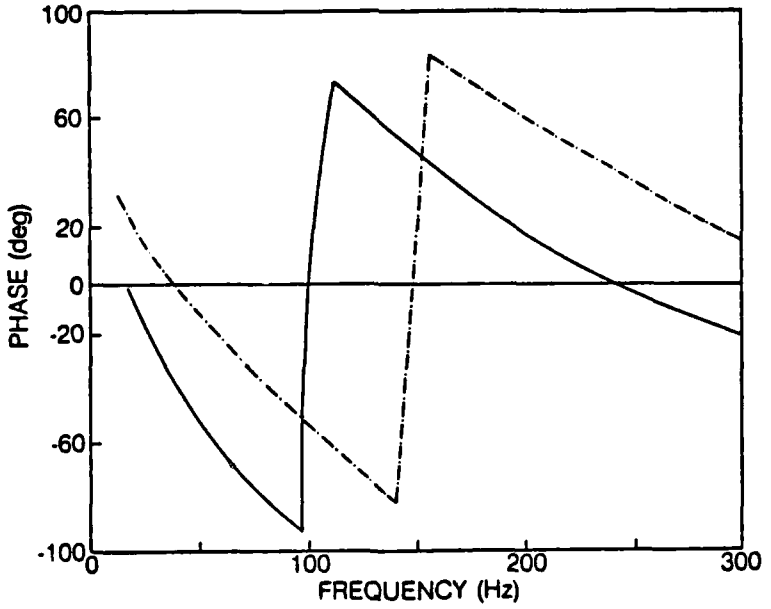

Figure 5.14. The calculated (-·-) and experimental (——) phases of the acoustic transfer function at Sardis.

Seismic Transfer Function

In the transfer function experiment, the seismic sensor was buried so that the top of the case was at depths of 5 and 25 cm. However, because of the physical size of the sensor (cylindrical, diameter = 20 cm, length = 18 cm), the transfer functions are calculated at 23 cm and 43 cm below the surface. At a depth of 43 cm, the lower clay layer is reached so we measure the seismic transfer function in both the porous soil and the non-porous clay. Figure 5.15, 5.16, 5.17 and 5.18 show the comparison of the magnitude and phase of the experimental and predicted seismic transfer function for both depths at Sardis. The experimental magnitude shows a strong minimum at 160 Hz and other fine structure which is not predicted by our single layer model. At Sardis the moisture content of the sand increased rapidly below 5 cm and became saturated at the depth of the clay layer. To predict the detailed structure of the seismic transfer functions in such a media it may be necessary to incorporate multiple layers in the physical model. In Figure 17, the UM test field measured seismic wave speeds for the clay were also used in the calculations along with a layer depth of 35 cm. Comparisons of the UM test field data to theory are not shown, but again the agreement is as good as at Sardis.

From the measured seismic wave speeds in the clay below the porous medium, the reflection coefficient for an air-clay boundary would be approximately .999 indicating almost no transmission into the surface. However, the measured magnitude of the seismic transfer function for the lower medium indicates as much seismic energy is transmitted into the clay as is coupled into the porous medium from the air. Theoretically, this is also seen. Transmission coefficients of .75 are computed at 200 Hz indicating that the porous layer acts as an impedance matching device for coupling acoustic energy into the non-porous clay below the porous medium.

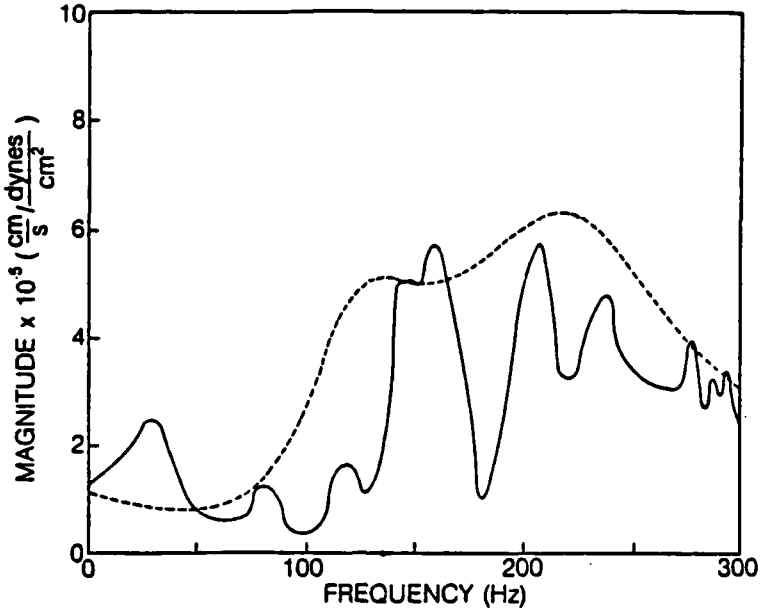

Figure 5.15. The magnitude of calculated (——) and experimental (——) seismic transfer function at Sardis at 20° and 23 cm.

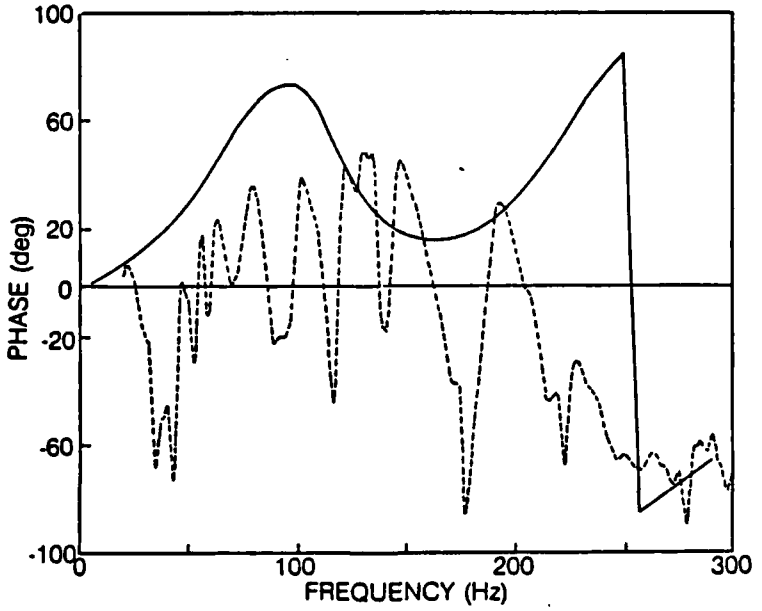

Figure 5.16. The phase of calculated (——) and experimental (——) seismic transfer function at Sardis at 20° and 23 cm.

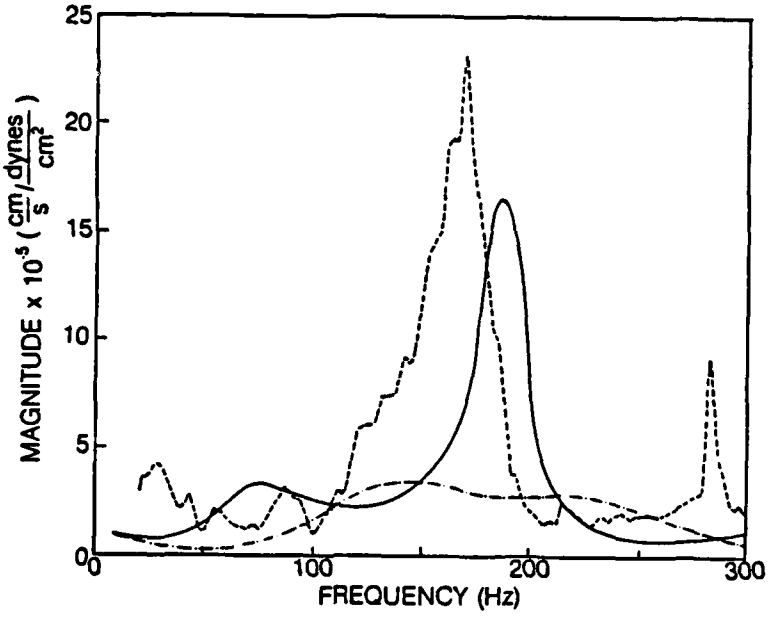

Figure 5.17. The magnitude of the calculated (-·-) and experimental (——) seismic transfer function at Sardis at 20° and 43 cm. The solid line is calculated with the UM test field clay velocities and a layer depth of 35cm substituted for the Sardis values.

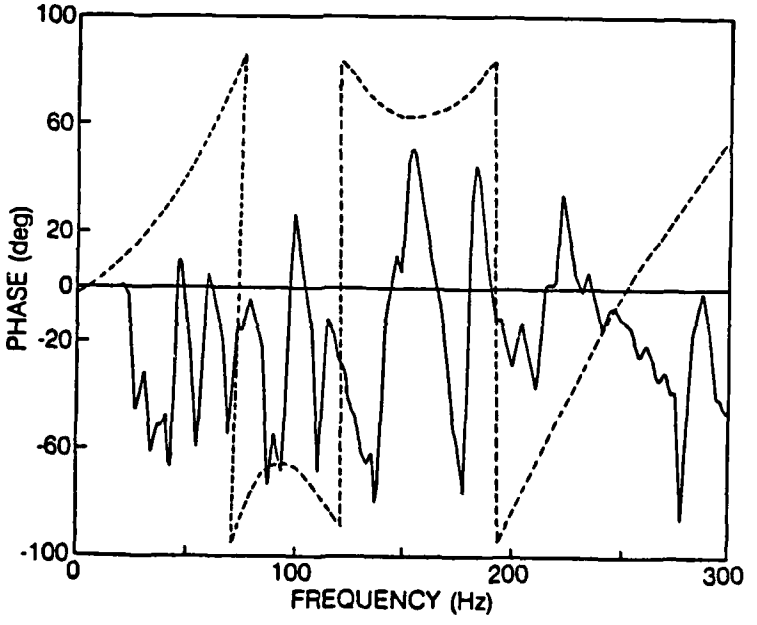

Figure 5.18. The phase of the calculated (---) and experimental (——) seismic transfer function at Sardis at 20° and 43 cm.

The very fact that the theoretical predictions come within a factor of 2 of the experimental data in all cases, compared to a factor of 1000 for a homogeneous layer theory, is remarkable considering that there are no empirical adjustments or parameters allowed.

Surface Impedance

The acoustic surface impedance at Sardis or the UM test field soil was not experimentally determined. However, Bolen and Bass have published normalized surface impedances for several ground covers which include a sand and two different soils. They compared experimentally measured values of surface impedance to that which is predicted from a single parameter model based on measured flow resistivity (see Reference 17). In each of the ground covers investigated, they found that the impedance necessary to reproduce the sound pressure level measured with above ground microphones required that a they use a flow resistivity in the single parameter model approximately one-half the measured flow resistivity (see Figure 5.19, 5.20). This was referred to as the best fit to measured values. The theoretical normalized surface impedance predicted by the Biot-Stoll Model developed here is plotted on the Bolen and Bass impedance curves for their measured values of flow resistivity. Note that no empirical adjustment of the flow resistance is required. In fact, there are no adjustable parameters allowed.

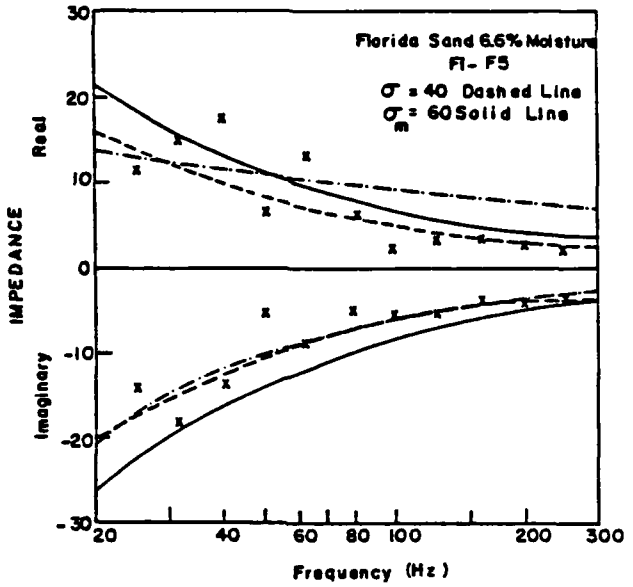

Figure 5.19. The real and imaginary impedance values for a Florida Sand determined by Bolen and Bass; experimental data (x), empirical Chessell model (——), the best fit (– – –). The dash dot line is calculated using the Biot-Stoll Model with the measured values of flow resistance, σ_m = 60 rayls/cm.

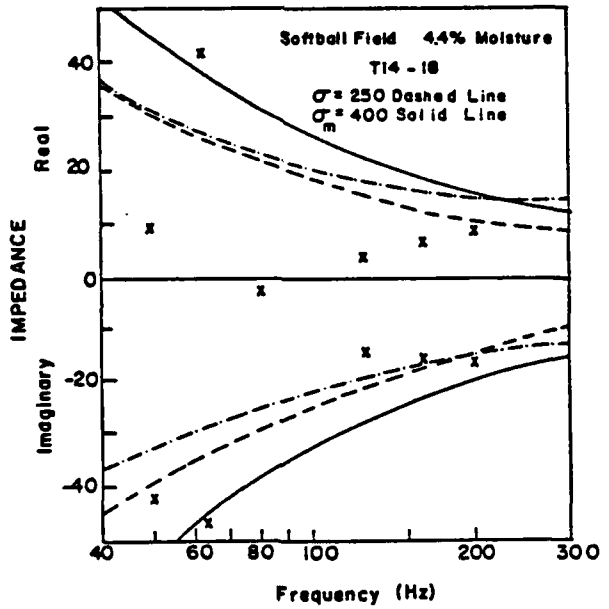

Figure 5.20. The real and imaginary impedance values for a Softball field determined by Bolen and Bass; experimental data (x), empirical Chessell model (——), the best fit (– – –). The dash dot line is calculated using the Biot-Stoll Model with the measured value of flow resistance, σ_m = 400 rayls/cm.

6. SUMMARY AND CONCLUSION

Using the Biot-Stoll Model of a porous elastic medium the compressional wave propagation constants have been numerically determined for a porous sand and a grass covered field. The earth's surface was modeled as a finite layer of porous material between two semi-infinite media, air and non-porous clay. The complex displacement amplitudes of compressional and shear waves in each medium were found using numerical techniques and a complex transfer function was defined in terms of these amplitudes. Compressional waves are emphasized here to clarify the physical properties. The surface impedance was also determined from the wave amplitudes. An outdoor experiment was performed in order to measure the transfer function so that theory could be compared to experiment.

A sensitivity analysis of the calculated transfer function revealed that the only physical quantities which significantly affect the computed transfer funtions are the flow resistivity of the porous surface, the depth of the porous layer, and the compressional and shear wave velocities of the underlying clay. The magnitudes of the calculated acoustic/seismic transfer function using independently measured values of the physical properties typically agrees with the measured values of the transfer function within factors of two. The theory does not predict observed fine structure in the acoutic/seismic transfer function. It may be necessary to include multiple layers and flow resistivity gradients in the porous surface if the fine structure is required.

The Biot-Stoll Model allows for an acoustic wave in the pores of the porous surface. In a separate experiment, attenuation coefficients and phase velocities of this acoustic wave were measured in sand using a probe microphone. The phase velocity of the acoustic wave in the pores was only tens of m/s and the attenuation was one to two dB/cm. Predicted attenuation and wave velocity agree well with experiment.

The mechanism for the coupling of acoustic energy into the ground as seismic energy is understood in the light of these measurements. As the airborne acoustic wave impinges upon the porous surface, it forces motion of air in the surface pores. The oscillating air in the pores is subjected to viscous drag at the pore walls. As a result of this drag, energy is taken out pore fluid motion and appears as motion of the pore walls - motion of the soil matrix. This motion is detected with a seismic sensor - a geophone. An alternative way of viewing this coupling process is to consider the porous layer as an impedance matching network. Without the pores, the acoustic resistance (ρc) in air is much less than in the earth. The pore wave, however, is very slow bringing the effective ρc product for the earth's surface more near that of air.

This physical model also explains a result which has mystified outdoor acousticians for a number of years. Specifically, when one measures the impedance of the earth's surface it is found, in almost all cases, to be locally reacting. This means that energy is refracted so that it is almost normal to the surface. The impedance then becomes essentially independent of the angle of incidence and regions of the surface very far away from the point where the acoustic wave strikes do not contribute to the refracted or reflected acoustic fields. This is difficult to understand if the wave speed in the earth is taken to be hundreds of meters per second but follows readily from Snell's Law if the wave speed in the surface (in the pores) is only tens of meters per second. The empirical result that the earth's surface is almost always locally reacting can, then, be understood as a natural consequence of the porous upper layer of the earth.

In conclusion, the Biot-Stoll Model for a porous elastic medium as presented here provides a good physical description of the coupling of airborne acoustic energy into the ground where it appears as seismic motion and an acoustic wave in the pores. This model predicts the measured

attenuation of the acoustic wave in the pores, surface impedance, and acoustic and seismic transfer functions and their dependence upon angle of incidence and frequency within factors of two of measured values even when one assumes only one porous homogeneous layer. Earlier calculation based upon semi-infinite homogeneous fluids in contact were in error by a factor of 1000 and these calculations predicted a strong angle of incidence not observed experimentally, and predicted incorrect frequency dependence.

The theoretical results presented here need three refinements in order to make this procedure a useful engineering tool:

1. Only plane incident waves are included when, in fact, most sources are more nearly spherical. Dr. Attenborough[18] has developed the mathematics necessary to treat the spherical case. His formalism needs to be included in our present computer programs and additional experiments need to be performed for angles of incidence less than 5^{o} where Attenborough predicts a difference between plane and spherical wave results.

2. The theoretical expressions need to be simplified by searching for realistic approximations so that one can treat impulsive sources using Fourier Transform techniques. This refinement will require extensive calculations be made to verify that the approximate relations are valid for practical surfaces. This refinement will allow comparison between experiment and the large data base developed by van Hoof[19] and co-workers for impulsive sources.

3. The model needs to be extended to allow for variation of flow resistance with depth and multiple porous layers. This refinement will be necessary before we can hope to predict the fine structure in the acoustic/seismic transfer functions. Experimentally, data is needed for a wider variety of surfaces as well as data with incident angles less than 5^{o}. Specifically, surfaces with very low and very high flow resistivities would help explore the range of validity of this model.

REFERENCES

1. H.E. Bass, L.N. Bolen, Daniel Cress, Jerry Lundien, and Mark Flohr, "Coupling of Airborne Sound into the Earth: Frequency Dependence", J. Acoust. Soc. Am. 67, 1502-1506 (1980).

2. M.D. Flohr and D.H. Cress, "Acoustic-to-Seismic Coupling: Properties and Applications to Seismic Sensors", Waterways Experiment Station Technical Rep. EL-79-1 (1979).

3. H. Lamb, "On the Propagation of Tremors over the Surface of an Elastic Solid", Philos, Trans. R. Soc. London 203, 1-42 (1904).

4. F. Press and M. Ewing, "Ground Roll Coupling to Atmospheric Compressional Waves", Geophysics 16, 416-438 (1951).

5. F. Press and J. Oliver, "Model Study of Air-Coupled Surface Waves", J. Acoust. Soc. Am. 27, 43-46 (1955).

6. Robert D. Stoll, "Acoustic Waves in Ocean Sediments", Geophysics 42, No. 2, 715-725 (June 1977).

7. Proceedings of the Symposium on Long Range Sound Propagation; Status and Future Directions, 19-20 Nov 81, H.E. Bass, Editor.

8. K. Attenborough, H. Bass, and L.N. Bolen, "Sound Transmission into Plane Porous Ground Surfaces", Acoustics Letters 6, 87-90 (1982).

9. K. Attenborough, "Acoustic-to-Seismic Coupling over Porous Ground Surfaces", ARO Europe Contract No: DAJA 37-81-C-0210, Fourth Periodic Report, march 1983.

10. M.A. Biot, "Theory of Propagation of Elastic Waves in a Fluid-Saturated Porous Solid. II. High Frequency Range", J. Acoust. Soc. Am. 28, 179-191 (1956).

11. D. Sides, "Absorption of Sound by Porous Fibrous Absorbents, PhD Thesis, University of Liverpool, (1973).

12. K. Attenborough, "Acoustical Characteristics of Rigid Fibrous Absorbents and Granuler Materials", J. Acoust. Soc. Am. 73, 785-799 (1983).

13. H. Deresiewicz, R. Sfalak, "On Uniqueness in Dynamic Poroelastivity", B. Seis. Soc. Am. 53,783-788 (1963).

14. M.A. Biot and D.G. Willis, "The elastic coefficients of the theory of consolidation," J. Appl. Mech. 24, 594-601 (1957).

15. R.W. Leonard, "Simplified Flow Resistance Measurements", J. Acoust. Soc. Am. 17m 240-241 (1946).

16. B. Redpath, "Seismic Refraction Exploration for Engineering Site Investigations", Waterways Experiment Station Technical Rep.I-73-4 (1973).

17. L.N. Bolen and H.E. Bass, "Effects of Ground Cover on the Propagation of Sound Through the Atmosphere", J. Acoust. Soc. Am. 69, 950-954 (1981).

18. Keith Attenborough, Nichlas W. Hoope, Trevor L. Richard and V.V.S.S. Sastry, "Acoustic-to-Seismic Coupling over Porous Ground Surfaces," Final Technical Report, U.S. Army European Research Office, Contract No. DAJA 37-81-C-0210 (January, 1984).

19. H.A.J.M. van Hoof and K.W.F.M. Doorman, "Coupling of Airborne Sound in a Sandy Soil," Laboratory for Electronic Developments for the Armed Forces, TNO Report No. TR 1983-09 (September, 1983).

The subroutine PROP.FORTRAN is used to drive the routine SOAIR.FORTRAN which computes the compressional wave propagation constants using equation 8. The frequency, FR, is the input parameter and the propagation constants, ZSLOW1, ZFAST1 are the output. The routine is in CGS units. SOAIR computes the viscosity correction factor (equation 6) with IARGT=0 and the complex compressibility with ICOMP=1 (see Reference 12). Parameters not defined in SOAIR are as follows:

NVISC	Static Shape Factor (n)
STATSF	Dynamic Shape Factor (s)
NTHER	Same as NVISC
QSQ	Tortuosity
RHO	Bulk Density
CP	Specific Heat of Air
COFUIS	Same as ETA
THECON	Thermal Conductivity of Air
PRN	Prandtl's Number
SHFT	Shape Factor Ratio
SHF	Same as SHFT
GAMA	Ratio of Specific Heats of Air
COMP	Compressibility of Air
HBAR	See equation 2a
CBAR	See equation 2b
MBAR	See equation 2c
D	See equation 2d

The subroutines CBESJ.FORTRAN and CBJ.FORTRAN compute the Bessel functions required for the viscosity correction factor and complex compressibility.

```
C     DRIVE SR ROUTINE FOR PROPAGATION PROGRAMS                          PR000010
C     FOR DEFINITION OF CONSTANTS SEE APPROPRIATE                        PR000020
C     SUBPROGRAMS.  SUBPROGRAM SOAIR COMPUTES THE                        PR000030
C     COMPLEX PROPAGATION CONSTANTS FOR THE POROUS                       PR000040
C     LAYER.                                                             PR000050
C                                                                        PR000060
      SUBROUTINE PROP(FR,ZSLOW1,ZFAST1)                                  PR000070
      IMPLICIT REAL *8 (A-H,O-Z)                                         PR000080
      REAL *8 MU,KBBAR,K,KR,NTHER,NVISC,NPRIME                           PR000090
      COMPLEX *16 ZSLOW1,ZFAST1,J,F                                      PR000100
      COMMON /BLK2/ J,F,ETA,K,Q2                                         PR000110
      COMMON /BLK4/ PHI                                                  PR000120
      COMMON /BLK/ DM,IARGT,ICOMP,MU,STATSF,NTHER,NVISC,NPRIME           PR000130
      COMMON /BLK3/ RHOF,GB,KBBAR,KR,RHOS,OMEGA                          PR000140
```

```
C                                                                       PR000150
        ICOMP = 0                                                       PR000160
      MU=.1495D0                                                        PR000170
      ETA=1.81D-04                                                      PR000180
      K=ETA/PHI                                                         PR000190
      CALL SOAIR(FR,ZSLOW1,ZFAST1)                                      PR000200
      RETURN                                                            PR000210
      END                                                               PR000220



C      SUBROUTINE SOAIR(FR,ZSLOW1,ZFAST1)                               SOA00010
CC     INPUTS           FR                                              SOA00020
C      OUTPUTS             ZSLOW1,ZFAST1                                SOA00030
C                                                                       SOA00040
C     TO OBTAIN PROPAGATION CONSTANTS FOR DILITATIONAL WAVES.           SOA00050
C     15TH NOV 82                                                       SOA00060
C     RECONSTRUCTED VERSION, 25TH APRIL 83.                             SOA00070
C     DATA TAKEN FROM STOLL'S PAPER JASA(1969) V 47, N 5,P1440-1447.    SOA00080
C                                                                       SOA00090
C     SUBROUTINES USED                                                  SOA00100
C                                                                       SOA00110
C           CBESJ                                                       SOA00120
C           CBJ                                                         SOA00130
C                                                                       SOA00140
      SUBROUTINE SOAIR(FR,ZSLOW1,ZFAST1)                                SOA00150
      IMPLICIT REAL *8 (A-H,O-Z)                                        SOA00160
C                                                                       SOA00170
      DIMENSION AKBDB(6),FAT(6)                                         SOA00180
      DIMENSION DEP(6),AT(6)                                            SOA00190
C                                                                       SOA00200
C                                                                       SOA00210
      REAL *8    MU,KBBAR,K,KR,NTHER,NVISC,NPRIME                       SOA00220
      COMPLEX *16 J,ROOTJ,CAPB,CAPC,SDISC,ARG,Z1,Z2,DISC                SOA00230
      COMPLEX *16 XARG1,XJ0,XJ1,T1,COMP,KF                              SOA00240
      COMPLEX *16 D,HBAR,CBAR,MBAR,CAPA                                 SOA00250
      COMPLEX *16 XARG2,RJ0,RJ1,T2,M                                    SOA00260
      COMPLEX *16 BJ0,BJ1,T,F,BBYA,BBYA2                                SOA00270
      COMPLEX *16 ZKRB                                                  SOA00280
      COMPLEX *16 ZFAST1,AKB1,ZKRB1,ZSLOW1                              SOA00290
      COMPLEX *16 CPS,CPB,ZSLOW,ZFAST,SRAT1,SRAT2,FRAT1,FRAT2           SOA00300
      COMPLEX *16 XARG,AKB                                              SOA00310
      COMPLEX *16 EP,EQ,ER,TOWS,TOWF,RAFTOS                             SOA00320
C     ------------------------------------------------------------      SOA00330
C                                                                       SOA00340
      COMMON /BLK/ DM,IARGT,ICOMP,MU,STATSF,NTHER,NVISC,NPRIME          SOA00350
      COMMON /BLK1/ EP,EQ,ER                                            SOA00360
      COMMON /BLK2/ J,F,ETA,K,QSQ                                       SOA00370
      COMMON /BLK3/ RHOF,GB,KBBAR,KR,RHOS,OMEGA                         SOA00380
     COMMON /BLK7/ HBAR,CBAR,MBAR                                       SOA00390
C                                                                       SOA00400
C      ------------------------------------------------------------     SOA00410
C                                                                       SOA00420
C                                                                       SOA00430
```

```
C     ------------------------------------------------------------      SOA00440
C                                                                       SOA00450
      PI = 4.D0*DATAN(1.D0)                                             SOA00460
C     OMEGA=POROSITY(NO UNITS).                                         SOA00470
C     KR=BULK MODULUS OF GRAINS (DYNES/CM**2)                           SOA00480
C                                                                       SOA00490
C     MU=KINEMATIC VISCOSITY (CM**2/SEC)                                SOA00500
C     ETA=DYNAMIC FLUID VISCOSITY (DYNE-SEC/CM**2)                      SOA00510
C     RHOS=DENSITY OF SOLID (GM/CM**3)                                  SOA00520
C     RHOF=DENSITY OF FLUID(GM/CM**3)                                   SOA00530
C                                                                       SOA00540
      RHO = (1.D0-OMEGA)*RHOS + OMEGA*RHOF                              SOA00550
C                                                                       SOA00560
C     ------------------------------------------------------------      SOA00570
C                                                                       SOA00580
C     COMPUTE PRANDTL NUMBER.                                           SOA00590
      CP      = 1006.D0                                                 SOA00600
      COFVIS = 1.81D-05                                                 SOA00610
      THECON  = 0.0257D0                                                SOA00620
      PRN     = COFVIS*CP/THECON                                        SOA00630
      SPRN    = DSQRT( PRN )                                            SOA00640
C                                                                       SOA00650
C     K=PERMEABILITY OF THE POROUS FRAME (CM**2)                        SOA00660
C                                                                       SOA00670
      SHFT = DSQRT(STATSF)/NTHER                                        SOA00680
      SHF  = DSQRT(STATSF)/NVISC                                        SOA00690
C                                                                       SOA00700
C                                                                       SOA00710
C     QSQ = (OMEGA)**(-NPRIME)                                          SOA00720
C                                                                       SOA00730
C     ------------------------------------------------------------      SOA00740
C                                                                       SOA00750
      GAMA   = 1.4D0                                                    SOA00760
      STWO   = DSQRT(2.D0)                                              SOA00770
      J      = (0.D0,1.D0)                                              SOA00780
      ROOTJ  = CDSQRT( J)                                               SOA00790
C     ROOTJ  = CMPLX( REAL (ROOTJ),-AIMAG(ROOTJ))                       SOA00800
      OM  = 2.D0*PI*FR                                                  SOA00810
      OM2 = OM*OM                                                       SOA00820
      OM4 = OM2*OM2                                                     SOA00830
C                                                                       SOA00840
C     ------------------------------------------------------------      SOA00850
C                                                                       SOA00860
C     COMPUTE COMPLEX COMPRESSIBILITY.                                  SOA00870
      XLAM1 = (8.D0*QSQ*K)/(MU*OMEGA)                                   SOA00880
      XLAM1 = SHFT*DSQRT(XLAM1)                                         SOA00890
      XLAM1 = XLAM1*DSQRT(OM)                                           SOA00900
      XARG1 = ROOTJ*SPRN*XLAM1                                          SOA00910
      AXARG1= CDABS(XARG1)                                              SOA00920
      IF( AXARG1 .GT. 7.0) GO TO 60                                     SOA00930
              CALL CBESJ(XARG1,0,XJ0)                                   SOA00940
              CALL CBESJ(XARG1,1,XJ1)                                   SOA00950
60    IF( AXARG1 .LE. 7.0) GO TO 70                                     SOA00960
              CALL CBJ(XARG1,0,XJ0)                                     SOA00970
              CALL CBJ(XARG1,1,XJ1)                                     SOA00980
70    T1   = XJ1/XJ0                                                   SOA00990
```

```
      COMP = (1.D0+2.D0*(GAMA-1.D0)*T1/XARG1)/(GAMA*1.01325D06)          SOA01000
      KF   = 1.D0/COMP                                                   SOA01010
      IF( ICOMP .NE. 1 ) GO TO 80                                        SOA01020
            COMP = 9.86923D-07                                           SOA01030
            KF   = 1.D0/COMP                                             SOA01040
80    CONTINUE                                                           SOA01050
C                                                                        SOA01060
C     ---------------------------------------------------------          SOA01070
C                                                                        SOA01080
      D    = KR*(1.D0 + OMEGA*(KR/KF - 1.D0))                            SOA01090
      HBAR = (KR-KBBAR)*(KR-KBBAR)/(D-KBBAR)                             SOA01100
     2       + KBBAR + (4.D0/3.D0)*GB                                    SOA01110
      CBAR = KR*(KR-KBBAR)/(D-KBBAR)                                     SOA01120
      MBAR = KR*KR/(D-KBBAR)                                             SOA01130
      M    = QSQ*(RHOF/OMEGA)                                            SOA01140
      CAPA = -HBAR*MBAR + CBAR*CBAR                                      SOA01150
C                                                                        SOA01160
C     VISCOSITY CORRECTION                                               SOA01170
C                                                                        SOA01180
      XARG = SHF*DSQRT((8.D0*QSQ*K)/(MU*OMEGA))                          SOA01190
      XX   = XARG*DSQRT(OM)                                              SOA01200
      ARG  = ROOTJ*XX                                                    SOA01210
      OM2  = OM*OM                                                       SOA01220
      OM4  = OM2*OM2                                                     SOA01230
      IF( IARGT .NE. 1) GO TO 90                                         SOA01240
            ARG = ROOTJ*XX                                               SOA01250
90    IF( IARGT .NE.2) GO TO 100                                         SOA01260
            AP  = SHF*DSQRT( 8.D0*QSQ*OMEGA)                             SOA01270
            ARG = ROOTJ*DSQRT(OM/ETA)*AP                                 SOA01280
100   IF( IARGT .NE. 3) GO TO 110                                        SOA01290
            APHI = (DM/3.D0)*(OMEGA/(1.D0-OMEGA))                        SOA01300
            ARG  = ROOTJ*APHI*DSQRT(OM/ETA)                              SOA01310
110   IF( IARGT .NE. 4) GO TO 120                                        SOA01320
            ARG  = ARG/OMEGA                                             SOA01330
120   CONTINUE                                                           SOA01340
      IF( CDABS(ARG) .GT. 7.0) GO TO 130                                 SOA01350
      CALL CBESJ(ARG,0,BJ0)                                              SOA01360
      CALL CBESJ(ARG,1,BJ1)                                              SOA01370
130   IF( CDABS(ARG) .LE. 7.0) GO TO 140                                 SOA01380
      CALL CBJ(ARG,0,BJ0)                                                SOA01390
      CALL CBJ(ARG,1,BJ1)                                                SOA01400
C     WRITE(6,*)' BJ0 = ',BJ0,'BJ1 = ',BJ1                               SOA01410
140   CONTINUE                                                           SOA01420
      T    = BJ1/BJ0                                                     SOA01430
C     WRITE(6,*)' T = ',T                                                SOA01440
      F    = (-0.25D0)*(ARG*T/(1.D0 - 2.D0*T/ARG))                       SOA01450
      FREAL  = DREAL(F)                                                  SOA01460
      FIMAG = DIMAG(F)                                                   SOA01470
      CAPB = OM2*(M*HBAR - 2.D0*CBAR*RHOF + RHO*MBAR)                    SOA01480
     2        +J*OM*F*ETA*HBAR/K                                          SOA01490
      CAPC = OM4*(RHOF*RHOF - M*RHO)                                     SOA01500
     2       - OM2*(RHO*J*OM*F*ETA/K)                                    SOA01510
      BBYA  = -CAPB/(2.D0*CAPA)                                          SOA01520
      BBYA2 = BBYA*BBYA                                                  SOA01530
```

```
      DISC = BBYA2 - CAPC/CAPA                                          SOA01540
      SDISC= CDSQRT(DISC)                                               SOA01550
      Z1   = BBYA + SDISC                                               SOA01560
      Z2   = BBYA - SDISC                                               SOA01570
      Z1   = CDSQRT(Z1)                                                 SOA01580
      Z2   = CDSQRT(Z2)                                                 SOA01590
C                                                                       SOA01600
      ZSLOW1 = Z1                                                       SOA01610
      ZFAST1 = Z2                                                       SOA01620
C                                                                       SOA01630
C                                                                       SOA01640
C                                                                       SOA01650
      RETURN                                                            SOA01660
      END                                                               SOA01670

C     SUBROUTINE CBESJ(X,N,CBJ)                                         CBE00010
C     INPUTS           X,N                                              CBE00020
C     OUTPUTS              CBJ                                          CBE00030
C     ROUTINE TO COMPUTE COMPLEX BESSEL FUNCTION JN(X)                  CBE00040
C     WHERE X IS A COMPLEX ARGUMENT                                     CBE00050
C*****************************************************************    CBE00060
C                                                                       CBE00070
      SUBROUTINE CBESJ(X,N,CBJ)                                         CBE00080
     IMPLICIT REAL *8 (A-H,O-Z)                                         CBE00090
      COMPLEX *16 X,CBJ,FM1,FM,BMK,ALPHA,CBPREV                         CBE00100
      CBPREV = (0.0,0.0)                                                CBE00110
      D = 1.0E-4                                                        CBE00120
      AX = CDABS(X)                                                     CBE00130
      NTEST = 20.0 + 10.0*AX - AX**2/3                                  CBE00140
      IF(AX.GT.15.0) NTEST = 90.0 + AX/2.0                              CBE00150
      IF(N.LT.NTEST) GO TO 20                                           CBE00160
      WRITE(6,1001)                                                     CBE00170
1001  FORMAT(1X,'RANGE OF X AND N IS INCORRECT')                        CBE00180
      RETURN                                                            CBE00190
20    N1=N+1                                                            CBE00200
      MA = AX + 6.0                                                     CBE00210
      IF(AX.GE.5.0)MA = 1.40*AX + 60.0/AX                               CBE00220
      IX = AX                                                           CBE00230
      MB = N+ IX/4 + 2                                                  CBE00240
      MO = MAXO(MA,MB)                                                  CBE00250
      MMAX = NTEST                                                      CBE00260
      DO 90 M = MO,MMAX,3                                               CBE00270
      FM1 = 1.0E-28                                                     CBE00280
      FM = 0.0                                                          CBE00290
      ALPHA = 0.D0                                                      CBE00300
      J1 = 1                                                            CBE00310
      IF(M.EQ.M/2*2) J1 = -1                                            CBE00320
      M2 = M - 2                                                        CBE00330
      DO 160 K=1,M2                                                     CBE00340
      MK = M-K                                                          CBE00350
      XMK = MK + 2                                                      CBE00360
      BMK = XMK*FM1/X - FM                                              CBE00370
      FM = FM1                                                          CBE00380
      FM1 = BMK                                                         CBE00390
      IF(MK-N-1.EQ.0.0) CBJ = BMK                                       CBE00400
      J1 = -J1                                                          CBE00410
      S = 1 + J1                                                        CBE00420
```

```
160     ALPHA = ALPHA + BMK*S                                          CBE00430
        BMK = 2.0*FM1/X - FM                                           CBE00440
        IF(N.EQ.0) CBJ = BMK                                           CBE00450
        ALPHA = ALPHA + BMK                                            CBE00460
        CBJ = CBJ/ALPHA                                                CBE00470
        IF(CDABS(CBJ-CBPREV).LT.(CDABS(D*CBJ)))GO TO 96                CBE00480
90      CBPREV = CBJ                                                   CBE00490
96      RETURN                                                         CBE00500
        END                                                            CBE00510

C       SUBROUTINE CBJ(X,N,J)                                          TEM00010
C       INPUTS          X,N                                            TEM00020
C       OUTPUT             J                                           TEM00030
C                                                                      TEM00040
C       ROUTINE TO COMPUTE COMPLEX *16BESSEL FUNCTION JN(X)            TEM00050
C       WHERE X IS COMPLEX *16                                         TEM00060
C                                                                      TEM00070
C       THE ROUTINE CBESSEL (YBESS.FTP FROM SOUTHAMPTON IS USED        TEM00080
C       IF CABS(X) IS GREATER THAN 7.0, OTHERWISE CBESJ IS USED.       TEM00090
C                                                                      TEM00100
C       ZERO AND FIRST ORDER BESSEL FUNCTIONS OF COMPLEX *16ARGUMENTS  TEM00110
C       ARE COMPUTED.                                                  TEM00120
C       N = 0; ZERO ORDER BESSEL FUNCTION.                             TEM00130
C       N = 1; FIRST ORDER BESSEL FUNCTION.                            TEM00140
C***************************************************************     TEM00150
C                                                                      TEM00160
        SUBROUTINE CBJ(X,N,J)                                          TEM00170
      IMPLICIT REAL *8 (A-H,O-Z)                                       TEM00180
        COMPLEX *16 X,J,FM1,FM,BMK,ALPHA,CBPREV                        TEM00190
        COMPLEX *16 Z,CHI,EZ,T0,T1,T2,T3,T4,T5,T6,T7,P0,Q0             TEM00200
        REAL *8 JR,JI                                                  TEM00210
        AX      = CDABS(X)                                             TEM00220
        IF(AX.GT.7.0) GO TO 100                                        TEM00230
        CBPREV  = (0.0,0.0)                                            TEM00240
        D       = 1.0E-04                                              TEM00250
        NTEST   = 20.0 + 10.0*AX - AX**2/3                             TEM00260
        IF(AX.GT.15.0) NTEST = 90.0 + AX/2.0                           TEM00270
        IF(N.LT.NTEST) GO TO 20                                        TEM00280
        WRITE(6,1001)                                                  TEM00290
1001    FORMAT(1X,'RANGE OF X AND N IS INCORRECT')                     TEM00300
        RETURN                                                         TEM00310
20      N1      = N + 1                                                TEM00320
        MA      = AX + 6.0                                             TEM00330
        IF(AX.GE.5.0) MA = 1.4D0*AX + 60.D0/AX                         TEM00340
        IX      = AX                                                   TEM00350
        MB      = N + IX/4 + 2                                         TEM00360
        MO      = MAX0(MA,MB)                                          TEM00370
        MMAX    = NTEST                                                TEM00380
        DO 90 M = MO,MMAX,3                                            TEM00390
        FM1     = 1.0E-28                                              TEM00400
        FM      = 0.0                                                  TEM00410
        ALPHA   = 0.0                                                  TEM00420
        J1      = 1                                                    TEM00430
        IF(M.EQ.M/2*2) J1 = -1                                         TEM00440
        M2      = M - 2                                                TEM00450
```

```
      DO 160 K=1,M2                                                    TEM00460
      MK       = M - K                                                 TEM00470
      XMK      = MK*2                                                  TEM00480
      BMK      = XMK*FM1/X - FM                                        TEM00490
      FM       = FM1                                                   TEM00500
      FM1      = BMK                                                   TEM00510
      IF(MK-N-1.EQ.0) J = BMK                                          TEM00520
      J1 =       -J1                                                   TEM00530
      S        = 1 + J1                                                TEM00540
160   ALPHA    = ALPHA + BMK*S                                         TEM00550
      BMK      = 2.0*FM1/X - FM                                        TEM00560
      IF(N.EQ.0) J = BMK                                               TEM00570
      ALPHA    = ALPHA + BMK                                           TEM00580
      J        = J/ALPHA                                               TEM00590
      IF(CDABS(J-CBPREV).LT.(CDABS(D*J))) GO TO 200                    TEM00600
90    CBPREV   = J                                                     TEM00610
      GO TO 200                                                        TEM00620
C     BEGIN CALCULATION USING LARGE ARGUMENT SERIES                    TEM00630
C     A.ANDS.EQU.9.2.5 (8 TERMS ARE USED)                              TEM00640
100   Z        = X                                                     TEM00650
      EZ       = 8.0*Z                                                 TEM00660
      IF(N.EQ.0) GO TO 189                                             TEM00670
C                                                                      TEM00680
C     FIRST ORDER CALCULATIONS                                         TEM00690
C                                                                      TEM00700
      CHI      = Z - 3.0*3.14159265/4.0                                TEM00710
C                                                                      TEM00720
C     TERMS IN P0 AND Q0 SERIES ARE FORMED BY                          TEM00730
C      CHAIN MULTIPLICATION                                            TEM00740
C                                                                      TEM00750
      T0       = 1.0                                                   TEM00760
      T1       = T0*(3.0/EZ)                                           TEM00770
      T2       = T1*(5.0/(2.0*EZ))                                     TEM00780
      T3       = T2*(21.0/(3.0*EZ))                                    TEM00790
      T4       = T3*(45.0/(4.0*EZ))                                    TEM00800
      T5       = T4*(77.0/(5.0*EZ))                                    TEM00810
      T6       = T5*(117.0/(6.0*EZ))                                   TEM00820
      T7       = T6*(165.0/(7.D0*EZ))                                  TEM00830
C                                                                      TEM00840
C     FORM P0 = 1.0+T2-T4+T6                                           TEM00850
C                                                                      TEM00860
      P0       = T6 - T4                                               TEM00870
      P0       = P0 + T2                                               TEM00880
      P0       = P0 +T0                                                TEM00890
C                                                                      TEM00900
C     FORM Q0 = T1-T3+T5-T7                                            TEM00910
C                                                                      TEM00920
      Q0       = T5 - T7                                               TEM00930
      Q0       = Q0 - T3                                               TEM00940
      Q0       = Q0 + T1                                               TEM00950
      GO TO 199                                                        TEM00960
C                                                                      TEM00970
C     ZERO ORDER CALCULATION                                           TEM00980
C                                                                      TEM00990
189   CHI      = Z - 3.14159265359/4.0                                 TEM01000
```

```
C                                                                       TEM01010
C       TERMS IN P0 AND Q0 SERIES ARE FORMED BY                         TEM01020
C       CHAIN MULTIPLICATION.                                           TEM01030
C                                                                       TEM01040
        T0      = 1.0                                                   TEM01050
        T1      = T0/EZ                                                 TEM01060
        T2      = T1*(9.0/(2.0*EZ))                                     TEM01070
        T3      = T2*(25.0/(3.0*EZ))                                    TEM01080
        T4      = T3*(49.0/(4.0*EZ))                                    TEM01090
        T5      = T4*(81.0/(5.0*EZ))                                    TEM01100
        T6      = T5*(121.0/(6.0*EZ))                                   TEM01110
        T7      = T6*(169.0/(7.0*EZ))                                   TEM01120
C                                                                       TEM01130
C       FORM P0 = 1.0 - T2 + T4 - T6                                    TEM01140
C                                                                       TEM01150
        P0      = T4 - T6                                               TEM01160
        P0      = P0 - T2                                               TEM01170
        P0      = P0 + T0                                               TEM01180
C                                                                       TEM01190
C       FORM Q0 = -T1+T3-T5+T7                                          TEM01200
C                                                                       TEM01210
        Q0      = T7 - T5                                               TEM01220
        Q0      = Q0 + T3                                               TEM01230
        Q0      = Q0 - T1                                               TEM01240
199     CONTINUE                                                        TEM01250
        J       = CDSQRT(2.0/(3.14159265359*Z))*(P0*CDCOS(CHI)-         TEM01260
     2                  Q0*CDSIN(CHI))                                 TEM01270
C       END OF CALCULATION USING SERIES EXPRESSION.                     TEM01280
200     CONTINUE                                                        TEM01290
        XR      = DREAL (X)                                             TEM01300
        XI      = DIMAG(X)                                              TEM01310
        JR      = DREAL (J)                                             TEM01320
        JI      = DIMAG(J)                                              TEM01330
C       FOR ZEROTH ORDER FUNCTION:                                      TEM01340
C       - IF XR=0.0 OR XI=0.0 THEN J IS REAL .                          TEM01350
C       - THUS SET IMAG. RESULT TO ZERO.                                TEM01360
C                                                                       TEM01370
        IF(((XR.EQ.0.0).OR.(XI.EQ.0.0)).AND.(N.EQ.0)) JI = 0.0          TEM01380
C                                                                       TEM01390
C       FOR FIRST ORDER FUNCTION                                        TEM01400
C       - IF XI = 0.0 THEN J IS REAL                                    TEM01410
C       - THUS SET IMAG. RESULT TO ZERO                                 TEM01420
C                                                                       TEM01430
C       - IF XR = 0.0 THEN J IS IMAGINARY                               TEM01440
C       - THUS SET REAL *8 RESULT TO ZERO                               TEM01450
C                                                                       TEM01460
        IF((XI.EQ.0.0).AND.(N.EQ.1)) JI = 0.0                           TEM01470
        IF((XR.EQ.0.0).AND.(N.EQ.1)) JR = 0.0                           TEM01480
        J       = DCMPLX(JR,JI)                                         TEM01490
        RETURN                                                          TEM01500
        END                                                             TEM01510
```

APPENDIX A.2

AMPL.FORTRAN solves for the amplitudes of the wave motion developed in the section Boundary Value Problem. This routine calls the subroutines PROP, SURIMP, LTRANR, TRANSF and RTRANS which are discussed in additional appendices. AMPL reads the following input from a data file:

VP1	p-wave Velocity in Sand
VP2	p-wave Velocity in Clay
VS1	s-wave Velocity in Sand
VS2	s-wave Velocity in Clay
OMEGA	Porosity
THETO	Incidence Angle from Normal
D	Propagation Depth
RHOS	Clay Density
PHI	Flow Resistivity
QSQ	Tortuosity
STATSF	Dynamic Shape Factor (s)
NTHER	Static Shape Factor (n)
NVISC	Same as NTHER
IARGT	Set to ϕ for this work
DM	Not used for IARGT = ϕ
DEP	Layer Thickness
D1	Propagation Height

For each frequency, AMPL calls PROP which returns the fast and slow wave propagation constants, then the constants in the nine boundary condition equations are computed. The IMSL routine LEQTIC is called and returns the wave amplitudes. Originally AMPL calculated attenuation coefficients, equation 73, but these lines (4710-4920) are no longer used.

```
C     ************************************************                AMP00010
C      NUMERICAL SOLUTION FOR WAVE AMPL. OF A BIOT LAYER              AMP00020
C      ************************************************               AMP00030
C                                                                     AMP00040
C                                                                     AMP00050
      IMPLICIT REAL * 8 (A-H,O-Z)                                     AMP00060
      DIMENSION WK(9)                                                 AMP00070
      DIMENSION ZREAL(12),ZIMAG(12),FRQ(12),PHSGEO(12),PHSPRB(12)     AMP00080
      REAL *8 ATDBG(12),ATDBP(12),MAGG2(12),MAGG1(12),MAGP1(12)       AMP00090
      REAL *8 MAGP2(12),MAGGEO(12),MAGPRB(12)                         AMP00100
      COMPLEX *16   HH1,CC1,MM1                                       AMP00110
        COMPLEX *16 WA(99)                                            AMP00120
C     DIMENSION WA(9)                                                 AMP00130
      COMPLEX *16 TEMP1,TEMP2,TEMP3,TEMP4,TEMP5                       AMP00140
      COMPLEX *16 Q3,Q4,Q5,C3,C4,C5                                   AMP00150
      COMPLEX *16  J,L1,L2,L1S,L2S,C1,C2,S1,S2,Q1,Q2                  AMP00160
      COMPLEX *16  EXP1,EXP2,EXP3,EXP4,EXP5,EXP11,EXP12               AMP00170
```

```
      COMPLEX *16  EXP13,EXP14,EXP15                                    AMP00180
      COMPLEX *16  V1,V2,Z1,Z2,M1,M2,F                                  AMP00190
      REAL *8  OMEGA,KR,KF,KBBAR,K                                      AMP00200
     REAL *8 MAGGO,MAGPB                                                AMP00210
      REAL *8 MU,STATSF,NTHER,NVISC,NPRIME                              AMP00220
      REAL *8  GB,GB2,LAM2                                              AMP00230
      COMPLEX *16    A(9,9),B(9)                                        AMP00240
      REAL *8  L0,L3,L4,L5,L0S,L3S,L4S,L5S,L0S0                         AMP00250
      COMMON /BLK3/ RHOF,GB,KBBAR,KR,RHOS,OMEGA,KF                      AMP00260
      COMMON /BLK2/ J,F,ETA,K,QSQ                                       AMP00270
      COMMON /BLK5/ V0,C0,S0,C1,L0,L1,C2,L2,S3,L3,C3                    AMP00280
      COMMON /BLK4/ PHI                                                 AMP00290
      COMMON /BLK/ DM,IARGT,ICOMP,MU,STATSF,NTHER,NVISC,NPRIME          AMP00300
        COMMON /BLK7/ HH1,CC1,MM1                                       AMP00310
        COMMON /BLK8/ S1,S2                                             AMP00320
        COMMON /BLK8/ C4,S4,C5,L4,L5                                    AMP00330
      J=(0.D0,1.D0)                                                     AMP00340
      E=DEXP(1.D0)                                                      AMP00350
      TWOPI=4.D0*DARSIN(1.D0)                                           AMP00360
C                                                                       AMP00370
C                                                                       AMP00380
C     DEP IS LAYER THICKNESS                                            AMP00390
C     D IS PROPAGATION DEPTH                                            AMP00400
C     D1 IS A PROPAGATION HEIGHT                                        AMP00410
C                                                                       AMP00420
C***********************************************************************AMP00430
C                                                                       AMP00440
      WRITE(6,20)                                                       AMP00450
20     FORMAT(1X,'IMPUT 1 FOR SARDIS, 2 FOR AUDI ACRES.')               AMP00460
      READ(5,*)NTYPE                                                    AMP00470
      IF(NTYPE .GT. 2)GO TO 9997                                        AMP00480
      READ(2,10,END=99)VP1,VP2,VS1,VS2,OMEGA,THETO,D,RHOS,PHI,QSQ,STATSFAMP00490
     2 ,NTHER,NVISC,IARGT,DM,DEP,D1                                     AMP00500
99     IF(NTYPE .NE. 1)GO TO 409                                        AMP00510
      READ(1,10,END=409)VP1,VP2,VS1,VS2,OMEGA,THETO,D,RHOS,PHI,QSQ,     AMP00520
     2 STATSF,NTHER,NVISC,IARGT,DM,DEP,D1                               AMP00530
10     FORMAT(/,1X,7(E10.3,1X),///,1X,6(E10.3,1X),I3,//,1X,3(E10.3,1X)) AMP00540
409   WRITE(11,21)VP1,VP2,VS1,VS2,OMEGA,THETO,D,PHI,QSQ,STATSF,         AMP00550
     2 NTHER,NVISC,IARGT,DM,D1,DEP                                      AMP00560
21     FORMAT(1X,'VP1 = ',E10.3,2X,'VP2 = ',E10.3,2X,'VS1 = '           AMP00570
     2  ,E10.3,3X,'VS2 = ',E10.3,/,1X,'OMEGA = ',E10.3,3X,              AMP00580
     2  'THETO = ',E10.3,3X,'+Z = ',E10.3,/,1X,'FLOW RESIST ='          AMP00590
     2  ,E10.3,3X,'TORTUOSITY = ',E10.3,3X,'STATSF = '                  AMP00600
     2 ,E10.3,/,1X,'NTHER = ',E10.3,3X,'NVISC = ',                      AMP00610
     2  E10.3,3X,'IARGT = ',I2,3X,'DM = ',E10.3,3X,/,1X,'-Z = ',E10.3,3XAMP00620
     2  ,'LAYER THICKNESS = ',E10.3)                                    AMP00630
C***********************************************************************AMP00640
C      FR IS FREQUENCY                                                  AMP00650
C      THETO IS INCIDENT ANGLE                                          AMP00660
C                                                                       AMP00670
      DO 9 I=1,300                                                      AMP00680
      FRQ(I)=I                                                          AMP00690
9     CONTINUE                                                          AMP00700
      FR=10.D0                                                          AMP00710
```

```
C                                                                       AMP00720
      LTHETI=THETO                                                      AMP00730
      THETO=TWOPI*THETO/360.DO                                          AMP00740
      D3=D                                                              AMP00750
C                                                                       AMP00760
C     D IS PROPAGATION DEPTH BELOW SURFACE.                             AMP00770
C     D1 IS PROPAGATION DEPTH ABOVE SURFACE/                            AMP00780
C                                                                       AMP00790
C***********************************************************************AMP00800
C     WAVE NUMBERS:     0  INCIDENT WAVE IN AIR AT THETO.               AMP00810
C                       1  FAST WAVE IN POROUS MEDIUM                   AMP00820
C                       2  SLOW WAVE IN POROUS MEDIUM                   AMP00830
C                       3  SHEAR WAVE IN POROUS MEDIUM                  AMP00840
C                       4  SHEAR WAVE  IN 3RD MEDIUM                    AMP00850
C                       5  FAST WAVE IN 3RD MEDIUM                      AMP00860
C                                                                       AMP00870
C                                                                       AMP00880
C     ******************************************************            AMP00890
C     VO TO V5 ARE THE WAVE VELOCITIES IN CGS UNITS                     AMP00900
C                                                                       AMP00910
C     VO= SOUND SPEED IN AIR                                            AMP00920
C     V1= BIOT FAST WAVE VELOCITY                                       AMP00930
C     V2= BIOT SLOW WAVE VELOCITY                                       AMP00940
C     V3= SHEAR WAVE VELOCITY IN LAYER                                  AMP00950
C     V4= SHEAR WAVE VELOCITY IN LOWER MIDIUM                           AMP00960
C     V5= COMPRESSIONAL WAVE VELOCITY IN LOWER MEDIUM                   AMP00970
C                                                                       AMP00980
C                                                                       AMP00990
C                                                                       AMP01000
C                                                                       AMP01010
C                                                                       AMP01020
C     DENSITIES OF MATERIALS FOR THE SYSTEM:                            AMP01030
C                                                                       AMP01040
C     DENSITY OF AIR, RHOF (CGS UNITS)                                  AMP01050
C                                                                       AMP01060
      RHOF=1.204D-03                                                    AMP01070
C                                                                       AMP01080
C     DENSITY OF CLAY, RHOS AND MEAS VAL. = 2.65 GCM**-3                AMP01090
C                                                                       AMP01100
C                                                                       AMP01110
C     DENSITY OF POROUS LAYER, RHO                                      AMP01120
C                                                                       AMP01130
C                                                                       AMP01140
      RHO=RHOS+OMEGA*(RHOF-RHOS)                                        AMP01150
C                                                                       AMP01160
C                                                                       AMP01170
C***********************************************************************AMP01180
C                                                                       AMP01190
C     GB AND GB2 ARE THE SHEAR MODULI FOR THE LAYER AND CLAY            AMP01200
C                                                                       AMP01210
        GB = VS1*VS1*RHO                                                AMP01220
C                                                                       AMP01230
        GB2 = VS2*VS2*RHOS                                              AMP01240
```

```
C                                                                       AMP01250
        KBBAR = VP1*VP1*RHO - 4.D0/3.D0*GB                              AMP01260
C                                                                       AMP01270
        KR = VP2*VP2*RHOS - 4.D0/3.D0*GB2                               AMP01280
C                                                                       AMP01290
C                                                                       AMP01300
C     ************************************************************      AMP01310
C     EQUATIONS TO CALCULATE H,C,M FOR THE POROUS MEDIUM                AMP01320
C     ARE TAKEN FROM  STEVE ADDISONS SEMINAR.                           AMP01330
C     H IS HH1,C IS CC1, M IS MM1                                       AMP01340
C                                                                       AMP01350
C                                                                       AMP01360
C     FOR THE LAYER:  BULK MOD FOR THE GRAINS IS SAME AS CLAY, KR       AMP01370
C                     BULK MOD FOR THE FRAME IS INPUT, KBBAR            AMP01380
C                     BULK MOD OF FLUID =ATM. PRES. 1.01E6 KF           AMP01390
      KF=1.01D06                                                        AMP01400
C                                                                       AMP01410
C                                                                       AMP01420
C     TEMP=KR*(1.D0+OMEGA*(KR/KF-1.D0))                                 AMP01430
C                                                                       AMP01440
C     HH1=(KR-KBBAR)**2.D0/(TEMP-KBBAR)+KBBAR+GB*4.D0/3.D0              AMP01450
C                                                                       AMP01460
C     CC1=KR*(KR-KBBAR)/(TEMP-KBBAR)                                    AMP01470
C                                                                       AMP01480
C     MM1=KR**2.D0/(TEMP-KBBAR)                                         AMP01490
C                                                                       AMP01500
C                                                                       AMP01510
CC    WRITE(6,30)HH1,CC1,MM1                                            AMP01520
30    FORMAT(1X,'H=',2E13.6,2X,'C=',2E13.6,2X,'M=',2E13.6)              AMP01530
C                                                                       AMP01540
C***********************************************************************AMP01550
C                                                                       AMP01560
C     DO 101 J1=5,10,5                                                  AMP01570
      DO 201 I=1,30                                                     AMP01580
11     CALL PROP(FR,L2,L1)                                              AMP01590
C                                                                       AMP01600
C                                                                       AMP01610
C       WRITE(6,30)HH1,CC1,MM1                                          AMP01620
C                                                                       AMP01630
      V1=TWOPI*FR/L1                                                    AMP01640
      V2=TWOPI*FR/L2                                                    AMP01650
C     WRITE(11,50) L2,L1                                                AMP01660
50    FORMAT(5X,'BIOT WAVE CONSTANTS',/                                 AMP01670
     2  ,10X,'SLOW WAVE CON. = ',E13.6,',',E13.6,                       AMP01680
     2  /,10X,'FAST WAVE CON. = ',E13.6,',',E13.6,/)                    AMP01690
C                                                                       AMP01700
      V0=3.43D4                                                         AMP01710
C                                                                       AMP01720
C                                                                       AMP01730
C                                                                       AMP01740
C                                                                       AMP01750
C     WRITE(6,65)KBBAR,KR,GB,GB2                                        AMP01760
65    FORMAT(1X,'KBBAR=',E13.2,2X,'KR=',E13.2,2X,'GB=',E13.2,2X         AMP01770
     2  ,'GB2=',E13.2,///)                                              AMP01780
```

```
C                                                                       AMP01790
C                                                                       AMP01800
C***********************************************************************AMP01810
C                                                                       AMP01820
C      M1 AND M2 ARE THE RATIOS OF THE  RELATIVE WAVE TO THE            AMP01830
C      MATRIX WAVE(FAST, SLOW)                                          AMP01840
C                                                                       AMP01850
C      EQUATIONS FOR M1 AND M2 TAKEN FROM GEERTSMA AND SMIT             AMP01860
C      GEOPHYSICS V.26 APR 1961                                         AMP01870
C      ASPECTS OG ELASTIC WAVE PROG. IN FLD. SAT. POROUS SOLIDS.        AMP01880
C                                                                       AMP01890
C***********************************************************************AMP01900
C                                                                       AMP01910
       Z1= HH1*L1*L1/(RHO*TWOPI*TWOPI*FR*FR)                            AMP01920
C                                                                       AMP01930
       Z2= HH1*L2*L2/(RHO*TWOPI*TWOPI*FR*FR)                            AMP01940
C                                                                       AMP01950
       M1= (HH1*(Z1-1.D0))/(Z1*CC1-RHOF*HH1/RHO)                        AMP01960
C                                                                       AMP01970
       M2= (HH1*(Z2-1.D0))/(Z2*CC1-RHOF*HH1/RHO)                        AMP01980
C                                                                       AMP01990
C      WRITE(11,40)M1,M2                                                AMP02000
40     FORMAT(1X,'M1=',E13.6,E13.6,2X,'M2=',E13.6,E13.6,///)            AMP02010
C                                                                       AMP02020
C*************************************************************        AMP02030
C                                                                       AMP02040
C LAME'S CONSTANTS FOR THE LOWER MEDIUM ARE LAM2,GB2                    AMP02050
C                                                                       AMP02060
       LAM2=KR + (4.D0/3.D0)*GB2                                        AMP02070
C                                                                       AMP02080
C                                                                       AMP02090
C                                                                       AMP02100
C                                                                       AMP02110
C*****************************************************************    AMP02120
C                                                                       AMP02130
C       L0  -  L5  ARE THE WAVE NUMBERS                                 AMP02140
C                                                                       AMP02150
C                                                                       AMP02160
       L0=TWOPI*FR/V0                                                   AMP02170
       L3=TWOPI*FR/VS1                                                  AMP02180
       L4=TWOPI*FR/VS2                                                  AMP02190
       L5=TWOPI*FR/VP2                                                  AMP02200
C                                                                       AMP02210
C                                                                       AMP02220
       L0S=L0*L0                                                        AMP02230
       L1S=L1*L1                                                        AMP02240
       L2S=L2*L2                                                        AMP02250
       L3S=L3*L3                                                        AMP02260
       L4S=L4*L4                                                        AMP02270
       L5S=L5*L5                                                        AMP02280
C      ***************************************************              AMP02290
C                                                                       AMP02300
C      S0,S1,C0,C1, ETC ATE THE SINES AND COSINES OF THE                AMP02310
C      INCIDENT, REFLECTED AND REFRACTED ANGLES.                        AMP02320
C
```

```
                                                                      AMP02330
C     ************************************************************    AMP02340
      SO=DSIN(THETO)                                                  AMP02350
      CO=DCOS(THETO)                                                  AMP02360
      SSQ=SO*SO                                                       AMP02370
      C1=CDSQRT(1.DO-LOS*SSQ/L1S)                                     AMP02380
      C2=CDSQRT(1.DO-LOS*SSQ/L2S)                                     AMP02390
      TEMP3=1.DO-LOS*SSQ/L3S                                          AMP02400
      TEMP4=1.DO-LOS*SSQ/L4S                                          AMP02410
      TEMP5=1.DO-LOS*SSQ/L5S                                          AMP02420
      C3=CDSQRT(TEMP3)                                                AMP02430
      C4=CDSQRT(TEMP4)                                                AMP02440
      C5=CDSQRT(TEMP5)                                                AMP02450
      LOSO=LO*SO                                                      AMP02460
      S1=LOSO/L1                                                      AMP02470
      S2=LOSO/L2                                                      AMP02480
      S3=LOSO/L3                                                      AMP02490
      S4=LOSO/L4                                                      AMP02500
      S5=LOSO/L5                                                      AMP02510
C                                                                     AMP02520
C     ******************************************************          AMP02530
C                                                                     AMP02540
C     Q1 - Q5 IS THE WAVE NUMBER * COS(ANGLE) * LAYER THICKNESS       AMP02550
C                                                                     AMP02560
C     DEP IS THE DEPTH OF LAYER                                       AMP02570
C                                                                     AMP02580
      Q1=L1*C1*DEP                                                    AMP02590
      Q2=L2*C2*DEP                                                    AMP02600
      Q3=L3*C3*DEP                                                    AMP02610
      Q4=L4*C4*DEP                                                    AMP02620
      Q5=L5*C5*DEP                                                    AMP02630
C     WRITE(6,*)Q1,Q2,Q3,Q4,Q5                                        AMP02640
C                                                                     AMP02650
C     ************************************************************    AMP02660
C                                                                     AMP02670
C     EXPI OR EXPII ARE THE EXPONENTIALS IN THE B. C. EQUATIONS       AMP02680
C                                                                     AMP02690
C                                                                     AMP02700
      EXP11 =CDEXP(-J*Q1)                                             AMP02710
      EXP1=CDEXP(J*Q1)                                                AMP02720
      EXP12=CDEXP(-J*Q2)                                              AMP02730
      EXP2=CDEXP(J*Q2)                                                AMP02740
      EXP3=CDEXP(J*Q3)                                                AMP02750
      EXP13=CDEXP(-J*Q3)                                              AMP02760
      EXP4=CDEXP(J*Q4)                                                AMP02770
      EXP14=CDEXP(-J*Q4)                                              AMP02780
      EXP5=CDEXP(J*Q5)                                                AMP02790
      EXP15=CDEXP(-J*Q5)                                              AMP02800
C                                                                     AMP02810
C      ************************************************************   AMP02820
C                                                                     AMP02830
C     THE A SUB II'S ARE THE COEF. IN THE B. C. EQUATIONS.            AMP02840
C                                                                     AMP02850
C                                                                     AMP02860
```

```
A(1,1)=(1.D0-M1)*C1                                                    AMP02870
A(1,2)=-A(1,1)                                                         AMP02880
A(1,3)=(1.D0-M2)*C2                                                    AMP02890
A(1,4)=-A(1,3)                                                         AMP02900
A(1,5)=S3                                                              AMP02910
A(1,6)=-S3                                                             AMP02920
A(1,7)=(0.D0,0.D0)                                                     AMP02930
A(1,8)=(0.D0,0.D0)                                                     AMP02940
A(1,9)=C0                                                              AMP02950
A(2,1)=2.D0*L1*S1*C1                                                   AMP02960
A(2,2)=-A(2,1)                                                         AMP02970
A(2,3)=2.D0*L2*C2*S2                                                   AMP02980
A(2,4)=-A(2,3)                                                         AMP02990
A(2,5)=-(L3*C3*C3-L3*S3*S3)                                            AMP03000
A(2,6)=-A(2,5)                                                         AMP03010
A(2,7)=(0.D0,0.D0)                                                     AMP03020
A(2,8)=(0.D0,0.D0)                                                     AMP03030
A(2,9)=(0.D0,0.D0)                                                     AMP03040
A(3,1)=L1*(HH1-M1*CC1-2.D0*GB*S1*S1)                                   AMP03050
A(3,2)=A(3,1)                                                          AMP03060
A(3,3)=L2*(HH1-M2*CC1-2.D0*GB*S2*S2)                                   AMP03070
A(3,4)=A(3,3)                                                          AMP03080
A(3,5)=2.D0*GB*L3*S3*C3                                                AMP03090
A(3,6)=A(3,5)                                                          AMP03100
A(3,7)=(0.D0,0.D0)                                                     AMP03110
A(3,8)=(0.D0,0.D0)                                                     AMP03120
  A(3,9)=-KF*L0                                                        AMP03130
A(4,1)=L1*(CC1-M1*MM1)                                                 AMP03140
A(4,2)= A(4,1)                                                         AMP03150
A(4,3)=L2*(CC1-M2*MM1)                                                 AMP03160
A(4,4)=A(4,3)                                                          AMP03170
A(4,5)=(0.D0,0.D0)                                                     AMP03180
A(4,6)=(0.D0,0.D0)                                                     AMP03190
A(4,7)=(0.D0,0.D0)                                                     AMP03200
A(4,8)=(0.D0,0.D0)                                                     AMP03210
  A(4,9)=-KF*L0                                                        AMP03220
A(5,1)=C1*EXP1                                                         AMP03230
A(5,2)=-C1*EXP11                                                       AMP03240
A(5,3)=C2*EXP2                                                         AMP03250
A(5,4)=-C2*EXP12                                                       AMP03260
A(5,5)=S3*EXP3                                                         AMP03270
A(5,6)=-S3*EXP13                                                       AMP03280
A(5,7)=-C5*EXP5                                                        AMP03290
A(5,8)=-S4*EXP4                                                        AMP03300
A(5,9)=(0.D0,0.D0)                                                     AMP03310
A(6,1)=S1*EXP1                                                         AMP03320
A(6,2)=S1*EXP11                                                        AMP03330
A(6,3)=S2*EXP2                                                         AMP03340
A(6,4)=S2*EXP12                                                        AMP03350
A(6,5)=-C3*EXP3                                                        AMP03360
A(6,6)=-C3*EXP13                                                       AMP03370
A(6,7)=-S5*EXP5                                                        AMP03380
A(6,8)=C4*EXP4                                                         AMP03390
A(6,9)=(0.D0,0.D0)                                                     AMP03400
A(7,1)=A(3,1)*EXP1                                                     AMP03410
```

```
      A(7,2)=A(3,2)*EXP11                                                AMP03420
      A(7,3)=A(3,3)*EXP2                                                 AMP03430
      A(7,4)=A(3,4)*EXP12                                                AMP03440
      A(7,5)=2.D0*GB*L3*S3*C3*EXP3                                       AMP03450
      A(7,6)=2.D0*GB*L3*S3*C3*EXP13                                      AMP03460
      A(7,7)=-L5*EXP5*(LAM2-2.D0*GB2*C5*C5)                              AMP03470
      A(7,8)=2.D0*GB2*L4*S4*C4*EXP4                                      AMP03480
      A(7,9)=(0.D0,0.D0)                                                 AMP03490
      A(8,1)=2.D0*GB*L1*S1*C1*EXP1                                       AMP03500
      A(8,2)=-2.D0*GB*L1*S1*C1*EXP11                                     AMP03510
      A(8,3)=2.D0*GB*L2*S2*C2*EXP2                                       AMP03520
      A(8,4)=-2.D0*GB*L2*S2*C2*EXP12                                     AMP03530
      A(8,5)=-GB*L3*(C3*C3-S3*S3)*EXP3                                   AMP03540
      A(8,6)=GB*L3*(C3*C3-S3*S3)*EXP13                                   AMP03550
      A(8,7)=-2.D0*GB2*L5*C5*S5*EXP5                                     AMP03560
      A(8,8)=GB2*L4*(C4*C4-S4*S4)*EXP4                                   AMP03570
      A(8,9)=(0.D0,0.D0)                                                 AMP03580
      A(9,1)=M1*C1*EXP1                                                  AMP03590
      A(9,2)=-M1*C1*EXP11                                                AMP03600
      A(9,3)=M2*C2*EXP2                                                  AMP03610
      A(9,4)=-M2*C2*EXP12                                                AMP03620
      A(9,5)=(0.D0,0.D0)                                                 AMP03630
      A(9,6)=(0.D0,0.D0)                                                 AMP03640
      A(9,7)=(0.D0,0.D0)                                                 AMP03650
      A(9,8)=(0.D0,0.D0)                                                 AMP03660
      A(9,9)=(0.D0,0.D0)                                                 AMP03670
C                                                                        AMP03680
C************************************************************************AMP03690
C                                                                        AMP03700
C       WRITING  AMPLITUDE RATIOS                                        AMP03710
C                                                                        AMP03720
C      DO 280 I=1,9                                                      AMP03730
C        WRITE(6,110)(A(I,K1),K1=1,9)                                    AMP03740
C280    CONTINUE                                                         AMP03750
C                                                                        AMP03760
110       FORMAT(1X,9(E18.8,',',E14.8,/))                                AMP03770
C                                                                        AMP03780
C     ******************************************************************AMP03790
C                                                                        AMP03800
C                                                                        AMP03810
      B(1)=C0                                                            AMP03820
      B(2)=(0.D0,0.D0)                                                   AMP03830
        B(3)=KF*L0                                                       AMP03840
        B(4)=KF*L0                                                       AMP03850
      B(5)=(0.D0,0.D0)                                                   AMP03860
      B(6)=(0.D0,0.D0)                                                   AMP03870
      B(7)=(0.D0,0.D0)                                                   AMP03880
      B(8)=(0.D0,0.D0)                                                   AMP03890
      B(9)=(0.D0,0.D0)                                                   AMP03900
C     WRITE(6,*)(B(I),I=1,9)                                             AMP03910
C                                                                        AMP03920
C                                                                        AMP03930
C     ******************************************************************AMP03940
```

```
C                                                                       AMP03950
C       SUBROUTINE LEQTIC                                               AMP03960
C                                                                       AMP03970
C       SOLVES SIMULTANEOUS ALGREBRAIC EQUATIONC                        AMP03980
C                                                                       AMP03990
C                                                                       AMP04000
C       ****************************************************************AMP04010
        IA=9                                                            AMP04020
        IB=9                                                            AMP04030
        N=9                                                             AMP04040
        IJOB=0                                                          AMP04050
        M=1                                                             AMP04060
        CALL LEQ2C(A,N,IA,B,M,IB,IJOB,WA,WK,IER)                        AMP04070
C                                                                       AMP04080
C                                                                       AMP04090
C       ****************************************************************AMP04100
C                                                                       AMP04110
C                                                                       AMP04120
        IFREQ=FR                                                        AMP04130
C204     WRITE(11,205)                                                  AMP04140
205     FORMAT(5X,'FREQUENCY',5X'INCIDENT ANGLE')                       AMP04150
C       WRITE(11,210)IFREQ,LTHETI                                       AMP04160
210     FORMAT(6X,I4,15X,I2,//)                                         AMP04170
C       WRITE(11,300)                                                   AMP04180
300     FORMAT(9X,'FAST WAVE (DOWN)',20X,' FAST WAVE (UP)')             AMP04190
C       WRITE(11,305)B(1),B(2)                                          AMP04200
305     FORMAT(1X,E14.8,1X,',',1X,E14.8,5X,E14.8,1X,',',1X,E14.8,//)    AMP04210
C       WRITE(11,310)                                                   AMP04220
310     FORMAT(9X,'SLOW WAVE (DOWN)',21X,'SLOW WAVE (UP)')              AMP04230
C       WRITE(11,305)B(3),B(4)                                          AMP04240
C       WRITE(11,320)                                                   AMP04250
320     FORMAT(9X,'SHEAR WAVE (DOWN)',20X,'SHEAR WAVE (UP)')            AMP04260
C       WRITE(11,305)B(5),B(6)                                          AMP04270
C       WRITE(11,330)                                                   AMP04280
330     FORMAT(9X,'TRANS. COMP. WAVE',20X,'TRANS. SHEAR WAVE')          AMP04290
C       WRITE(11,305)B(7),B(8)                                          AMP04300
        WRITE(6,340)                                                    AMP04310
340     FORMAT(9X,'REFL WAVE')                                          AMP04320
        WRITE(6,305)B(9)                                                AMP04330
C       WRITE(6,*)(B(I),I=1,9)                                          AMP04340
C                                                                       AMP04350
C***********************************************************************AMP04360
        CALL SUFIMP(B,LO,KF,RHOF,VO,CO,FR,ZREAL1,ZIMAG1)                AMP04370
        ZREAL(I)=ZREAL1                                                 AMP04380
        ZIMAG(I)=ZIMAG1                                                 AMP04390
C         IF(D.GT.DEP) GO TO 1090                                       AMP04400
C       CALL TRANSF(B,M1,M2,FR,D,D1,MAGGO,MAGPB,PHSGO,PHSPB)            AMP04410
C         CALL RTRANS(B,FR,D,D1,RMAG,RPHAS)                             AMP04420
          GO TO 1095                                                    AMP04430
C1090     CALL LTRANF(B,LO,RHOF,KF,FR,DPRIME,MAGGO,PHSGO)               AMP04440
1095     CONTINUE                                                       AMP04450
        MAGGEO(I)=MAGGO                                                 AMP04460
C         WRITE(6,13)FR,MAGGO,MAGPB                                     AMP04470
C13       FORMAT(1X,3(E14.3))                                           AMP04480
```

```
      MAGPRB(I)=MAGPB                                                    AMP04490
      PHSGEO(I)=PHSGO                                                    AMP04500
      PHSPRB(I)=PHSPB                                                    AMP04510
C                                                                        AMP04520
C     WRITING VALUES FOR TRANSFER FUNCTION AND SURFACE IMPEDANCE.        AMP04530
C                                                                        AMP04540
C     WRITE(6,256)MAGGEO(I),PHSGEO(I),MAGPRB(I),PHSPRB(I),ZREAL(I)       AMP04550
C    2   ,ZIMAG(I),RMAG,RPHAS                                           AMP04560
256   FORMAT(1X,8E12.4)                                                  AMP04570
        WRITE(6,257)ZREAL(I),ZIMAG(I)                                    AMP04580
257     FORMAT(1X,2E12.4)                                                AMP04590
505   FORMAT(1X,'MAD FOR VERT GEO. = ',E14.8,/                           AMP04600
     2  ,1X,'PHAS FOR VERT GEO. = ',E14.8,//                            AMP04610
     2  ,1X,'MAG FOR PROBE = ',E14.8,/,                                 AMP04620
     2  1X,'PHAS FOR PROBE = ',E14.8,//                                 AMP04630
     2  ,1X,'REAL PART OF IMPEDANCE = ',E14.8,/,                        AMP04640
     2  1X,'IMAG PART OF IMPEDANCE = ',E14.8,//)                        AMP04650
C                                                                        AMP04660
C     MAGG2(I)=MAGGEO(I)                                                 AMP04670
C     MAGP2(I)=MAGPRB(I)                                                 AMP04680
        FR = FR + 10.0D0                                                 AMP04690
201   CONTINUE                                                           AMP04700
C     IF(J1.GE.10)GO TO 1100                                             AMP04710
C     DO 301 I1=1,12                                                     AMP04720
C     MAGG1(I1)=MAGG2(I1)                                                AMP04730
C     MAGP1(I1)=MAGP2(I1)                                                AMP04740
C301   CONTINUE                                                          AMP04750
C     D = D + 1.D0                                                       AMP04760
C     FR = 25.D0                                                         AMP04770
C101   CONTINUE                                                          AMP04780
1100  CONTINUE                                                           AMP04790
C     FR = 25.                                                           AMP04800
C     DELD = D - D3                                                      AMP04810
C     DO 401 I=1,12                                                      AMP04820
C     ATDBG(I)=(-1.D0)*(DLOG(MAGG2(I))-DLOG(MAGG1(I)))*20.D0*DLOG10(E)/AMP04830
C    2 DELD                                                              AMP04840
C     ATDBP(I)=(-1.D0)*(DLOG(MAGP2(I))-DLOG(MAGP1(I)))*20.D0*DLOG10(E)/AMP04850
C    2 DELD                                                              AMP04860
C     FR = FR + 25.D0                                                    AMP04870
C401   CONTINUE                                                          AMP04880
C     WRITE(11,203)                                                      AMP04890
203   FORMAT(1X,'FREQ, ATTENUATION IN DB OF PROBE AND VERT. GEO.')       AMP04900
C     WRITE(11,506)(FRQ(I),ATDBP(I),ATDBG(I),I=1,12)                     AMP04910
506   FORMAT(1X,3(E14.8,1X))                                             AMP04920
9997        STOP                                                         AMP04930
      END                                                                AMP04940
```

APPENDIX A.3

The routine SUFIMP.FORTRAN computes the real (ZREAL) and imaginary (ZIMAG) parts of the acoustic surface impedance relative to air using equation 67. The input arguments passed are all defined in AMPL.FORTRAN (see Appendix A.2).

```
C         SUBROUTINE TO CALCULATE THE                                    SUF00010
C         REAL AND IMAGINARY PARTS OF                                    SUF00020
C         THE SURFACE IMPEDANCE.                                         SUF00030
          SUBROUTINE SUFIMP(B,LO,KF,RHOF,VO,CO,FR,ZREAL,ZIMAG)           SUF00040
          IMPLICIT REAL *8 (A-H,O-Z)                                     SUF00050
         COMPLEX *16 B(9)                                                SUF00060
         COMPLEX *16 J,PRES,VEL,ZNOT                                     SUF00070
         REAL *8 KF,LO                                                   SUF00080
C        CALCULATE PRESSURE AND VELOCITY AT THE SURFACE.                 SUF00090
         J=(0.D0,1.D0)                                                   SUF00100
         TWOPI=4.D0*DARSIN(1.D0)                                         SUF00110
C        PRES = RHOF*VO*CO*(1.D0+B(9))*(-J*TWOPI*FR)                     SUF00120
         PRES = -J*KF*LO*(1.D0+B(9))                                     SUF00130
         VEL=CO*(1.D0-B(9))*(-J*TWOPI*FR)                                SUF00140
         ZNOT=PRES/VEL                                                   SUF00150
         ZREAL=DREAL(ZNOT)/(RHOF*VO)                                     SUF00160
         ZIMAG=DIMAG(ZNOT)/(RHOF*VO)                                     SUF00170
C        WRITE(6,13)ZREAL,ZIMAG                                          SUF00180
13     FORMAT(1X,'IMPEDANCE = ',2(E14.3))                                SUF00190
         RETURN                                                          SUF00200
         END                                                             SUF00210
```

APPENDIX A.4

The subroutine TRANSF.FORTRAN computes the acoustic and vertical seismic transfer functions for the porous sand using equations 77 and 79, respectively. TRANSF returns the magnitudes (DMAG, DMMAG) and phases (PHAS, PHAS2) of these transfer functions. Input parameters are defined in AMPL.FORTRAN.

```
C*********************************************************************  TRA00010
C                                                                       TRA00020
C      LET WAVES PROPAGATE  AND CALCULATE  VERTICAL TRANSFER FUNCTION   TRA00030
C         FOR MIC AND VERT GEOPHONE                                     TRA00040
C                                                                       TRA00050
          SUBROUTINE TRANSF(B,M1,M2,FR,DPRIME,D1,DMAG,DMMAG,PHAS,PHAS2) TRA00060
          IMPLICIT REAL *8 (A-H,O-Z)                                    TRA00070
          COMPLEX *16 J,L1,L2,C1,C2,C3                                  TRA00080
          COMPLEX *16 TEMP4,TPRES,M1,M2,TEMP6                           TRA00090
          COMPLEX *16 MOVRM,T1,T2,P1,P2,P3,P4                           TRA00100
          COMPLEX *16 PRES,NVEL1,NVEL2,NVEL3,NVEL4,NVEL5,NVEL6         TRA00110
          COMPLEX *16 TNVEL,GOVRM                                       TRA00120
          COMPLEX *16 B(9)                                              TRA00130
          REAL *8 M,KF,KBBAR,KR,L0,L3                                   TRA00140
          COMMON /BLK7/ H,C,M                                           TRA00150
          COMMON /BLK5/ V0,C0,S0,C1,L0,L1,C2,L2,S3,L3,C3                TRA00160
          COMMON /BLK3/ RHOF,GB,KBBAR,KR,RHOS,OMEGA,KF                  TRA00170
          J = (0.D0,1.D0)                                               TRA00180
          TWOPI = 4.D0*DARSIN(1.D0)                                     TRA00190
C                                                                       TRA00200
C     DPRIME IS PROPAGATION DEPTH                                       TRA00210
C     D1 IS PROPAGATION HEIGHT                                          TRA00220
C                                                                       TRA00230
C                                                                       TRA00240
C      CALCULATE PRESSURE AT ABOVE GROUND MIC                           TRA00250
C                                                                       TRA00260
          PRES = -J*KF*L0*(1.D0+B(9))                                   TRA00270
C                                                                       TRA00280
C        CALCULATE NORMAL COMPONENTS OF PARTICLE VELOCITY               TRA00290
C                                                                       TRA00300
          NVEL1 = -J*TWOPI*FR*B(1)*C1*CDEXP(J*L1*C1*DPRIME)             TRA00310
          NVEL2 =  J*TWOPI*FR*B(2)*C1*CDEXP(-J*L1*C1*DPRIME)            TRA00320
          NVEL3 = -J*TWOPI*FR*B(3)*C2*CDEXP(J*L2*C2*DPRIME)             TRA00330
          NVEL4 =  J*TWOPI*FR*B(4)*C2*CDEXP(-J*L2*C2*DPRIME)            TRA00340
          NVEL5 =  J*TWOPI*FR*B(5)*S3*CDEXP(J*L3*C3*DPRIME)             TRA00350
          NVEL6 =  J*TWOPI*FR*B(6)*S3*CDEXP(-J*L3*C3*DPRIME)            TRA00360
          TNVEL = NVEL1 + NVEL2 + NVEL3 + NVEL4 + NVEL5 + NVEL6         TRA00370
          T1 = (C - M1*M)                                               TRA00380
          T2 = (C - M2*M)                                               TRA00390
          P1 = B(1)*L1*T1*CDEXP(J*L1*C1*DPRIME)                         TRA00400
          P2 = B(2)*L1*T1*CDEXP(-J*L1*C1*DPRIME)                        TRA00410
          P3 = B(3)*L2*T2*CDEXP(J*L2*C2*DPRIME)                         TRA00420
          P4 = B(4)*L2*T2*CDEXP(-J*L2*C2*DPRIME)                        TRA00430
          TPRES = P1 + P2 + P3 + P4                                     TRA00440
```

```
C     WRITE(6,13)PRES,TPRES                                          TRA00450
13      FORMAT(1X,4(E8.2,2X))                                        TRA00460
        MOVRM = TPRES/PRES                                           TRA00470
        GOVRM = TNVEL/PRES                                           TRA00480
        TEMP4 = DCONJG(GOVRM)                                        TRA00490
        TEMP6 = DCONJG(MOVRM)                                        TRA00500
        TEMP5 = GOVRM*TEMP4                                          TRA00510
        TEMP7 = MOVRM*TEMP6                                          TRA00520
        DMAG  = DSQRT(TEMP5)                                         TRA00530
        DMMAG = DSQRT(TEMP7)                                         TRA00540
        TEMP1 = DIMAG(GOVRM)                                         TRA00550
        TEMP8 = DIMAG(MOVRM)                                         TRA00560
        TEMP2 = DREAL(GOVRM)                                         TRA00570
        TEMP9 = DREAL(MOVRM)                                         TRA00580
        ARG   = TEMP1/TEMP2                                          TRA00590
        ARG2  = TEMP8/TEMP9                                          TRA00600
        PHAS  = DATAN(ARG)*360.D0/TWOPI                              TRA00610
        PHAS2 = DATAN(ARG2)*360.D0/TWOPI                             TRA00620
        RETURN                                                       TRA00630
        END                                                          TRA00640
```

APPENDIX A.5

The subroutine LTRANF.FORTRAN computes the vertical seismic transfer function in the clay by taking the ratio of the normal seismic response to the acoustic pressure at the surface. LTRANF then returns the magnitude (DMAG) and phase (PHAS) of the transfer function. Input arguments are all defined in the main routine AMPL.FORTRAN.

```
C*****************************************************************      LTR00010
C                                                                        LTR00020
C      LET WAVES PROPAGATE  AND CALCULATE  VERTICAL TRANSFER FUNCTION    LTR00030
C         FOR MIC AND VERT GEOPHONE IN CLAY                              LTR00040
C                                                                        LTR00050
          SUBROUTINE LTRANF(B,L0,RHOF,KF,FR,DPRIME,DMAG,PHAS)            LTR00060
          IMPLICIT REAL *8 (A-H,O-Z)                                     LTR00070
          COMPLEX *16 J                                                  LTR00080
          COMPLEX *16 TEMP4,NVEL1,NVEL2                                  LTR00090
          COMPLEX *16 TNVEL,GOVRM,PRES                                   LTR00100
          COMPLEX *16 B(9),C4,C5                                         LTR00110
          REAL *8 L0,KF,L4,L5                                            LTR00120
          COMMON /BLK8/ C4,S4,C5,L4,L5                                   LTR00130
          J = (0.D0,1.D0)                                                LTR00140
          TWOPI = 4.D0*DARSIN(1.D0)                                      LTR00150
C                                                                        LTR00160
C     DPRIME IS PROPAGATION DEPTH                                        LTR00170
C     D1 IS PROPAGATION HEIGHT                                           LTR00180
C                                                                        LTR00190
C                                                                        LTR00200
C      CALCULATE PRESSURE AT ABOVE GROUND MIC                            LTR00210
C                                                                        LTR00220
          PRES = -J*KF*L0*(1.D0+B(9))                                    LTR00230
C                                                                        LTR00240
C        CALCULATE NORMAL COMPONENTS OF PARTICLE VELOCITY                LTR00250
C                                                                        LTR00260
          NVEL1 =  -J*TWOPI*FR*B(8)*S4*CDEXP(J*L4*C4*DPRIME)             LTR00270
          NVEL2 =  -J*TWOPI*FR*B(7)*C5*CDEXP(J*L5*C5*DPRIME)             LTR00280
          TNVEL = NVEL1 + NVEL2                                          LTR00290
          GOVRM = TNVEL/PRES                                             LTR00300
          TEMP4 = DCONJG(GOVRM)                                          LTR00310
          TEMP5 = GOVRM*TEMP4                                            LTR00320
          DMAG  = DSQRT(TEMP5)                                           LTR00330
          TEMP1 = DIMAG(GOVRM)                                           LTR00340
          TEMP2 = DREAL(GOVRM)                                           LTR00350
          ARG   = TEMP1/TEMP2                                            LTR00360
          PHAS  = DATAN(ARG)*360.D0/TWOPI                                LTR00370
          RETURN                                                         LTR00380
          END                                                            LTR00390
```

RTRANS.FORTRAN returns the manitude (DMAG) and phase (PHAS) of the radial seismic transfer function for the porous sand. The routine is the same as TRANSF except that the radial component is taken as opposed to the normal component. The arguments in the call statement are defined in the calling routine, AMPL.FORTRAN.

```
C*****************************************************************      RTR00010
C                                                                        RTR00020
C      LET WAVES PROPAGATE  AND CALCULATE RADIAL  TRANSFER FUNCTION      RTR00030
C                                                                        RTR00040
         SUBROUTINE RTRANS(B,FR,DPRIME,D1,DMAG,PHAS)                     RTR00050
         IMPLICIT REAL *8 (A-H,O-Z)                                      RTR00060
         COMPLEX *16 J,L1,L2,C1,C2,C3,S1,S2                              RTR00070
         COMPLEX *16 TEMP4,TPRES,M1,M2,TEMP6                             RTR00080
         COMPLEX *16 PRES,NVEL1,NVEL2,NVEL3,NVEL4,NVEL5,NVEL6            RTR00090
         COMPLEX *16 TNVEL,GOVRM                                         RTR00100
         COMPLEX *16 B(9)                                                RTR00110
         REAL *8 M,KF,KBBAR,KR,L0,L3                                     RTR00120
         COMMON /BLK8/ S1,S2                                             RTR00130
         COMMON /BLK7/ H,C,M                                             RTR00140
         COMMON /BLK5/ V0,C0,S0,C1,L0,L1,C2,L2,S3,L3,C3                  RTR00150
         COMMON /BLK3/ RHOF,GB,KBBAR,KR,RHOS,OMEGA,KF                    RTR00160
         J = (0.D0,1.D0)                                                 RTR00170
         TWOPI = 4.D0*DARSIN(1.D0)                                       RTR00180
C                                                                        RTR00190
C    DPRIME IS PROPAGATION DEPTH                                         RTR00200
C    D1 IS PROPAGATION HEIGHT                                            RTR00210
C                                                                        RTR00220
C                                                                        RTR00230
C     CALCULATE PRESSURE AT ABOVE GROUND MIC                             RTR00240
C                                                                        RTR00250
         PRES = -J*KF*L0*(1.D0+B(9))                                     RTR00260
C                                                                        RTR00270
C       CALCULATE RADIAL COMPONENTS OF PARTICLE VELOCITY                 RTR00280
C                                                                        RTR00290
         NVEL1 = -J*TWOPI*FR*B(1)*S1*CDEXP(J*L1*C1*DPRIME)               RTR00300
         NVEL2 =  J*TWOPI*FR*B(2)*S1*CDEXP(-J*L1*C1*DPRIME)              RTR00310
         NVEL3 = -J*TWOPI*FR*B(3)*S2*CDEXP(J*L2*C2*DPRIME)               RTR00320
         NVEL4 =  J*TWOPI*FR*B(4)*S2*CDEXP(-J*L2*C2*DPRIME)              RTR00330
         NVEL5 =  J*TWOPI*FR*B(5)*C3*CDEXP(J*L3*C3*DPRIME)               RTR00340
         NVEL6 =  J*TWOPI*FR*B(6)*C3*CDEXP(-J*L3*C3*DPRIME)              RTR00350
         TNVEL = NVEL1 + NVEL2 + NVEL3 + NVEL4 + NVEL5 + NVEL6           RTR00360
         GOVRM = TNVEL/PRES                                              RTR00370
         TEMP4 = DCONJG(GOVRM)                                           RTR00380
         TEMP5 = GOVRM*TEMP4                                             RTR00390
         DMAG  = DSQRT(TEMP5)                                            RTR00400
         TEMP1 = DIMAG(GOVRM)                                            RTR00410
         TEMP2 = DREAL(GOVRM)                                            RTR00420
         ARG   = TEMP1/TEMP2                                             RTR00430
         PHAS  = DATAN(ARG)*360.D0/TWOPI                                 RTR00440
         RETURN                                                          RTR00450
         END                                                             RTR00460
```

APPENDIX A.7

This routine was used to compute the magnitude and phase of the experimental transfer function. Tranff.Bas program first accepts the calibrations (typically 10-15 seconds depending on the length of data record to be analyzed) on channel 0 (always the reference microphone above the ground). The digitized record is always collected in blocks of 1024 points. Due to finite transfer rates, a few points could be dropped between successive 1024 point records. After the calibration tone is digitized, each 1024 point record is Fourier transformed. The magnitudes of the transform at each frequency (512 of these) are added together and these are added to the magnitude determined from each successive 1024 point data record. The total sum is then divided by the number of data records - this is referred to as the calibration level for channel 0. The tape is then moved to the calibration tone on the channel to be analyzed and this process is repeated to give the calibration level for channel 1.

Next the tape is moved to the data for the first third octave band (31.5 Hz). At this point, the data from the reference microphone and channel of interest are simultaneously digitized. Actually channel 0 is sampled first; channel one is sampled a few hundred microseconds later. This small delay gives a small phase difference which must be corrected for later. Once the data is all digitized and stored in memory, each 1024 point data record from channel 0 is Fourier transformed. The simultaneous 1024 point record from channel 1 is next Fourier transformed and the transfer function for these 1024 points is computed giving the transfer function at 512 frequencies. Only those frequencies within the third octave band being considered are kept. The next pair of 1024 point records is transformed and the transfer function computed is added to the first. This process is continued for all the data records for that third octave band.

AD-A146 231 COUPLING OF AIRBORNE SOUND INTO THE EARTH(U) 2/2
MISSISSIPPI UNIV UNIVERSITY PHYSICAL ACOUSTICS RESEARCH
LAB H E BASS ET AL. 01 AUG 84 PARGUM-84-01
UNCLASSIFIED ARO-17560.2-GS DAAG29-81-K-0078 F/G 17/1 NL

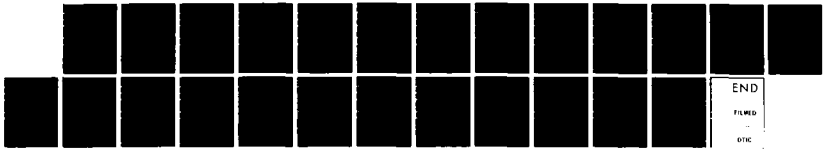

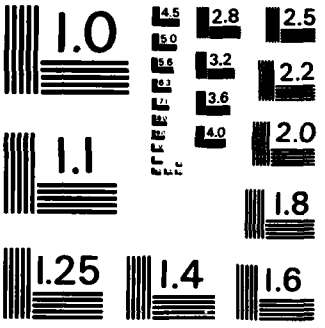

MICROCOPY RESOLUTION TEST CHART
NATIONAL BUREAU OF STANDARDS-1963-A

Next, the tape is advanced to the next third octave band and the process is repeated.

The raw transfer function at each frequency is divided by the calibration levels to get absolute values for the real and imaginary parts of the transfer function. Finally, the real and imaginary parts are converted to a magnitude and phase at each frequency; the results are plotted on an X-Y plotter (program Plotff.Bas, Appendix A.8) and stored on disks.

The plotted transfer function was, in many cases, quite noisy (many sharp spikes). For comparison to theory, sometimes smoothed this data. A seven point averaging routine was used, twice, to smooth the data which was then replotted. The smoothing routine (Program Smooth.Bas, Appendix A.9) computed:

$$Y(0) = \{[Y(-3)+Y(3)]+4[Y(-2)+Y(2)]+11[Y(-1)+Y(1)]+14Y(0)\}/42$$

which replaced Y(0). This procedure was executed twice to result in graphs referred to later as smoothed curves.

As noted earlier, samples from the two channels are actually taken sequentially which means that there is a small time delay between samples on the two channels. This delay was determined experimentally. An oscillator generating a sine wave at one of the 1/3 octave band center frequencies was coupled directly into channel 0 of the computer and the same signal was put through an RC filter (time constant .002 sec) into channel 1. Through such a circuit, the amplitude should vary between 0 (at 0 Hz) and 1 (well above 80 Hz, where $\omega = 1/RC$). The phase should decrease from 90° at 0 Hz to 0° well above 80 Hz. When the amplitude of channel 1 is 0.707 times the amplitude of channel 0, the phase difference should be $+45^{\circ}$. Experimentally, the phase was found to be slightly larger than 45° requiring that we introduce a phase correction of .06 x frequency. Note that at a frequency of 6 kHz, the phase corrections would be 360° implying

a channel to channel delay of 167 sec which is close to the manufacturer's (DEC) specfications. This correction appears on line 5297 of program Tranff.

```
20 OPEN "VM:FILE1.DAT" AS FILE #1
30 OPEN "VM:FILE2.DAT" AS FILE #2
40 OPEN "VM:FILE3.DAT" AS FILE #3
45 OPEN "VM:FILE4.DAT" AS FILE #4
47 OPEN "LP:" FOR OUTPUT AS FILE #7
50 DIM #1,A1%(33768)
60 DIM #2,D1(1024)
70 DIM #3,F1(1024)
75 DIM #4,O(14)
78 DIM C%(1024)
80 COMMON A%(2048)
85 V%=0
100 PRINT "NUMBER OF SECONDS TO BE DIGITIZED?";
110 INPUT S3%
120 S4=S3%-1
130 PRINT "LISTEN FOR CAL. TONE ON CH."V%", PUSH RETURN";
140 INPUT Z$
160 FOR I%=0 TO S4
170 AIN(,A%(),1024,1/1000,V%,1)
180 BLOCK_MOVE(A%(0),A1%(I%*1024),1024)
190 NEXT I%
210 PRINT "STOP TAPE"
230 S2=0
240 FOR I%=1 TO 512
250 D1(I%)=0
260 F1(I%)=0
270 NEXT I%
280 FOR I%=0 TO S3%-1
290 N1=1024*I% \ N2=N1+1023 \ S9%=1
300 GOSUB 7370
310 FFT(,1024,A%(),C%(),S%)
320 FOR J%=1 TO 512
330 D1(J%)=D1(J%)+SQR((A%(J%)*2^S%)^2+(C%(J%)*2^S%)^2)
350 NEXT J%
360 NEXT I%
370 FOR I%=1 TO 512
380 S2=S2+D1(I%)
390 NEXT I%
400 S2=S2/S3%
410 IF V%=1 THEN 460
420 V%=V%+1
430 S1=S2
440 GO TO 130
460 J%=0
470 PRINT S1,S2
570 O(0)=20 \ O(1)=25 \ O(2)=31.5 \ O(3)=40 \ O(4)=50 \ O(5)=63 \ O(6)=80
```

```
670 O(7)=100 \ O(8)=125 \ O(9)=160 \ O(10)=200 \ O(11)=250 \ O(12)=315
870 F0=1000/1024
880 FOR I%=1 TO 1024
900 D1(I%)=0
910 F1(I%)=0
920 NEXT I%
930 S4=S3%-1
970 FOR L%=1 TO 12
1070 CLOSE #1
1170 OPEN "VM:FILE1.DAT" AS FILE #1
1270 Q8%=53
1370 F1=(2^.1667)*O(L%-1)
1470 F2=(2^.1667)*O(L%)
1570 I1%=F1/F0
1670 I2%=F2/F0
1770 PRINT "START TAPE ";O(L%);" HZ AND PRESS RETURN.";
1870 INPUT D9$



1970 SCHMITT(1,8070)
2070 IF Q8%<>-999 THEN 2070
2170 SCHMITT
2370 FOR I%=0 TO S4
2470 AIN(,A%(),2048,1/1000,0,2)
2570 BLOCK_MOVE(A%(0),A1%(I%*2048),2048)
2670 NEXT I%
2870 PRINT "STOP TAPE!!!!!!!!!!!!! "
3370 FOR I%=0 TO S3%-1
3470 N1=2*1024*I% \ N2=N1+2046 \ S9%=2
3570 GOSUB 7370
3670 FFT(,1024,A%(),C%(),S%)
3770 FOR M%=I1% TO I2%
3870 J%=M%+512
3970 D1(M%)=(A%(M%)*2^S%)/S1
4070 D1(J%)=(C%(M%)*2^S%)/S1
4170 NEXT M%
4470 N1=2*1024*I%+1 \ N2=N1+2046 \ S9%=2
4570 GOSUB 7370
4670 FFT(,1024,A%(),C%(),S%)
4770 FOR M%=I1% TO I2%
4870 J%=M%+512
4880 M=D1(M%)^2+D1(J%)^2
4890 R=(A%(M%)*D1(M%)+C%(M%)*D1(J%))*2^S%/S2
4900 I2=(D1(M%)*C%(M%)-A%(M%)*D1(J%))*2^S%/S2
4970 F1(M%)=F1(M%)+SQR((R^2+I2^2)/M^2)
5070 F1(J%)=F1(J%)+ATN(I2/R)
5170 NEXT M%
5270 NEXT I%
5280 FOR I%=I1% TO I2%
5290 M%=I%+512
5291 D1(I%)=I%*F0
5293 F1(I%)=F1(I%)/S3%
```

```
5297 F1(M%)=180*((F1(M%)/S3%)/3.14159)-D1(I%)*60/1000
5310 NEXT I%
5370 NEXT L%
5870 I1%=(2^.1667)*O(0)/FO
5970 I2%=(2^.1667)*O(13)/FO
6070 FOR I%=I1% TO I2%
6170 M%=I%+512
6780 PRINT #7,"FREQ="D1(I%),"MAG="F1(I%),"PHASE="F1(M%)
6970 NEXT I%
7229 CLOSE
7250 CHAIN "PLOTFF.BAS"
7270 STOP
7370 J%=0
7380 FOR I3%=N1 TO N2 STEP S9%
7470 J%=J%+1
7570 C%(J%)=0
7670 A%(J%)=A1%(I3%)
7770 NEXT I3%
7870 RETURN
7970 END
8070 Q8%=-999
8170 RETURN
```

APPENDIX A.8

PLOTFF.BAS was written to plot the output of TRANFF.BAS on an HP 7470A digital plotter.

```
60 OPEN "VM:FILE2.DAT" AS FILE #2
70 OPEN "VM:FILE3.DAT" AS FILE #3
80 DIM #2,D1(1024)
90 DIM #3,F1(1024)
100 L9=2 \ O=1 \ O1=1 \ Q=1
200 DISPLAY_CLEAR
1400 PRINT " input the size of plot (1) full page, and (2) quarter page ? ";
1500 INPUT A%
1600 X9=0 \ X8=0
3400 FOR I=1 TO 2
3450 PRINT "PLEASE PUT PAPER IN H.P. PLOTTER AND PRESS RETURN"; \ INPUT E7$
3475 Y9=0 \ Y8=0 \ L9=2 \ O=1 \ O1=1 \ Q=1
3500 FOR J=1 TO 362
3600 IF I=1 THEN IF Y9<F1(J) THEN Y9=F1(J)
3700 IF I=1 THEN IF Y8>F1(J) THEN Y8=F1(J)
3800 IF I=2 THEN IF Y9<F1(J+512) THEN Y9=F1(J+512)
3900 IF I=2 THEN IF Y8>F1(J+512) THEN Y8=F1(J+512)
3950 IF I=2 THEN 4500
4000 IF X9<D1(J) THEN X9=D1(J)
4100 IF X8>D1(J) THEN X8=D1(J)
4500 NEXT J
4600 IF Y9<3 THEN O1=10000
4700 IF X9<3 THEN O=10000
5100 PAUSE(3)
5200 IF Y9*O1<0 THEN P1=-1
5300 IF Y9*O1>=0 THEN P1=1
5400 Y2=INT(LOG10(ABS(Y9*O1)))
5500 IF Y2<0 THEN Y2=Y2-1
5600 Y3=Y9*O1/10^Y2
5700 IF ABS(Y3)=1 THEN S1=1
5800 IF ABS(Y3)>1 THEN S1=2
5900 IF ABS(Y3)>2 THEN S1=2.5
6000 IF ABS(Y3)>2.5 THEN S1=5
6100 IF ABS(Y3)>5 THEN S1=10
6200 U1=(S1*10^Y2)*P1
6300 IF ABS(Y8*O1)<(1.00000E-03*(Y9*O1)) THEN 7600
6400 IF Y8*O1<0 THEN P2=-1
6500 IF Y8*O1>=0 THEN P2=1
6600 Y4=INT(LOG10(ABS(Y8*O1)))
6700 IF Y4<0 THEN Y4=Y4-1
6800 Y5=Y8*O1/10^Y4
6900 IF ABS(Y5)=1 THEN S2=1
7000 IF ABS(Y5)>1 THEN S2=2
7100 IF ABS(Y5)>2 THEN S2=2.5
7200 IF ABS(Y5)>2.5 THEN S2=5
7300 IF ABS(Y5)>5 THEN S2=10
7400 L1=(S2*10^Y4)*P2
7500 GO TO 8300
7600 L1=0
```

```
8200 PAUSE(3)
8300 IF A%=1 THEN X6=9200 \ Y6=7560
8400 IF A%=2 THEN X6=5150 \ Y6=4180
8410 IF ABS(U1)>30000 THEN Q=100
8420 IF ABS(L1)>30000 THEN Q=100
8500 COUT(,"IN;SP1;",,1)
8600 M$="IP 1100,1600,"+STR$(X6)+","+STR$(Y6)+";"
8700 COUT(,M$,,1)
8800 M$="SC "+STR$(X8*0)+","+STR$(X9*0)+","+STR$(L1/Q)+","+STR$(U1/Q)+";"
8900 COUT(,M$,,1)
9000 M$="PA "+STR$(X8*0)+","+STR$(L1/Q)+",PD,"+STR$(X9*0)+","+STR$(L1/Q)+","
9100 M$=M$+STR$(X9*0)+","+STR$(U1/Q)+","+STR$(X8*0)+","+STR$(U1/Q)+",
     "+STR$(X8*0)+","+STR$(L1/Q)+",PU;"
9200 COUT(,M$,,1)
9300 PAUSE(2)



9900 COUT(,"SR 1,2;",,1)
10000 T1=(ABS(X9*0)+ABS(X8*0))/5
10100 T2=(ABS(L1/Q)+ABS(U1/Q))/5
10200 C=X8*0
10300 FOR J=1 TO 6
10400 M$="PA "+STR$(C)+","+STR$(L1/Q)+";XT;"
10500 COUT(,M$,,1)
10600 M$="PR "+STR$(-(T1*.15))+","+STR$(-(T2*.2))+";"
10700 COUT(,M$,,1)
10800 M$="LB"+STR$(C/0)+CHR$(3)
10900 COUT(,M$,,1)
10950 PAUSE(2)
11000 C=C+T1
11100 NEXT J
11200 PAUSE(4)
11300 C=L1/Q
11400 FOR J=1 TO 6
11500 M$="PA "+STR$(X8*0)+","+STR$(C)+";YT;"
11600 COUT(,M$,,1)
11700 M$="PR "+STR$(-(T1*.4))+",0;LB"+STR$((C/01)*Q)+CHR$(3)
11800 COUT(,M$,,1)
11900 C=C+T2
12000 NEXT J
12050 PAUSE(5)
12600 M$="PA "+STR$(X8*0)+",0;PR "+STR$(-(T1*.4))+",0;LB0 "+CHR$(3)
12700 COUT(,M$,,1)
12800 M$="PA "+STR$(X8*0)+",0,PD,"+STR$(X9*0)+",0,PU;"
12900 COUT(,M$,,1)
13000 PAUSE(5)
13100 IF I=1 THEN A2$="MAGNITUDE"
13200 IF I=2 THEN A2$="PHASE"
13300 A1$="FREQUENCY"
14000 Z1=LEN(A1$)
14100 Z2=LEN(A2$)
14200 M$="PA "+STR$(((X8*0)+(X9*0))/2)+","+STR$(L1/Q)+";"
```

```
14300 COUT(,M$,,1)
14400 M$="PR 0,"+STR$(-(T2*.4))+";"
14500 COUT(,M$,,1)
14600 PAUSE(1)
14700 M$="PR "+STR$(-(T1*.05)*(Z1/2))+",0;LB"+A1$+CHR$(3)
14800 COUT(,M$,,1)
14900 PAUSE(2)
15000 M$="PA "+STR$(X8*O)+","+STR$(((L1/Q)+(U1/Q))/2)+";"
15100 COUT(,M$,,1)
15200 M$="PR "+STR$(-(T1*.6))+",0;"
15300 COUT(,M$,,1)
15400 M$="PR 0,"+STR$(-(T2*.06)*(Z2/2))+";DR 0,1;LB"+A2$+CHR$(3)
15500 COUT(,M$,,1)
15550 COUT(,"SP2;",,1)
16200 PAUSE(20)
17200 M$="PA "+STR$(D1(1)*O)+","+STR$((F1((I-1)*512+1)*O1)/Q)+";PD;"
17300 COUT(,M$,,1)
17400 FOR J=2 TO 362
17450 IF INT(J/100)=J/100 THEN PAUSE(1)
17600 M$="PA "+STR$(D1(J)*O)+","+STR$((F1(((I-1)*512)+J)*O1)/Q)+";"
17700 COUT(,M$,,1)
17800 NEXT J
18000 COUT(,"PU;",,1)
18100 PAUSE(3)
18200 NEXT I
18210 PRINT "WOULD YOU LIKE TO SAVE THESE NUMBERS ON DISK? IF SO TYPE A FILE"
18220 PRINT "NAME IN. IF YOU DON'T WANT TO SAVE THESE NUMBER JUST PRESS RETURN"
18230 PRINT "INPUT FILE NAME"; \ INPUT F4$


18240 IF F4$="" THEN 18300
18250 OPEN "DY1:"+F4$+".XYZ" AS FILE #1
18260 FOR L%=1% TO 362%
18270 PRINT #1,D1(L%)","F1(L%)","F1(L%+512%)
18280 NEXT L%
18290 CLOSE
18300 END
```

APPENDIX A.9

SMOOTH.BAS is a seven point smoothing routine used to smooth the output of TRANFF.BAS and is discussed in Chapter 4 of this report.

```
10 OPEN "VM:FILE2.DAT" AS FILE #2
20 OPEN "VM:FILE3.DAT" AS FILE #3
30 DIM #2,D1(1024)
40 DIM #3,F1(1024)
50 DIM X(512),Y(512),Z(512)
60 PRINT "INPUT FILE NAME"; \ INPUT A1$
70 OPEN "DY1:"+A1$+".XYZ" AS FILE #1
80 FOR I%=1 TO 353
90 INPUT #1,X(I%),Y(I%),Z(I%)
100 NEXT I%
110 N%=0
120 FOR I%=4 TO 350
130 Y(I%)=Y(I%)*14+11*(Y(I%-1)+Y(I%+1))+4*(Y(I%-2)+Y(I%+2))
140 Y(I%)=(Y(I%)-(Y(I%-3)+Y(I%+3)))/42
141 IF Z(I%)<90 GO TO 143
142 Z(I%)=90
143 IF Z(I%)>-90 GO TO 150
144 Z(I%)=-90
150 Z(I%)=Z(I%)*14+11*(Z(I%-1)+Z(I%+1))+4*(Z(I%-2)+Z(I%+2))
160 Z(I%)=(Z(I%)-(Z(I%-3)+Z(I%+3)))/42
170 NEXT I%
171 Y(350)=0
172 Z(350)=0
180 N%=N%+1
190 IF N%=1 GO TO 120
200 BLOCK_MOVE(X(0),D1(0),512)
210 BLOCK_MOVE(Y(0),F1(0),512)
220 BLOCK_MOVE(Z(0),F1(513),512)
230 CLOSE
240 CHAIN "PLOTFF.BAS"
250 END
```

APPENDIX B

Included here is a larger and more complete sample of the experimental data collected. The purpose is twofold; one, to present a sample of the raw data before smoothing calculations were done and two, to make available samples of the radial and transverse seismic transfer function which were not included in the body of the report. The data chosen for presentation were collected at the UM test field and have not been scaled. The units have been left off the axes, however, they are the same as on earlier graphs. On each figure is a legend which includes the date, angle of incidence, depth of the sensor and the axis of the geophone or probe.

Figures 1-4 indicate the poor signal to noise ratio obtained as the angle of incidence was changed from 20^{o} to 5^{o}. The remaining eight figures are the magnitudes and phases of the vertical, radial and transverse seismic transfer function and the probe transfer function.

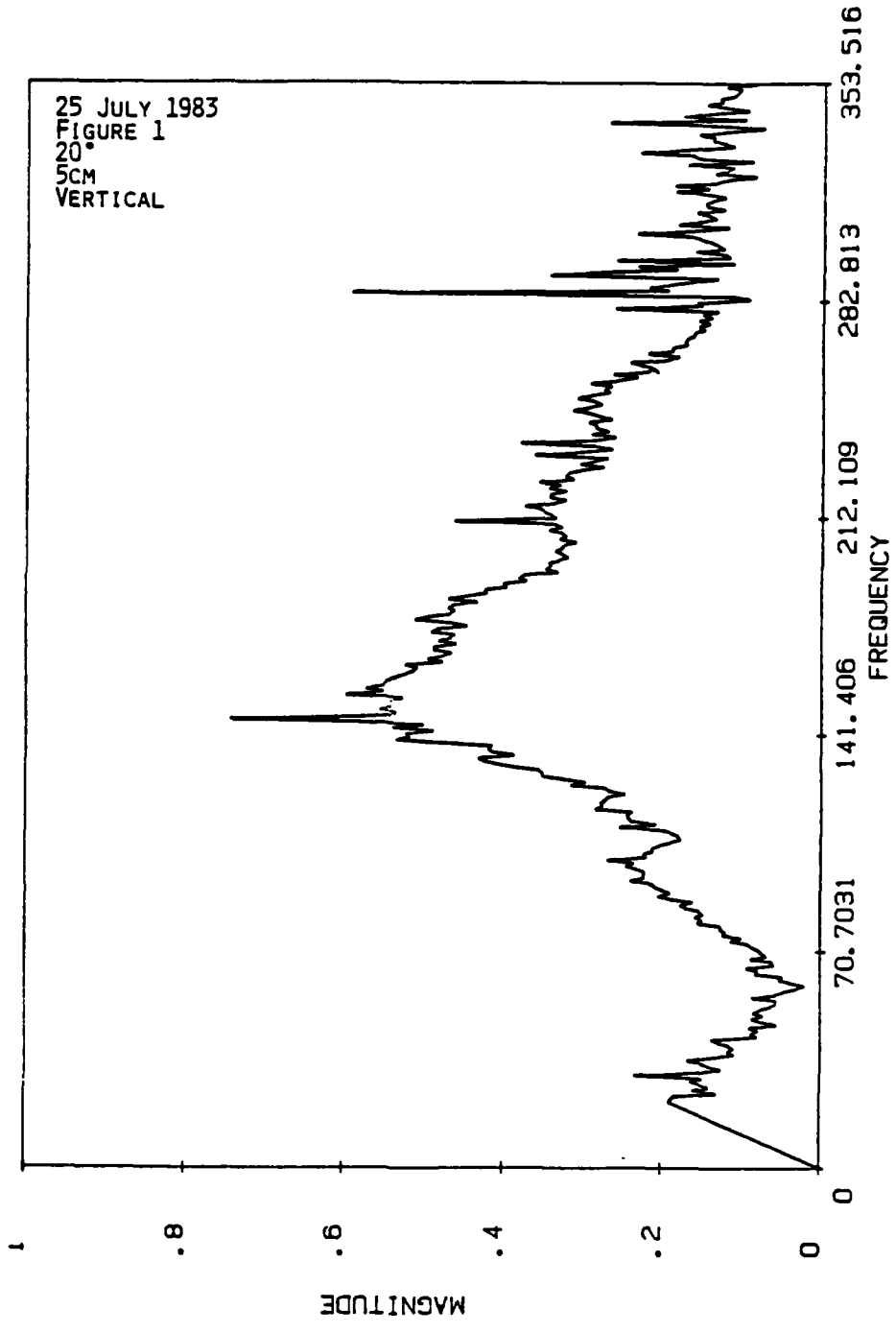
25 JULY 1983
FIGURE 1
20°
5CM
VERTICAL
353.516
282.813
212.109
141.406
70.7031
0
FREQUENCY
1
.8
.6
.4
.2
0
MAGNITUDE

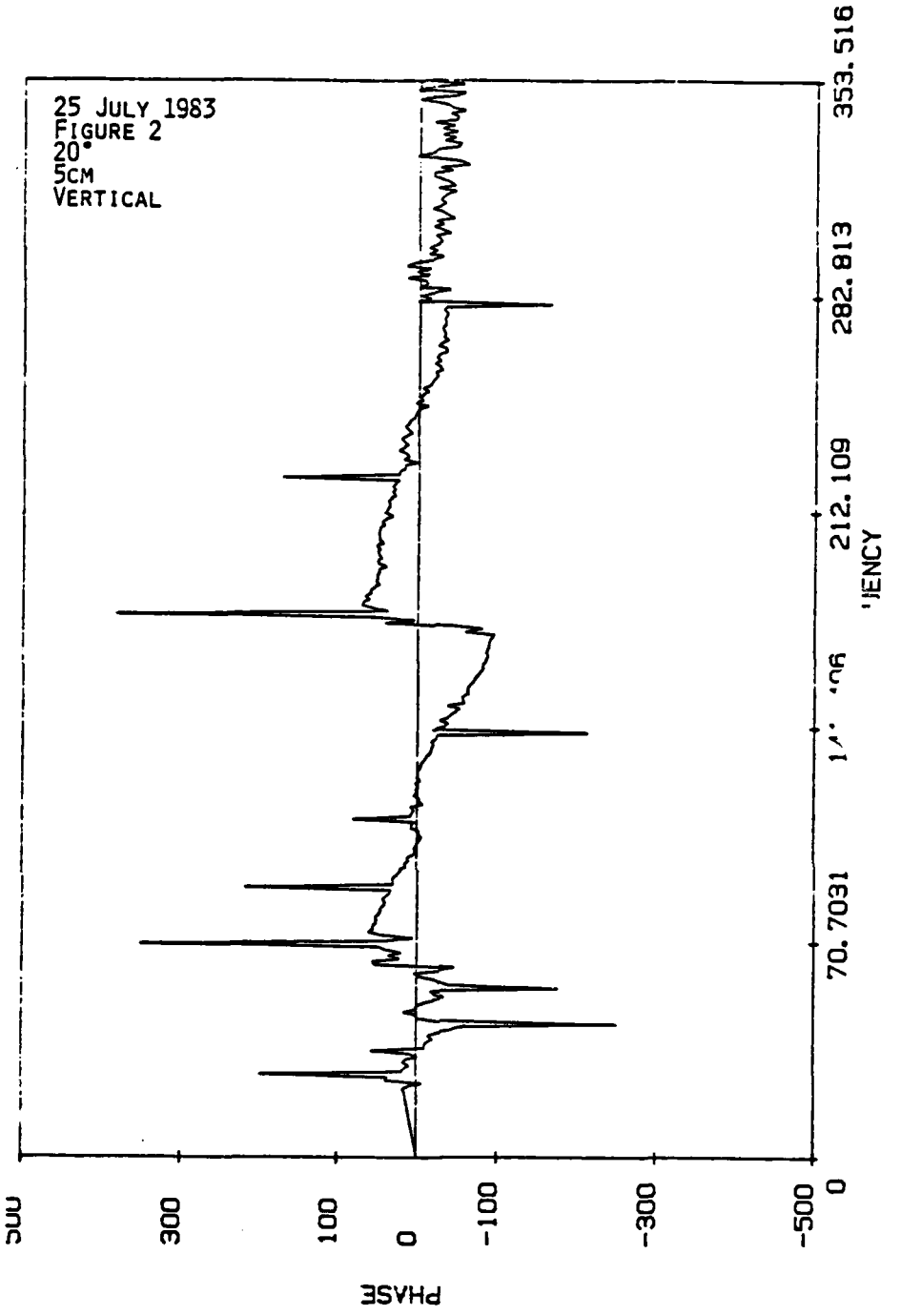
25 JULY 1983
FIGURE 2
20°
5CM
VERTICAL
353.516
282.813
212.109
70.7031
FREQUENCY
500
300
100
0
-100
-300
-500
PHASE

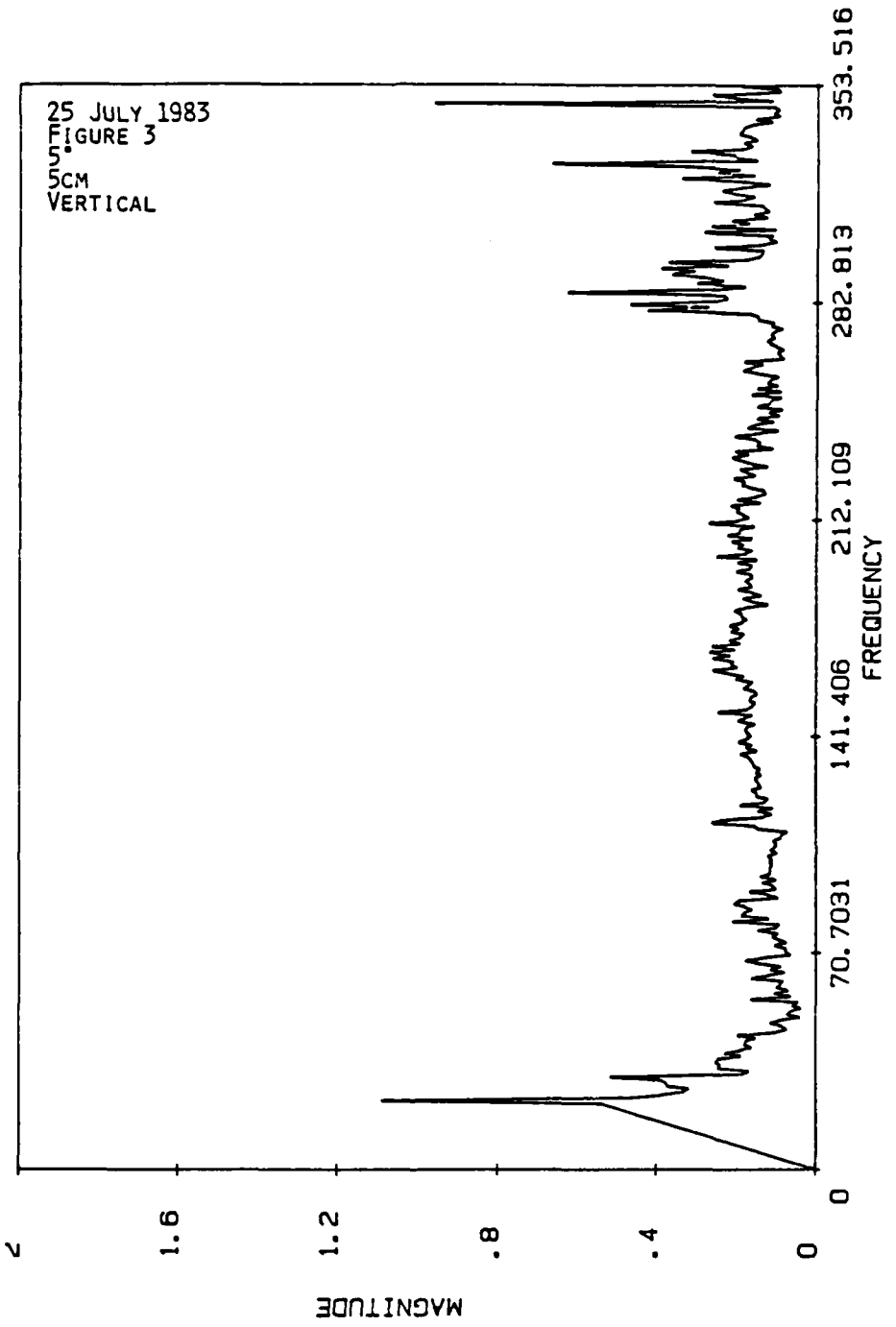
25 JULY 1983
FIGURE 3
5°
5CM
VERTICAL
MAGNITUDE
2
1.6
1.2
.8
.4
0
0
70.7031
141.406
212.109
282.813
353.516
FREQUENCY

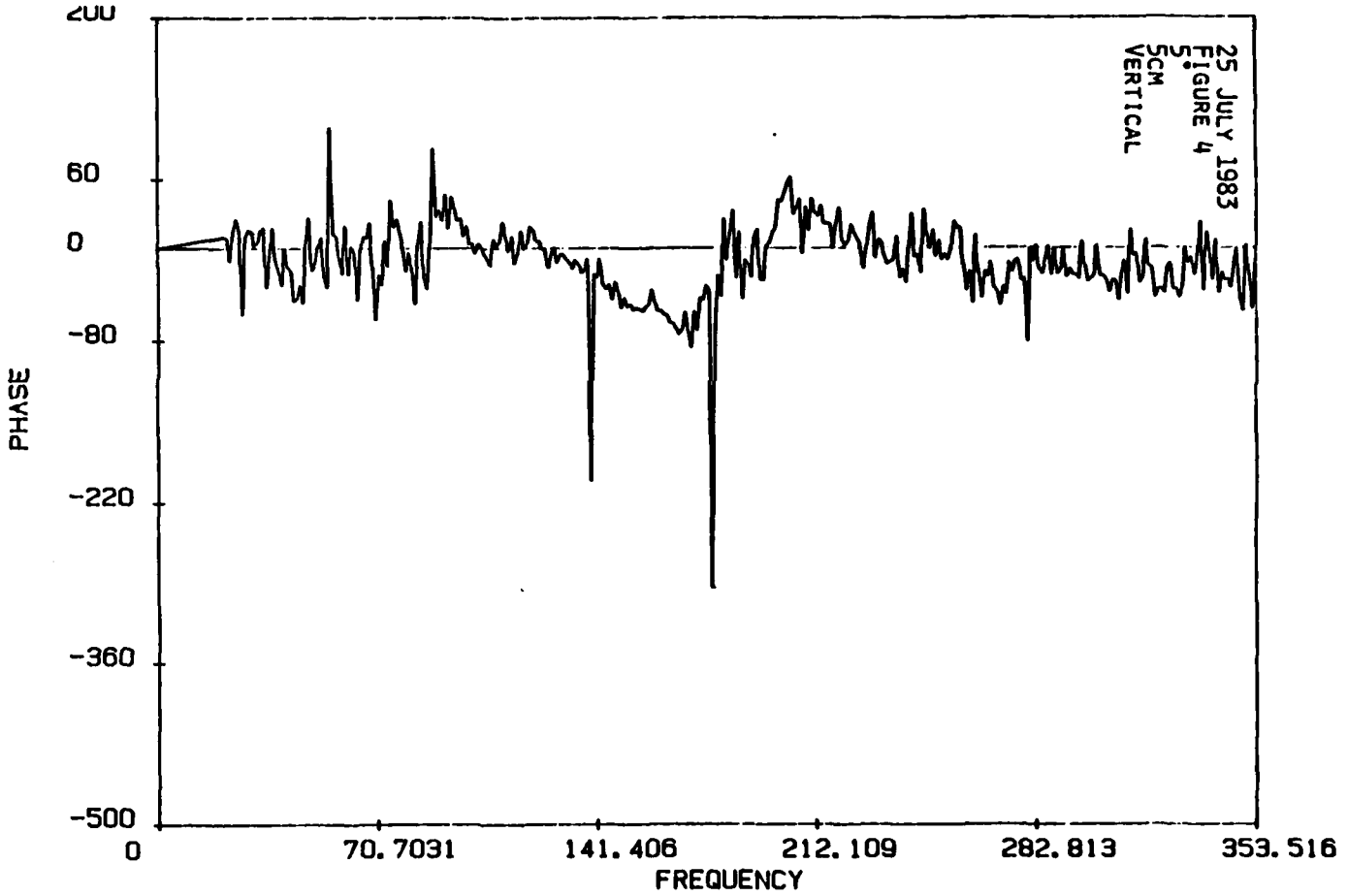
25 JULY 1983
FIGURE 4
5.
5CM
VERTICAL
200
60
0
-80
-220
-360
-500
PHASE
0
70.7031
141.406
212.109
282.813
353.516
FREQUENCY

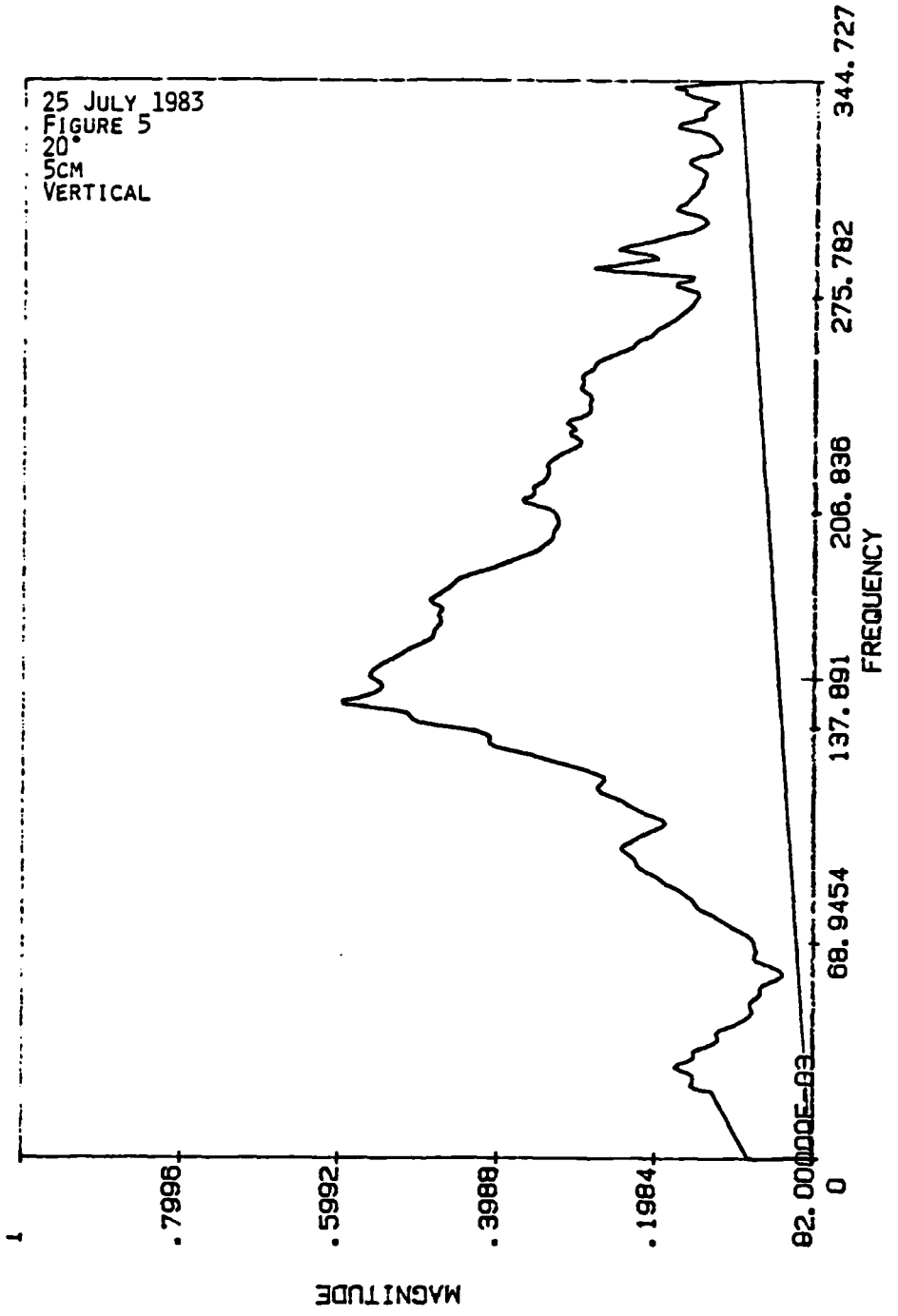
25 JULY 1983
FIGURE 5
20°
5CM
VERTICAL
MAGNITUDE
1
.7996
.5992
.3988
.1984
82.00000E-03
0
68.9454
137.891
206.836
275.782
344.727
FREQUENCY

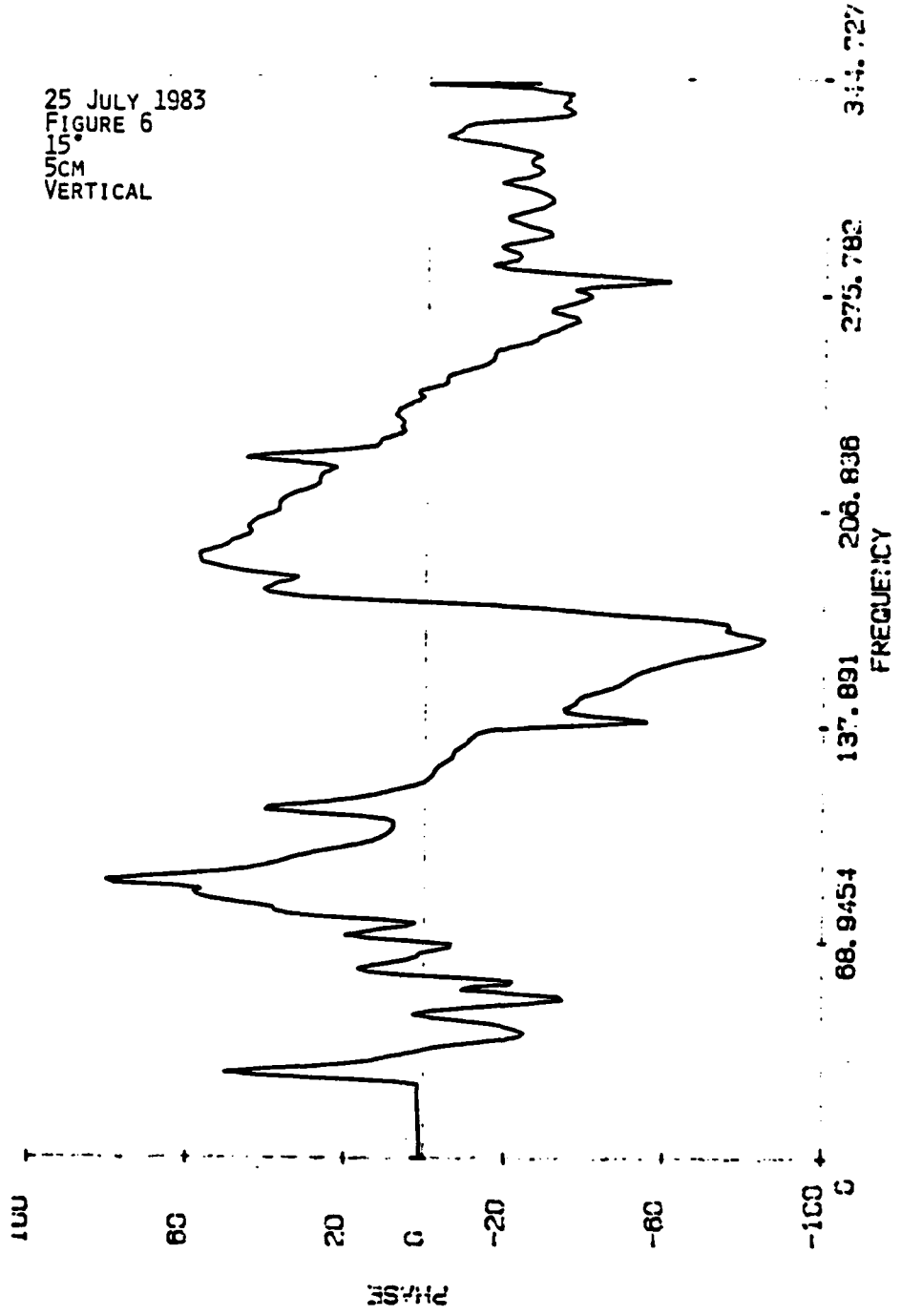
25 JULY 1983
FIGURE 6
15°
5CM
VERTICAL
88.9454
137.891
208.836
275.782
FREQUENCY
100
60
20
0
-20
-60
-100
PHASE

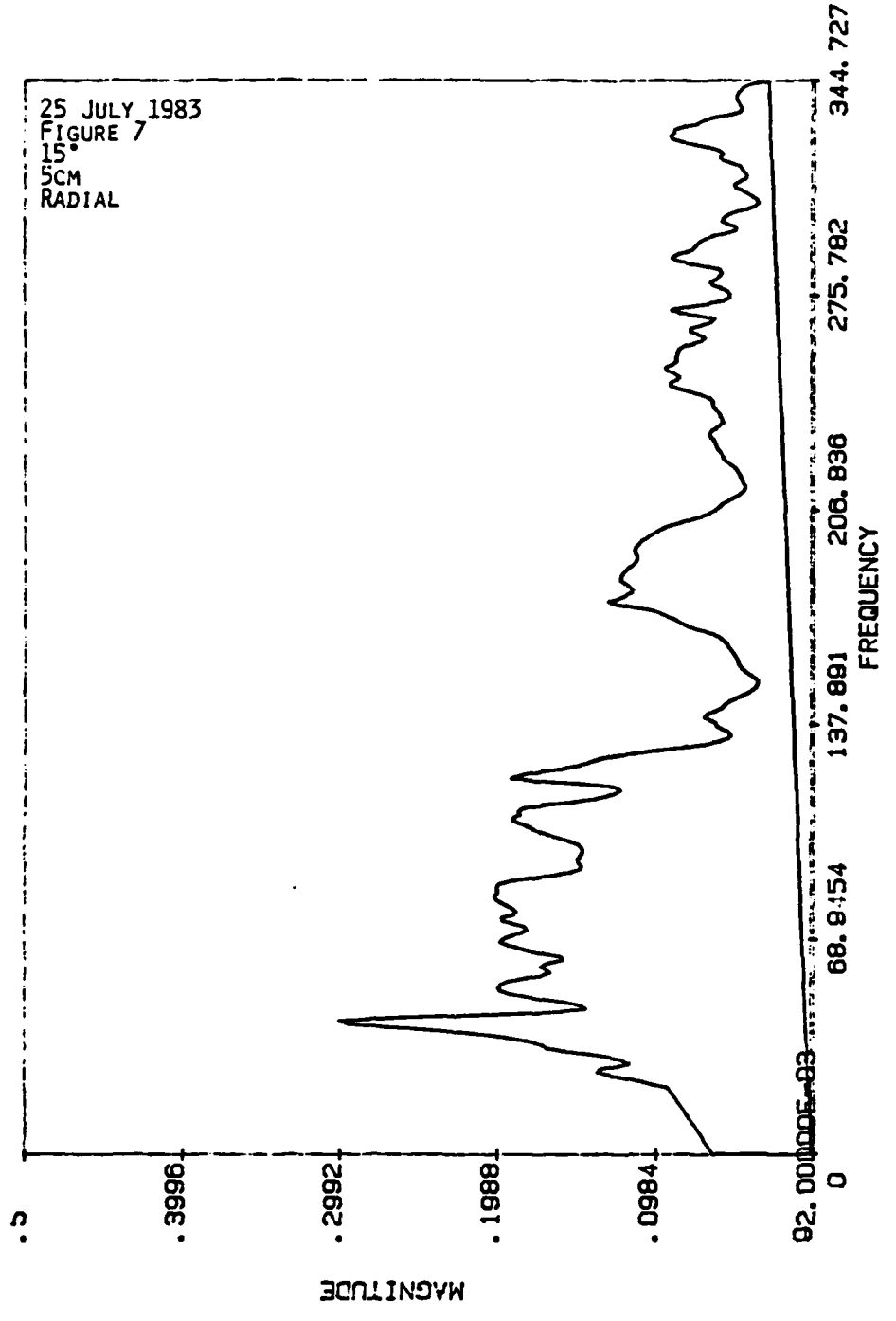
25 JULY 1983
FIGURE 7
15°
5CM
RADIAL
MAGNITUDE
.5
.3996
.2992
.1988
.0984
0
FREQUENCY
0
68.8154
137.891
206.836
275.782
344.727

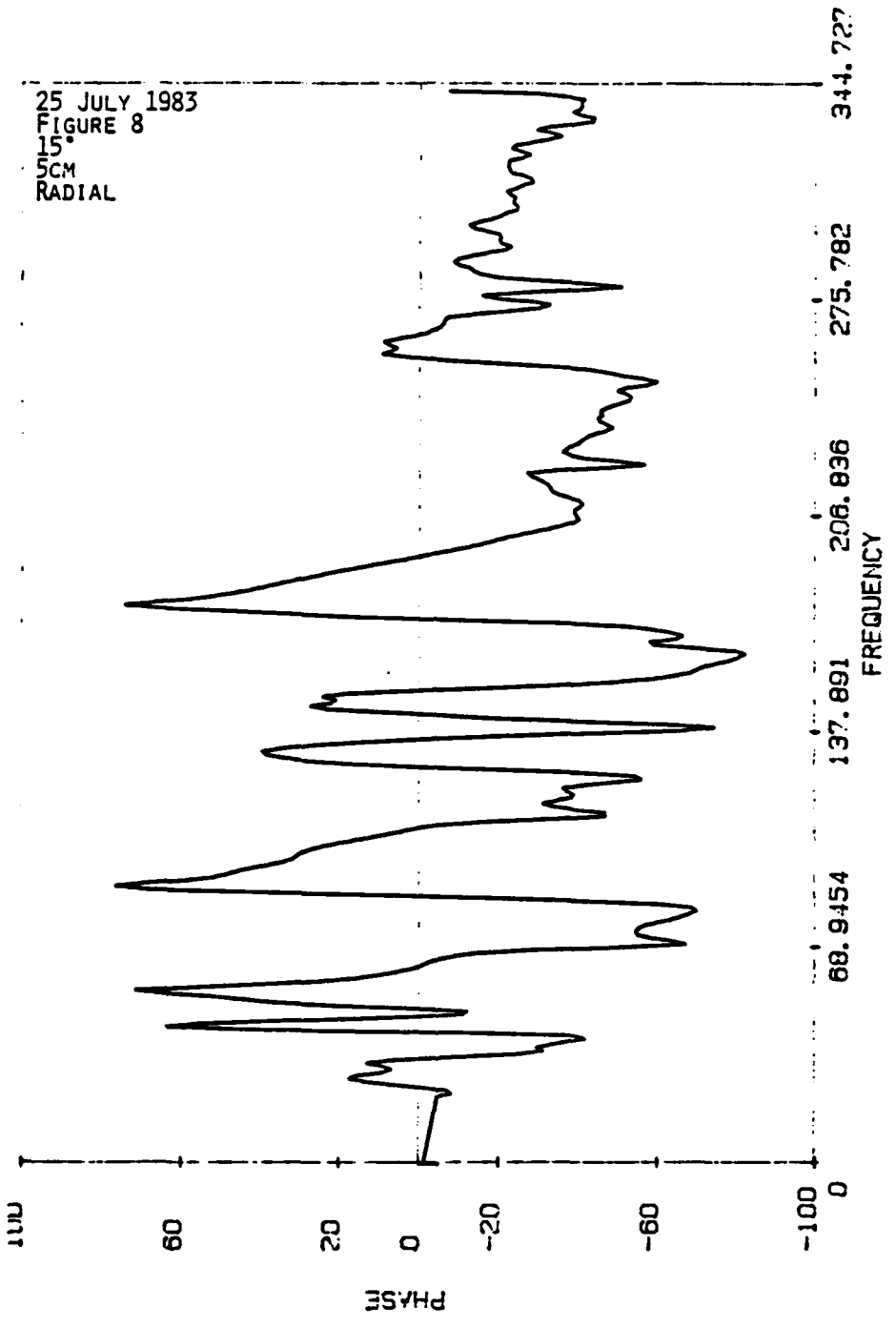
25 JULY 1983
FIGURE 8
15°
5CM
RADIAL
344.727
275.782
206.836
137.891
68.9454
FREQUENCY
100
60
20
0
-20
-60
-100
PHASE

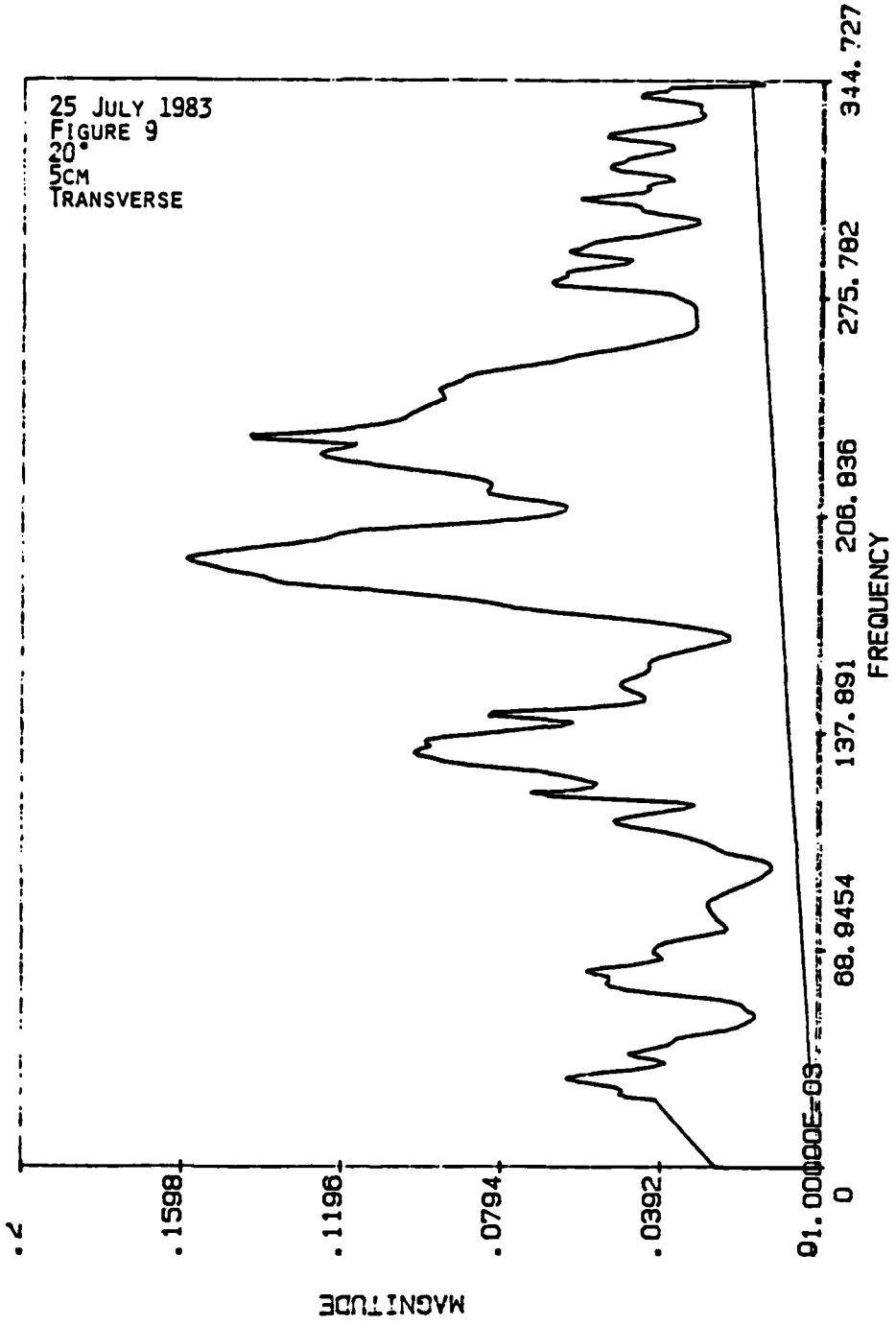
25 JULY 1983
FIGURE 9
20°
5CM
TRANSVERSE
MAGNITUDE
.1598
.1196
.0794
.0392
1.00000E-03
0
68.9454
137.891
206.836
275.782
344.727
FREQUENCY

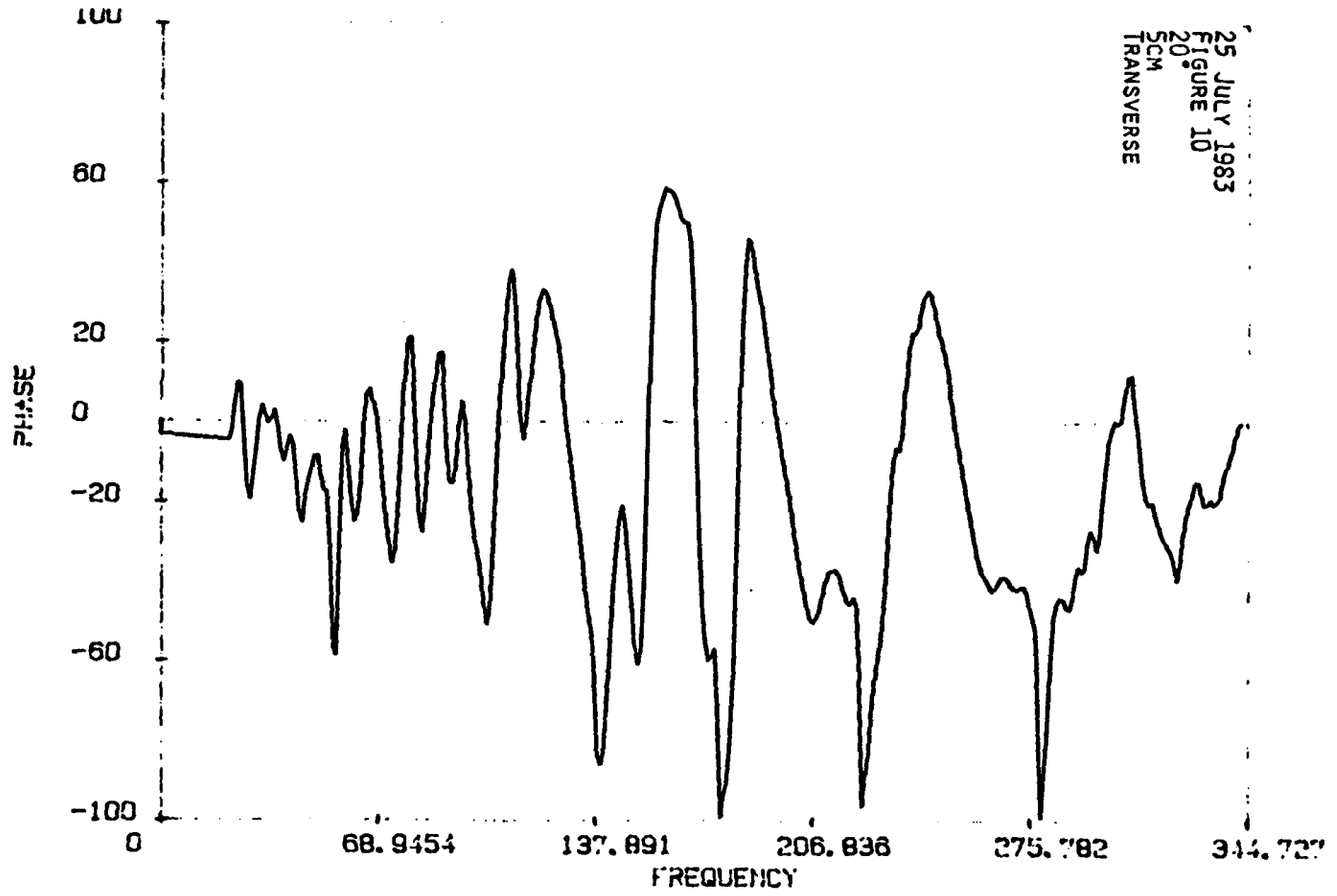
25 JULY 1983
FIGURE 10
20°
5CM
TRANSVERSE
100
60
20
0
-20
-60
-100
PHASE
0
68.9454
137.891
206.836
275.782
344.727
FREQUENCY

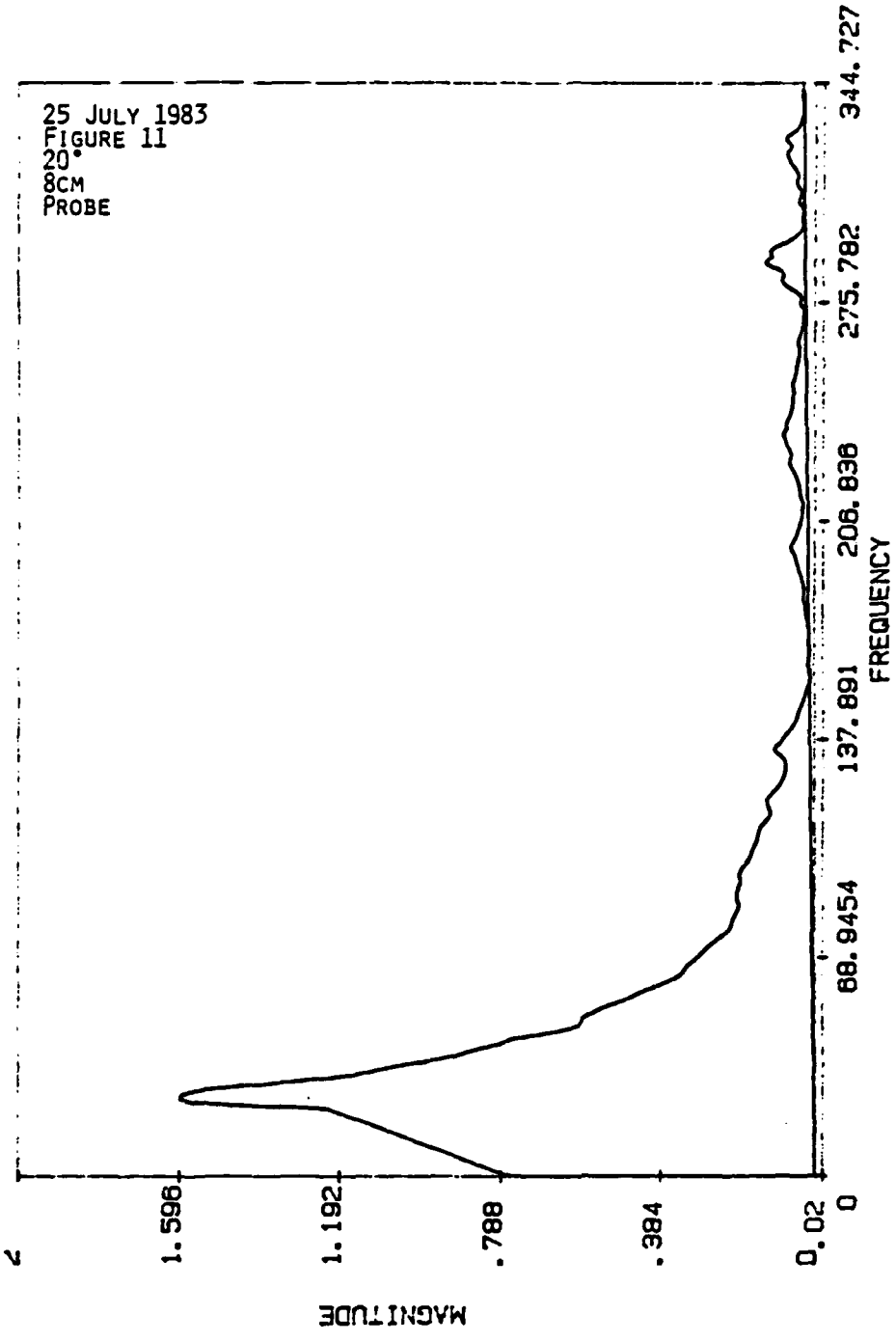
25 JULY 1983
FIGURE 11
20°
8CM
PROBE
MAGNITUDE
1.596
1.192
.788
.384
0.02
0
88.9454
137.891
206.836
275.782
344.727
FREQUENCY

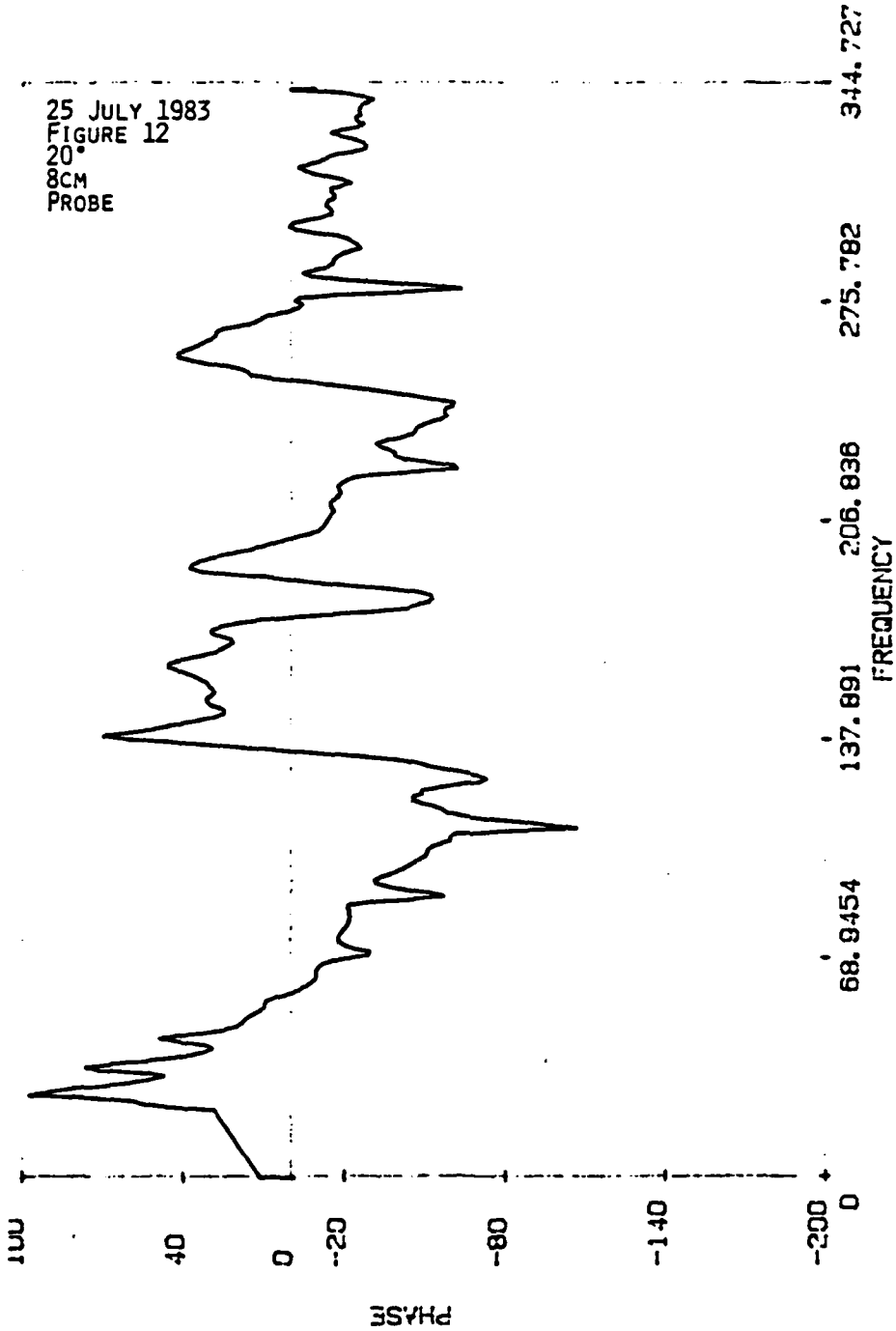
25 JULY 1983
FIGURE 12
20°
8CM
PROBE
344.727
275.782
206.836
137.891
68.9454
FREQUENCY
100
40
0
-20
-80
-140
-200
PHASE

APPENDIX C.1

The UM test field is located two miles south of Oxford, Mississippi and a map of the site is shown below. The experiment was carried out near the center of the field and the experimental site is marked with an X.

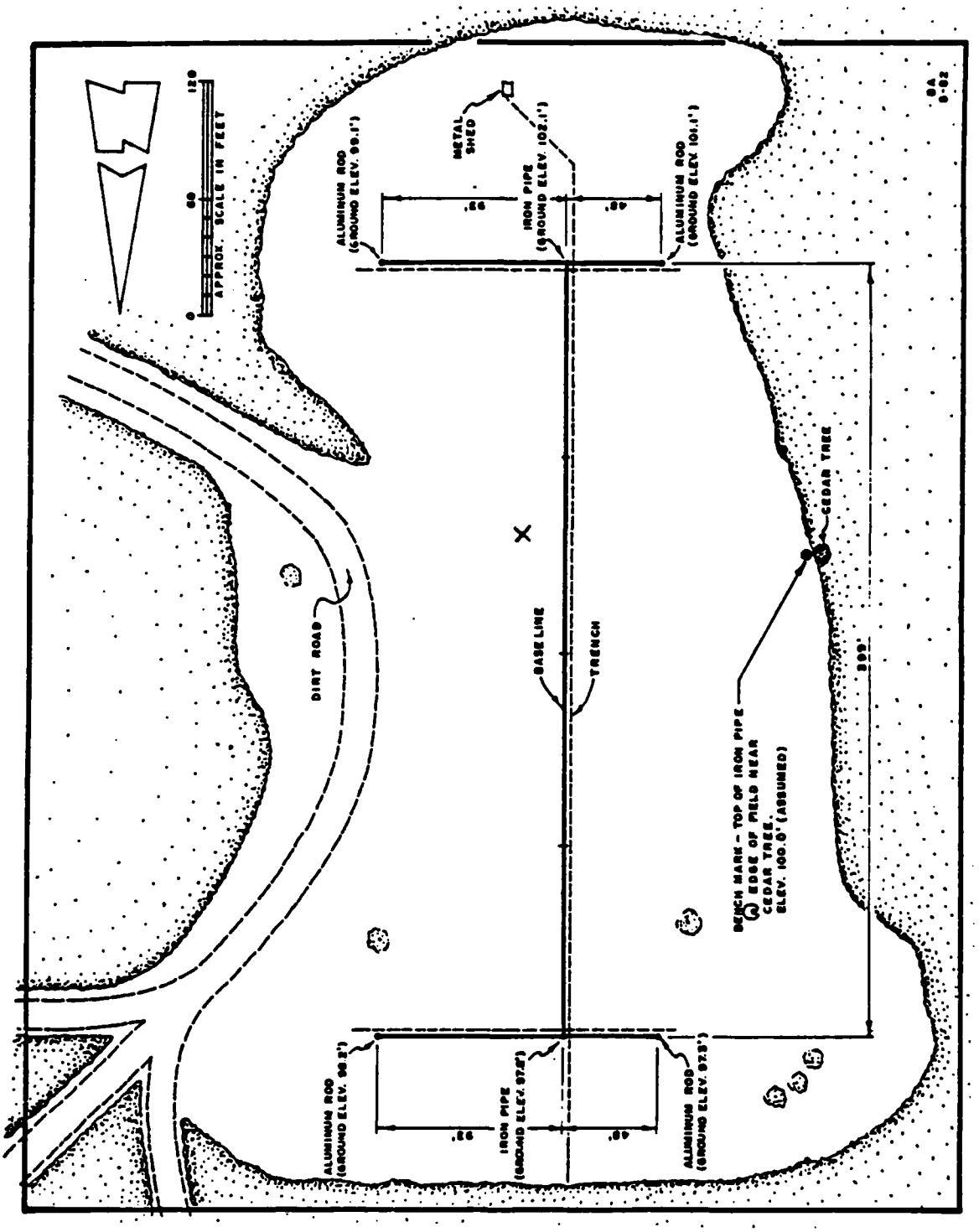

APPENDIX C.2

Sardis beach is located in the John W. Kyle State Park which is approximately 10 miles west of Oxford, Mississippi. The experiment was carried out on the lower lake beach immediately below the eastern most end of the dam. The experimental site is marked with an X.

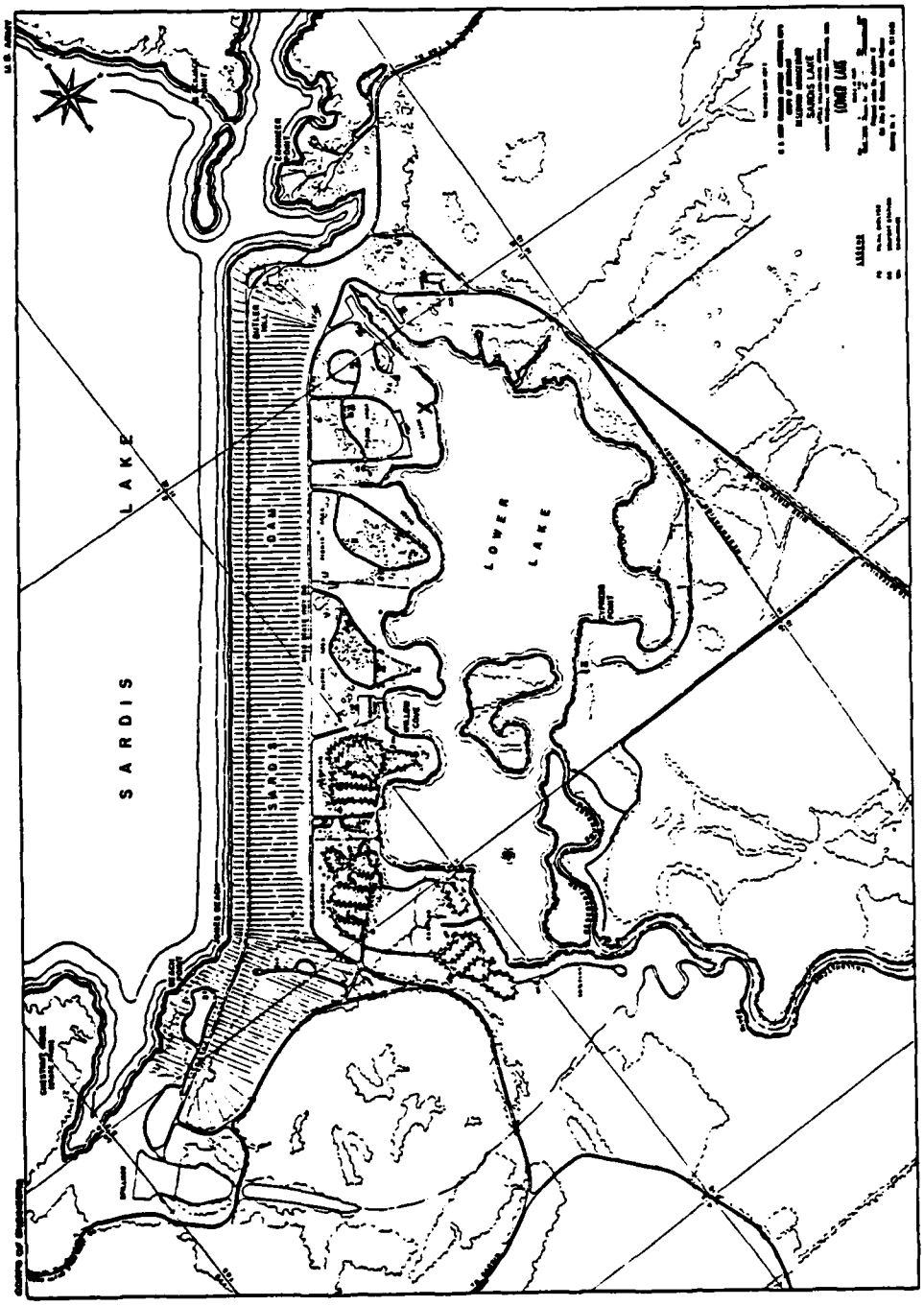

APPENDIX D

Participating Scientific Personnel

Bass, Henry E.	Co-Principal Investigator
Bolen, Lee N.	Co-Principal Investigator
Attenborough, Keith	Research Scientist
Sabatier, James	Ph.D. - Sept. 1984 (estimated)
Rish, Jeff	Ph.D. Candidate
Fortenberry, Rance M.	B.S. - May 1981
Sisler, Peter H.	M.S. - May 1982
Ezell, Jean E.	B.S. - May 1983
Horsburgh, Steven D.	M.S. - Aug. 1984
Wittchen, Bruce D.	B.S.E. - Dec. 1983
Logue, Lawrence C.	B.S. - May 1983
Fisher, Donald	B.S. Candidate
Rogers, Richard	M.S. Candidate
Givens, William J.	M.S. Candidate
Fortenberry, Steven D.	B.S. Candidate
McGee, Brenda Jo	B.A. Candidate